2016-06-02

Mechanisms Regulating Early Mesendodermal Differentiation of Human Embryonic Stem Cells: A Dissertation

Jennifer J. VanOudenhove
University of Massachusetts Medical School

MECHANISMS REGULATING EARLY MESENDODERMAL DIFFERENTIATION OF HUMAN EMBRYONIC STEM CELLS

A Dissertation Presented

By

Jennifer J. VanOudenhove

Submitted to the Faculty of the

University of Massachusetts Graduate School of Biomedical Sciences, Worcester

in partial fulfillment of the requirements for the degree of

DOCTOR OF PHILOSOPHY

June 2, 2016

Program in Cell Biology

MECHANISMS REGULATING EARLY MESENDODERMAL DIFFERENTIATION OF HUMAN EMBRYONIC STEM CELLS

A Dissertation Presented By
Jennifer J. VanOudenhove

This work was undertaken in the Graduate School of Biomedical Sciences
Program in Cell Biology
The signature of the Thesis Advisor signifies validation of Dissertation content

Gary S. Stein, Ph. D., Thesis Advisor

The signatures of the Dissertation Defense Committee signify completion and approval as to style and content of the Dissertation

Jeanne Lawrence, Ph. D., Member of Committee

Jaime Rivera, Ph. D., Member of Committee

Paul Odgren, Ph. D., Member of Committee

Janice Telfer, Ph. D., Member of Committee

The signature of the Chair of the Committee signifies that the written dissertation meets the requirements of the Dissertation Committee

Anthony Imbalzano, Ph.D., Chair of Committee

The signature of the Dean of the Graduate School of Biomedical Sciences signifies that the student has met all graduation requirements of the School.

Anthony Carruthers, Ph.D., Dean of the Graduate School of Biomedical Sciences

June 2, 2016

Dedication

This thesis is dedicated to my friends and family that have supported me throughout my Ph. D. journey; my good friends, Kate G. and Laurel D., as well as all my other friends who encouraged me and put up with me; my mother Dawn VanOudenhove for answering my phone calls (sometimes) and her loving support. I would also like to specifically dedicate this thesis to Andrew J. Hatt, an important part of my life, who passed away during my Ph. D. journey, but will always remain in my heart.

Acknowledgements

I would like to thank Dr. Gary Stein, Dr. Janet Stein and Dr. Jane Lian for their support and encouragement. I would like to acknowledge their many years of advice and direction; without which this experience would not have been the positive experience it was. Additional thanks to the current and previous members of the Stein, Stein, and Lian laboratory. Specific thanks go to Dr. Prachi Ghule, Dr. Rodrigo Grandy and Dr. Ricardo Medina for their help and advice with learning how to design and execute experiments and Dr. Kaleem Zaidi for his help with manuscript preparations and overall project direction. Additional thanks to Joseph Boyd for his assistance with bioinformatics analysis. I would also like to thank Dr. Julie Dragon for her help with microarray quality control, and explaining the basics of microarray data analysis as well as Dr. Roxana del Rio for her help with executing and analyzing flow cytometry.

I would also like to thank my thesis research and defense committee members Dr. Anthony Imbalzano, Dr. Jeanne Lawrence, and Dr. Jaime Rivera for their suggestions and guidance throughout my thesis research. I also would like to thank DEC members Dr. Janice Telfer, and Dr. Paul Odgren.

Abstract

Key regulatory events take place at very early stages of human embryonic stem cell (hESC) differentiation to accommodate their ability to differentiate into different lineages; this work examines two separate regulatory events.

To investigate precise mechanisms that link alterations in the cell cycle and early differentiation, we examined the initial stages of mesendodermal lineage commitment and observed a cell cycle pause that occurred concurrently with an increase in genes that regulate the G2/M transition, including WEE1. Inhibition of WEE1 prevented the G2 pause. Directed differentiation of hESCs revealed that cells paused during commitment to the endo- and mesodermal, but not ectodermal, lineages. Functionally, WEE1 inhibition during meso- and endodermal differentiation selectively decreased expression of definitive endodermal markers SOX17 and FOXA2. These findings reveal a novel G2 cell cycle pause required for endodermal differentiation.

A role for phenotypic transcription factors in very early differentiation is unknown. From a screen of candidate factors during early mesendodermal differentiation, we found that RUNX1 is selectively and transiently up-regulated. Transcriptome and functional analyses upon RUNX1 depletion established a role for RUNX1 in promoting cell motility. In parallel, we discovered a loss of repression for several epithelial genes, indicating that RUNX1 knockdown impaired an epithelial to mesenchymal transition during differentiation. Cell biological and biochemical approaches revealed that RUNX1 depletion

compromised TGFβ2 signaling. Both the decrease in motility and deregulated epithelial marker expression upon RUNX1 depletion were rescued by reintroduction of TGFβ2, but not TGFβ1. These findings identify novel roles for RUNX1-TGFβ2 signaling in mesendodermal lineage commitment.

Table of Contents

List of Figures

List of Tables

List of Symbols and Abbreviations

Bromodeoxyuridine (BrdU)

Core Binding Factor β (CBFβ)

Cyclin dependent kinases (cdks)

Cyclin Dependent Kinase 1 (CDK1)

Embryoid Bodies (EBs)

Epithelial to Mesenchymal Transition (EMT)

Hematopoietic Stem Cells (HSCs)

Human Embryonic Stem Cells (hESC)

Latent Transforming Growth Factor β Binding Protein (LTBP)

Maturation-promoting Factor or M phase-promoting Factor (MPF)

Mouse Embryonic Stem Cells (mESCs)

Nuclear Localization Signal (NLS)

Nuclear Matrix Targeting Signal (NMTS)

Receptor-activated SMADs (R-SMADs)

Runt Homology Domain (RHD)

Preface

Portions of this thesis have appeared in the following works:

VanOudenhove JJ, Medina, R, Ghule PN, Lian JB, Stein JL, Zaidi SK, Stein, GS. Transient RUNX1 Expression during Early Mesendodermal Differentiation of hESCs Promotes Epithelial to Mesenchymal Transition through TGFβ2 Signaling. *Submitted to Stem Cell Reports*.

VanOudenhove JJ, Grandy RA, Ghule PN, del Rio R, Lian JB, Stein JL, Zaidi SK, Stein, GS. Lineage-Specific Early Differentiation of Human Embryonic Stem Cells Requires a G2 Cell Cycle Pause. *Stem Cells.* [Epub ahead of print]. PMID: 26946228

Other works published during graduate study that are not presented in this thesis:

Browne G, Dragon JA, Hong D, Messier TL, Gordon JA, Farina NH, Boyd JR, **VanOudenhove JJ**, Perez AW, Zaidi SK, Stein JL, Stein GS, Lian JB. (2016) MicroRNA-378-mediated suppression of Runx1 alleviates the aggressive phenotype of triple negative MDA-MB-231 human breast cancer cells. *Tumour Biol.* [Epub ahead of print]. PMID: 26749280

Grandy RA, Whitfield TW, Wu H, Fitzgerald MP, **VanOudenhove J**, Zaidi SK, Montecino M, Lian JB, vanWijnen AJ, Stein JL, Stein GS. (2015) Genome-wide Studies Reveal that H3K4me3 Modification in Bivalent Genes is Dynamically Regulated During the Pluripotent Cell Cycle and Stabilized Upon Differentiation. *Mol Cell Bio.* 36(4), 615–27. PMID: 26644406

Saxena P, Trerotola M, Wang T, Li J, Sayeed A, **VanOudenhove J**, Adams DS, Fitzgerald TJ, Altieri DC, Languino L.R. (2012) PSA regulates androgen receptor expression in prostate cancer cells. *Prostate.* 72(7), 769-76. PMID: 21956655

CHAPTER I. Introduction

1.1 Human embryonic stem cells

How can a full human being originate from a single zygotic cell? This central question, while simple, leads to a host of more detailed and complex questions. Since early development takes place inside a female human being, and is therefore inaccessible, it makes studying the early mechanistic details of the process very difficult. Thus, human embryonic stem cells (hESCs) were isolated from the inner cell mass of a blastocyst stage embryo, which forms within five days of fertilization of an oocyte (Reubinoff et al., 2000; Thomson et al., 1998), providing a model system for the study of early human development.

Human embryonic stems have unique properties, which include an unlimited replicative potential and the capability to differentiate into any somatic cell type, termed pluripotency (Thomson et al., 1998). The unlimited replicative potential of hESCs is maintained through high levels of expression of telomerase, which ensures retention of the telomere ends on chromosomes with each cell division and prevents the cells from reaching the Hayflick limit and undergoing senescence (Amit et al., 2000). The expression of telomerase is part of a regulatory network that maintains the self-renewal and pluripotency of hESCs. This regulatory network contains both auto-regulatory and feed-forward loops, and is dominated by three transcription factors, OCT4 (Niwa et al., 2000), NANOG (Chambers et al., 2003), and SOX2 (Avilion et al., 2003; Fong et al.,

2008), which are essential for maintenance of pluripotency and self-renewal (Boyer et al., 2005).

In order to be maintained in culture, hESC are grown on either a feeder layer (typically mouse embryonic fibroblasts) or under feeder-free conditions. When hESCs are kept under feeder-free conditions, as they were for the work in this dissertation, they are grown on a matrix composed of one of several substrates (including Matrigel, vitronection, laminin, fibronectin, or collagen IV among others) (Xu et al., 2001) with media containing specific growth factors that promote pluripotency. The two most important growth factors are bFGF and TGFβ1/Nodal, which are thought to suppress BMP signaling that induces differentiation (Xu et al., 2005), while TGFβ1 also specifically increases *NANOG* expression (Chen et al., 2011; Xu et al., 2008).

1.2 Unique Cell Cycle Regulation in hESCs

Maintenance of human embryonic stem cell pluripotency is tightly linked to cell cycle control (Kapinas et al., 2013; White and Dalton, 2005). Human embryonic stem cells have a unique cell cycle with a G1 phase shorter than that of somatic cells (~3h vs. ~10h) (Becker et al., 2006). Lengthening of the G1 phase has been linked to differentiation and loss of pluripotency (Calder et al., 2013; Filipczyk et al., 2007). Recent studies have shown that onset of differentiation likely occurs in the G1 phase, with endo- and mesodermal differentiation initiating in early G1 and the neuroectodermal lineage arising during late G1 (Pauklin and Vallier, 2013; Sela et al., 2012). The G2/M/S phases

of the hESC cell cycle are minimally responsive to differentiation cues (Pauklin and Vallier, 2013).

Regulation of the cell cycle during the differentiation process has been primarily attributed to known negative regulators of proliferation in somatic cells, including p21 and p27 (Calder et al., 2013; Egozi et al., 2007; Zhu et al., 2014). The levels of p21 and p27 remain low in pluripotent hESCs, and increase upon differentiation. A recent study found that to maintain pluripotency the expression of p21 and p27 must be repressed, as elevated levels of p21 and p27 resulted in an increased G1 phase occupancy (Menchón et al., 2011; Zhu et al., 2014). Additionally, p27 can directly repress SOX2 during differentiation (Li et al., 2012). While a correlation between the lengthening of the cell cycle and initiation of hESC differentiation has been established, mechanisms that coordinate changes in the cell cycle and differentiation are not fully understood.

1.3 Regulation of the G2/M Transition of the Cell Cycle

Since much of the focus on cell cycle regulation in hESCs has been on the role of the G1 phase, and the G1/S transition, this allows for potential novel discoveries in the other phases of the cell cycle. The G2 phase of the cell cycle begins at the completion of DNA replication and includes a period of rapid protein production and cell growth that concludes upon initiation of prophase of mitosis. The events that modulate the transition from G2 to mitosis form a checkpoint that prevents premature mitosis in cells with defects such as incomplete DNA replication or DNA damage that needs more time to be corrected (O'Connell and

Cimprich, 2005; Zhou and Elledge, 2000). Progress through the mammalian cell cycle is mediated by the sequential activation of cyclin dependent kinases (cdks) (Pines, 1995). The activation of the cdks is regulated by both stage specific cyclin binding and phosphorylation events.

A key regulatory event in the activation of cdks and the transition from G2 to mitosis is the formation of a complex between CDK1 and one of the five isoforms of Cyclin B (Nigg, 1995). This complex was originally identified as the maturation-promoting factor or M phase-promoting factor (MPF) in meiotic frog eggs, since it was capable of inducing mitosis in immature G2 phase oocytes (Masui and Markert, 1971). While in humans it is generally thought that the levels of CDK1 remain constant throughout the cell cycle, the levels of Cyclin B1 mRNA and protein change with cell cycle progression (Smits and Medema, 2001). The transcription from the Cyclin B1 promoter increases after S phase and decreases during the beginning of G1, and Cyclin B1 protein is degraded during the metaphase-anaphase transition during mitosis (Piaggio et al., 1995; Pines and Hunter, 1989).

During interphase Cyclin B interacts with importin β, is imported into the nucleus, and then is swiftly shuttled out of the nucleus due to an N-terminal nuclear export signal (Hagting et al., 1998; Takizawa et al., 1999; Toyoshima et al., 1998). Once the MPF complex levels in the cytoplasm increase, due to an increase in total Cyclin B, the Cyclin B portion of the complex is phosphorylated near the nuclear export signal on residues S133 and S147, creating a nuclear

localization signal, which increases the rate of nuclear import beyond what would be caused by simply blocking the nuclear export signal (Hagting et al., 1999; Toyoshima-Morimoto et al., 2001).

In addition to the regulation of the formation and localization of the MPF, there are multiple phosphorylation events on CDK1 that control the transition from G2 to mitosis. An activating phosphorylation of CDK1 is placed on T161 in the T-loop by the Cyclin Activating Kinase (CAK), which is a heterotrimeric complex composed of Cdk7, Cyclin H, and MAT1 (Tassan, 1994). This activating phosphorylation is opposed by a set of inhibitory phosphorylations. The WEE1 and MYT1 kinases are responsible for placing these inhibitory phosphorylations on CDK1 in the MPF complex. WEE1 primarily phosphorylates Y15 of CDK1, while the MYT1 kinase can phosphorylate either T14 or Y15 (Booher et al., 1997; Liu et al., 1997; Parker and Piwnica-Worms, 1992). Phosphorylation of Y15 on CDK1 interferes with phosphate transfer to a bound substrate, while the phosphorylation of T14 interferes with ATP binding (Atherton-Fessler et al., 1993; Endicott et al., 1994). Cyclin B binding mediates these inhibitory phosphorylations on CDK1 (Meijer et al., 1991).

Once CDK1 is bound to Cyclin B and phosphorylated by CAK and WEE1/MYT1, it is primed and ready to be activated through the dephosphorylation of T14 and Y15, which triggers the initiation of mitosis. Dephosphorylation of T14 and Y15 is performed by the dual specificity phosphatase CDC25, which can dephosphorylate phospho-tyrosine as well as

phospho-threonine residues (Gautier et al., 1991; Kumagai and Dunphy, 1991; Strausfeld et al., 1991). Conversely, the MPF complex can then phosphorylate WEE1 and CDC25, which inhibits WEE1 and further activates CDC25, which can then further dephosphorylate CDK1 on T14 and Y15 (Hoffmann et al., 1993; Mueller et al., 1995). This amplifies the signal and contributes to a burst of MPF activity, which initiates mitosis through the phosphorylation of downstream targets. Importantly, these targets include nuclear lamins that cause nuclear-envelope breakdown, microtubule-associated proteins that promote assembly of the mitotic spindle assembly, and condensin subunits that are responsible for chromosome condensation (Heald and McKeon, 1990; Kimura et al., 1998; Miake-Lye et al., 1983; Tombes et al., 1991).

Interestingly, in mice, of the CDKs, only CDK1 is essential for survival (lethality by E1.5)(Santamaría et al., 2007). Of the cyclins, only disruption of cyclin A2 and cyclin B1, which have roles in the S/G2/M phases, results in embryonic lethality early in development (E5.5 and before E10.5/not determined, respectively) (Brandeis et al., 1998; Gong and Ferrell, 2010; Gong et al., 2007; Murphy et al., 1997). Additionally, information regarding a role for WEE1 in mammalian development has been limited because there is a requirement for WEE1 prior to blastocyst formation in development that ends with embryonic lethality prior to E3.5 in WEE1-deficient mice due to apoptosis as a result of an accumulation of DNA damage (Tominaga et al., 2006). Together, these studies indicate the importance of the regulation of G2/M transition.

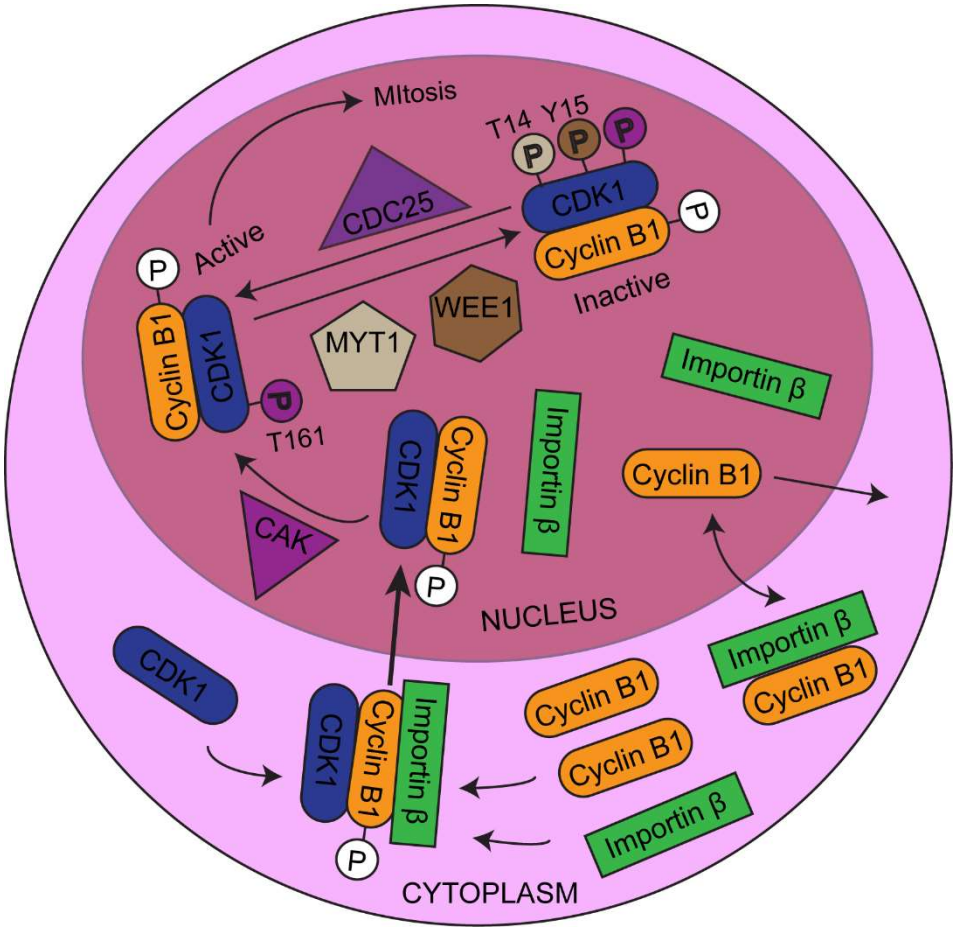

Figure 1.1. Overview of the Regulation of the G2/M Transition.

1.4 Strategies for Differentiating hESCs

A key property of hESCs is their ability to differentiate into cell types from all three germ layers. The most widely used method to differentiate hESCs involves formation of three-dimensional spheroids designated embryoid bodies (EBs), which can spontaneously differentiate into ectoderm, mesoderm and endoderm (Itskovitz-Eldor et al., 2000; Keller, 1995; Segev et al., 2004; Xu,

2002). There are also numerous studies using EB differentiation protocols that require several days to weeks that focus on creating defined cell types (D'Amour et al., 2005; Gerrard et al., 2005; Takasato et al., 2014). Typically, embryoid body formation requires long incubation periods to induce differentiation (minimum 4-5d to form EB spheroids), providing a challenge to investigate mechanisms operative in the earliest stages of differentiation. This method of differentiation does have the advantage that the three-dimensional culture more closely recapitulates an environment that would be found *in vivo*, with signals and cellular interactions coming from all directions, than two-dimensional culture.

Another common method of inducing differentiation is to co-culture hESCs with another cell line/type that will produce the cues to induce the hESCs to differentiate to the desired lineage (Mummery et al., 2003; Vodyanik et al., 2005). The issues that arise with this method of differentiation include removal of the co-cultured cell line after the desired lineage is generated, and the possibility of transmission of a pathogen, activation of retroviruses, or induction of immunogenicity resulting from exposure of the hESCs to cells or products from non-human species. The simplest method to induce differentiation is through a monolayer differentiation, which is used for the experiments in this dissertation, avoids the pitfalls of other methods of differentiation and allows for the study of early differentiation (D'Amour et al., 2005; Gerrard et al., 2005; Takasato et al., 2014).

1.5 Mesendoderm

Studies in lower vertebrates (*C.elegans*, *Xenopus*, and zebrafish) have shown that mesoderm and endoderm arise from a bipotent progenitor population (Maduro et al., 2001; Rodaway and Patient, 2001) known as the mesendoderm. Several studies have shown that there is a bipotent mesendodermal population during mammalian development as well, though whether the population is composed of cells that are truly bipotent or if the population is composed of a mix of progenitors that are already committed to each lineage is still up for debate (Lickert et al., 2002; Tada, 2005). Both mouse embryonic stem cells (mESCs) and hESCs can differentiate into mesendoderm (Kubo et al., 2004; Mahmood and Aldahmash, 2015; Tada, 2005), which is marked by early gene expression patterns similar to that of primitive streak with high expression of the markers *BRACHYURY*, *MIXL1*, or *GSC* (Pereira et al., 2011), though the exact timing of expression varies based on the method of differentiation (S. A. Jackson et al., 2010; Mahmood and Aldahmash, 2015; Tada, 2005). From mesendoderm, both mESCs and hESCs can then differentiate to definitive endoderm or mesoderm (D'Amour et al., 2005; Lam et al., 2014). The activation of canonical Wnt/β-catenin signaling in hESCs induces mesoderm (Davidson et al., 2012), whereas Activin A has been shown to mimic nodal, inducing differentiation into anterior primitive streak/endoderm progenitors (Sulzbacher et al., 2009).

1.6 The RUNX Family

While much is known about the maintenance of pluripotency (Boward et al., 2016; Boyer et al., 2005; Chambers et al., 2003; Huang et al., 2015; Kapinas et al., 2013), how differentiation signals regulate the dissolution of pluripotency and the establishment of phenotype is not well understood. Studies in hESCs have shown that many genes responsible for early developmental events are poised for either activation or repression by epigenetic mechanisms (Bernstein et al., 2006; Grandy et al., 2015; Szutorisz and Dillon, 2005). Once a differentiation signal has been introduced, early factors are expressed that prime the gene expression program of cells for lineage acquisition (Zaret and Carroll, 2011). One category of factors that has potential to regulate the gene expression program of differentiating cells is transcription factors.

The RUNX (Runt-related transcription factor) family of genes, which is also known as the acute myeloid leukemia (AML), core-binding factor (CBF) or polyoma enhancer-binding protein-2α (PEBP2α) family of genes, contains three members: RUNX1, RUNX2, and RUNX3 (Ito, 2004). Each of the RUNX family transcription factors has known roles in development (Chuang et al., 2013). RUNX1 is necessary for definitive hematopoiesis (Okuda et al., 1996), RUNX2 for bone formation (Otto et al., 1997), and RUNX3 for gastrointestinal and nervous system development (Inoue et al., 2002; Levanon et al., 2002; Li et al., 2002). All three of the family members are implicated in malignancies as either

tumor suppressors or oncogenes in a context specific manner (Blyth et al., 2005; Ito, 2004).

All RUNX genes are transcribed from two promoters, the distal P1 and the proximal P2 (Bangsow et al., 2001; Drissi et al., 2000; Fujiwara et al., 1999; Ghozi et al., 1996), and contain similar structural domains. Each family member contains a highly conserved 128 amino acid region in the N-terminal region known as the runt domain due to its homology to the *Drosophila* Runt protein (Kagoshima et al., 1993; Ogawa et al., 1993b). This runt homology domain (RHD) is responsible for mediating heterodimerization with the Core Binding Factor β (CBFβ) protein, which stabilizes the protein complex, and binding the RUNX family's consensus DNA sequence PyGPyGGTPy, where Py stands for either pyrimidine base (cytosine or thymine) (Melnikova et al., 1993; Ogawa et al., 1993a). CBFβ alone does not bind DNA (Ogawa et al., 1993a). A nuclear targeting signaling (NLS) is found on the C-terminal end of the RHD, which is required for the nuclear localization of the RUNX proteins and allows for access to its DNA targets (Kanno et al., 1998).

The RUNX family also has conserved regions on the C-terminus. Each family member has a nuclear matrix targeting signal (NMTS) in addition to the NLS. The NMTS is an ~31-38 amino acid sequence that is responsible for the sub-nuclear localization of the RUNX proteins to distinct nuclear sites to facilitate gene regulation (Stein et al., 2009; Zeng et al., 1998, 1997). The C-terminus is also comprised of additional domains that mediate gene regulation such as an

activation and inhibitory domain, the PPxY (or PY) motif, and the VWRPY motif. The PY motif is a proline-rich peptide that interacts with proteins containing the WW domain such as YAP, whereas the VWRPY motif interacts with proteins containing tryptophan-aspartic acid repeats, like Groucho/TLE transcription corepressors (Aronson et al., 1997; Chuang et al., 2013; Ito, 2004; Javed et al., 2000).

1.7 RUNX1 in Development

Developmental hematopoiesis begins with primitive hematopoiesis, where a limited number of blood lineages (mostly large erythroblasts) that sustain early embryonic development are produced primarily from the yolk sac (Chen et al., 2014). A second wave of blood development, termed definitive hematopoiesis, occurs intra-embryonically in the aorta-gonad-mesonephros. During this stage of development, hematopoietic stem cells (HSCs) are formed that have the ability to produce any of the hematopoietic lineages and having long term repopulation capacity (Chen et al., 2014). RUNX1 is required for definitive hematopoiesis, as no definitive HSCs are formed in the absence of RUNX1. When genetically deleted in mice, *Runx1* loss causes embryonic lethality due to major defects in the formation of the fetal liver and hemorrhaging in the central nervous system (Okuda et al., 1996; Wang et al., 1996). RUNX1 appears to be mostly dispensable once HSCs are formed, however, loss of RUNX1 has some effects on differentiation toward specific hematopoietic lineages (Growney et al., 2005; Ichikawa et al., 2008, 2004). It is hypothesized that RUNX1 is required to alter

chromatin, through unfolding and modification of the epigenetic landscape, to allow early hematopoiesis (Hoogenkamp et al., 2009; Lichtinger et al., 2012).

The RUNX1 transcript is expressed as three major isoforms, two from a proximal (isoforms a and b) and one from a distal (isoform c) promoter (Ghozi et al., 1996; Ran et al., 2013; Sroczynska et al., 2009). A study looking at *Runx1* isoform expression in early mouse hematopoietic development found that primitive erythrocytes that are produced prior to definitive hematopoiesis express mainly proximal promoter derived isoforms (Bee et al., 2009). However, in definitive HSCs from the yolk sac or aorta-gonad-mesonephros, transcription occurs from both the distal and proximal promoters, with isoforms from each promoter having non-redundant functions (Bee et al., 2010). Once cells have migrated to the fetal liver to establish adult hematopoiesis, the distal promoter gradually becomes the main hematopoietic promoter (Bee et al., 2009).

Previous studies of hematopoietic differentiation of hESCs have found an increase in RUNX1c mRNA levels between 8 and 12 days of differentiation from embryoid bodies that correlates with the emergence of the definitive hematopoietic lineage marker CD34. Also, low RUNX1b mRNA levels were observed throughout differentiation (Challen and Goodell, 2010; Zambidis et al., 2005). Of note, in undifferentiated hESCs, the *RUNX1* proximal promoter that expresses the RUNX1b transcript is bivalently marked with H3K27me3 and H3K4me3, indicating that it is poised for expression, while the distal promoter is not (Figure 1.2) (Mikkelsen et al., 2007). This could indicate that RUNX1

transcription from the proximal promoter is more permissive early in development and may have a role that is not linked to emergence of HSCs. The role of RUNX1 in differentiation at very early time points in either directed or undirected differentiation of hESCs has been minimally explored, which was a major objective of Chapter III.

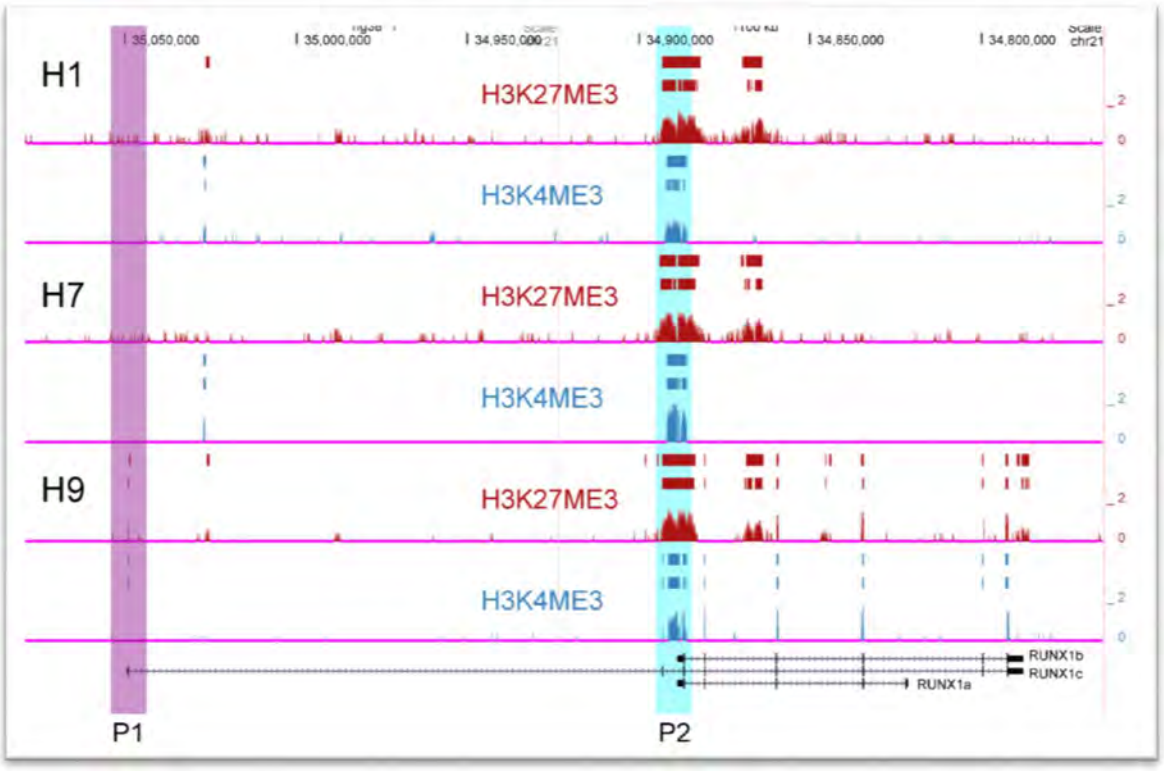

Figure 1.2. The *RUNX1* promoter is bivalently marked in pluripotent hESCs. Tracks marking H3K4ME3 and H3K27ME3 across the *RUNX1* gene in three different hESC lines (H1, H7, and H9). H1 and H7 data is taken from GEO datasets GSE51334 and GSE35583, respectively, while the H9 data is taken from data from different cell cycle stages pooled together from the GEO dataset GSE55502. The P1 or distal promoter is marked in purple, while the P2 or proximal promoter is marked in cyan. Both H3K4ME3 and H3K27ME3 markers are found at the P2 promoter in all three cell lines.

Emerging evidence indicates that RUNX1 has roles in non-hematopoietic lineages (Osorio et al., 2008; Scheitz and Tumbar, 2013; Stifani et al., 2008). Multiple reports have detailed a role for RUNX1 in epithelial biology (Scheitz and Tumbar, 2013). Studies have shown that RUNX1 modulates developmental activation and proliferation of hair follicle stem cells and inner olfactory nerve layer olfactory ensheathing cells (Hoi et al., 2010; Lee et al., 2014; Murthy et al., 2014; Osorio et al., 2011, 2008). RUNX1 is a key regulator of the differentiation of mammary epithelium stem cells from a state of ductal and lobular bipotency (Sokol et al., 2015). Additional roles have been shown in other mesodermal derivatives such as mesenchymal stem cells, myofibroblasts and skeletal progenitors (Kim et al., 2014; Lian et al., 2003).

1.8 TGFβ signaling

TGFβ signaling is a major contributor to specification of the body plan during metazoan development as well as other cellular processes including proliferation, apoptosis, recognition, and differentiation (Kitisin et al., 2007; Wu and Hill, 2009). The TGFβ superfamily is comprised of the TGFβ ligands (1,2, and 3), bone morphogenetic proteins, activins, inhibins, and other cytokines, all of which contain monomers with six cysteine residues in a “knot” formation (Kitisin et al., 2007; Sun and Davies, 1995). The TGFβ ligands are synthesized in a latent state with large N-terminal pro-domains, which are necessary for the proper folding and homodimerization of the C-terminal regions of the proteins (Gray and Mason, 1990). Before secretion, the pro-domains are cleaved from the C-terminal

portion of the protein intracellularly by Furin, however the pro-domains still remain non-covalently associated with the rest of the protein to maintain latency (Dubois et al., 1995). Another peptide, termed the latent transforming growth factor β binding protein (LTBP), forms disulfide bonds with the N-terminal end of the TGFβ pro-domain within fifteen minutes of synthesis and aids in secretion and targeting of latent TGFβ to sites within the extracellular matrix (Miyazono et al., 1991; Taipale et al., 1994). TGFβ can be activated by a variety of methods, including integrin, thrombospondin, matrix glycoprotein, and protease mediated activation, as well as by potentially by mechanisms yet to be discovered (Alcaraz et al., 2014; Annes, 2003; Giacomini et al., 2012).

Once TGFβ has been activated, the ligand can then initiate signaling by binding to and bringing together type I and type II receptor serine/threonine kinases on the surface of a cell (Wrana et al., 1992). This binding induces transphosphorylation of the type I receptor by the type II receptor constitutively active kinases. The type I receptor then phosphorylates a set of receptor-activated SMADs (R-SMADs), which include SMAD1, 2, 3, 5, and 8, on C-terminal serines that then form complexes with SMAD4. SMADS 2 and 3 are mostly activated by activin/nodal/TGFβ ligand bound type I receptors, whereas SMADSs 1, 5 and 8 are mostly activated by BMP bound type I receptors (Miyazawa et al., 2002). The R-SMAD/SMAD4 complexes translocate into the nucleus, where they regulate transcription of target genes by interacting with or binding to DNA-binding transcription factors, CREB-binding protein, p300

coactivators, or many other factors (Itoh et al., 2000; Massagué, 2000, 1998; Shi and Massagué, 2003).

Activation of R-SMADs by type I receptor kinases is inhibited by SMAD6 or SMAD7 as part of a negative feedback loop thought to function in signal termination (Itoh and ten Dijke, 2007; Schmierer and Hill, 2007). SMAD6 competes with SMAD4 for binding to activated SMAD1, sequestering the activated SMAD1 in apparently inactive complex (Hata et al., 1998). SMAD7 interaction with the type I receptors leads to the ubiquitination and degradation of these receptors (Ebisawa et al., 2001; Tajima et al., 2003).

TGFβ can activate RUNX genes at the transcriptional level and at the posttranscriptional level through activation or stabilization of RUNX proteins (Jin et al., 2004; Klunker et al., 2009; Miyazono et al., 2004). Additionally, RUNX1 can physically interact with SMAD factors to form complexes together with SMAD4 that appear to be critical for efficient transcriptional activation of target genes (Hanai et al., 1999). This allows the possibility that there could be additional regulation or interaction between RUNX1 and the TGFβ pathway to discover.

1.9 Epithelial Mesenchymal Transition in Development

An epithelial-mesenchymal transition (EMT) is a biologic process that allows an epithelial or epithelial-like cell to undergo a series of changes that allow acquisition of a mesenchymal phenotype, including an enhanced migratory capacity, invasiveness, elevated resistance to apoptosis, and increased

production of ECM components (Kalluri and Neilson, 2003; Kalluri and Weinberg, 2009). Elizabeth Hay first described the concept of EMT over 40 years ago in 1968 (Hay, 1968).

During EMT, epithelial cells lose their junctions and apical–basal polarity, reorganize their cytoskeleton, and lose the expression of markers of an epithelial phenotype like *E-Cadherin (CDH1)*, *Occludin*, *Claudins*, and *Cytokeratins*, while gaining expression of mesenchymal markers like *Vimentin*, *N-Cadherin*, *CD44*, *Fibronectin*, *Fibroblast Specific Protein 1 (FSP-1)*, and *α-Smooth Muscle Actin (α-SMA)* (Kalluri and Weinberg, 2009; Lamouille et al., 2014). E-cadherin loss is considered to be necessary, but not on its own sufficient to induce EMT, as mesenchymal trait acquisition is required. The mechanisms controlling the loss of E-Cadherin are the most studied in EMT regulation. The transcription factors SNAIL1, SNAIL2 (SLUG), ZEB1, ZEB2, and TWIST1 bind to the *E-Cadherin* promoter and represses transcription of this gene (Cano et al., 2000; Comijn et al., 2001; Eger et al., 2005; Hajra et al., 2002; Vesuna et al., 2008; Yang et al., 2004). These EMT promoting transcription factors also have additional roles beyond repression of E-Cadherin. SNAIL1 also directly represses claudins and Occludin expression (Ikenouchi et al., 2003). Additionally, ZEB2 is able to regulate genes crucial to formation of tight junctions, desmosomes and gap junctions, such as *P-Cadherin*, *Claudin 4*, *Tight junction protein 3* (*ZO-3*), *Plakophilin 2*, *Desmoplakin*, *Connexin 26* (*GJB2*) and *Connexin 31* (*GJB3*) (Vandewalle et al., 2005). The EMT inducing transcription factors are regulated

by a variety of signaling pathways (including TGFβ, Wnt, and FGF, among many others) that can work in a cooperative manner to orchestrate the EMT process (Gonzalez and Medici, 2014; Moustakas and Heldin, 2007).

The EMT process is divided into three main types, developmental, wound healing and fibrosis, and metastasis (Zeisberg and Neilson, 2009). Since this dissertation focuses on mechanisms involved on early lineage commitment, only the developmental variety of EMT will be discussed. The first noted post-implantation example of EMT is during the formation of the early mesoderm and endoderm during gastrulation (Viebahn, 1995). A subset of cells from the epiblast/primitive ectoderm, which arose from the inner cell mass of the embryo, moves to the embryo's midline to form the primitive streak along the anterior-posterior axis. These cells undergo EMT and move inward to generate mesoderm and endoderm, while those remaining in the epiblast become ectoderm (Acloque et al., 2009). Further waves of EMT occur as development progresses, including the formation of the neural crest, cardiac valve, and the secondary palate (Duband et al., 1995; Yang and Weinberg, 2008). Several studies have shown that early developmental EMT events can be recapitulated during hESCs differentiation, specifically in regard to mesendodermal lineages (D'Amour et al., 2005; Eastham et al., 2007; Evseenko, 2010).

CHAPTER II. Lineage-Specific Early Differentiation of Human Embryonic Stem Cells Requires a G2 Cell Cycle Pause

2.1 Introduction

In this chapter, we investigated the link between cell cycle progression and early differentiation using monolayer hESC cultures. Unexpectedly, we observed a cell cycle pause in G2 during differentiation to several lineages that was regulated by WEE1. When WEE1 was inhibited, this cell cycle pause was disrupted, and lineage determinant gene expression was compromised. These findings provide a novel mechanistic dimension to functional relationships between control of proliferation and induction of phenotype.

A large portion of this chapter comes from the published work:

VanOudenhove JJ, Grandy RA, Ghule PN, del Rio R, Lian JB, Stein JL, Zaidi SK, Stein, GS. Lineage-Specific Early Differentiation of Human Embryonic Stem Cells Requires a G2 Cell Cycle Pause. *Stem Cells.* [Epub ahead of print]. PMID: 26946228

All data and figures in this chapter were obtained/created by Jennifer J. VanOudenhove, with the exception of the raw FACS data was collected on the LSRII and the ModFit analysis of FACS data was performed by Dr. Roxanna del Rio in the Flow Cytometry and Cell Sorting Facility at the University of Vermont.

2.2 Materials and Methods

2.2.1 Stem Cell Culture

The female H9 (WA09) line and the male H1 (WA01) line of hESCs were maintained on Matrigel using WiCell Research Institute (Madison, WI) Standard Operating Procedures (SOP-SH-002 or SOP-SH-004) for Feeder Independent Growth using pluripotency supporting mTeSR1 medium (Stem Cell Technologies, Vancouver, BC, Canada) or E8 medium (Life Technologies, Carlsbad, CA) respectively, and the EDTA passaging method, using a shorter (5 min) exposure to EDTA. For fetal bovine serum (FBS)-induced mesendodermal differentiation, undifferentiated monolayer hESC cultures were switched from mTeSR1 to differentiation medium containing KNOCKOUT™ Dulbecco's modified Eagle's medium (DMEM), 20% heat inactivated, defined FBS, 1mM L-glutamine with 1% v/v 2-mercaptoethanol, and 0.1 mM nonessential amino acids. For retinoic acid (RA)-induced ectodermal differentiation, undifferentiated monolayer hESC cultures were switched from E8 to differentiation medium with E6 basal medium (E8 medium without the pluripotency supporting growth factors: TGFβ1 and bFGF) and the addition of 1 μM all-trans retinoic acid. For the mesodermal differentiation protocol, undifferentiated monolayer hESC cultures were switched from E8 to differentiation medium with RPMI 1640 with B-27 supplement without insulin (Life Technologies), which is a serum free growth supporting supplement and 12 μM CHIR99021 (Selleck Chemicals S2924, Houston, TX), a GSK-3 inhibitor that activates WNT signaling (Lian et al., 2013).

For the endodermal differentiation protocol, undifferentiated monolayer hESC cultures were switched from E8 to differentiation medium with RPMI 1640 with 1X Glutamax and 100 ng/mL Activin A (R&D Systems, Minneapolis, MN). For treatment past 24h, 0.2% FBS was added (D'Amour et al., 2005).

2.2.2 Microarray Expression Analysis

RNA was extracted using Trizol Reagent (Life Technologies) according to the manufacturer's protocol. Genomic DNA was removed from isolated RNA using the Zymo DNA-Free RNA Kit, and then RNA quality was assessed using the Agilent 2100 BioAnalyzer. Fifty nanograms of RNA was used to synthesize cDNA using the GeneChip® WT PLUS Reagent Kit. The cDNA was hybridized to the Affymetrix GeneChip Human Transcriptome Array 2.0 for 16.5h overnight at 45ºC. Arrays were stained using the Affymetrix GeneChip® Fluidics Station 450 and scanned with the Affymetrix GeneChip® Scanner 3000. All target preparation and microarray hybridization/ scanning was performed in the VGN Microarray Facility at UVM. The dataset generated has been deposited in the NCBI Gene Expression Omnibus database according to MIAME guidelines with accession number GSE74004**.**

Due to evident fold change compression, Affymetrix (Santa Clara, CA) used a GC content leveling and signal space transformation to reduce background levels. Transformed CEL files were then imported into Affymetrix Expression Console Build 1.3.1.187 where the data were normalized using the default

Robust Multi-Array Average algorithm. Further analysis was performed using the Gene Level Differential Expression Analysis function available in the Affymetrix Transcriptome Analysis Console Version 1.0.0.234. Differential gene expression was defined as a fold change greater than 1.5, an ANOVA *p* value less than 0.05, and a FDR *p* value less than 0.05. Partek Genomic Suite software (St. Louis, MO) was used to generate the principal component analysis (PCA). EulerAPE version 3.0.0 was used to generate the proportional Venn Diagram and then recolored (Micallef and Rodgers, 2014). The heatmap was visualized using the heatmap.2 function in the R language package (http://www.r-project.org/). Pathway analysis was performed using QIAGEN's Ingenuity Pathways Analysis (Qiagen, Valencia, CA, www.qiagen/com/ingenuity) and Reactome – A Curated Pathway Database (http://www.reactome.org/) v53 (Croft et al., 2014; Milacic et al., 2012).

2.2.3 Quantitative Real-Time PCR Analysis

RNA was isolated as described for microarray analysis; however, cDNA was synthesized with random hexamer primers using Super Script III First Strand Synthesis System (Life Technologies Cat No. 18080-051). QRT-PCR was performed using SYBR Green PCR Master Mix (Bio-Rad, Hercules, CA) and samples were normalized to HPRT and fold change was determined using the ΔΔCt method. Primers used are as specified in Table 2.1.

Gene	Primer	Sequence
SOX17	FW	CGCACGGAATTTGAACAGTA
	REV	GGATCAGGGACCTGTCACAC
PAX6	FW	CTTTGCTTGGGAAATCCGAG
	REV	AGCCAGGTTGCGAAGAACTC
MESP1	FW	GAAGTGGTTCCTTGGCAGAC
	REV	TCCTGCTTGCCTCAAAGTGT
NESTIN	FW	GAAACAGCCATAGAGGGCAAA
	REV	TGGTTTTCCAGAGTCTTCAGTGA
GBX2	FW	GTTCCACTGCAAAAAGTACCTCT
	REV	GGGACGACGATCTTAGGGTTC
BRACHYURY	FW	TGCTTCCCTGAGACCCAGTT
	REV	GATCACTTCTTTCCTTTGCATCAAG
MIXL1	FW	GGTACCCCGACATCCACTTG
	REV	TAATCTCCGGCCTAGCCAAA
GATA4	FW	TCCAAACCAGAAAACGGAAG
	REV	GAAGGCTCTCACTGCCTGAA
AFP	FW	AAATGCGTTTCTCGTTGCTT
	REV	GCCACAGGCCAATAGTTTGT
HPRT1	FW	TGCTGACCTGCTGGATTACA
	REV	TCCCCTGTTGACTGGTCATT
WEE1	FW	ATTTCTCTGCGTGGGCAGAAG
	REV	CAAAAGGAGATCCTTCAACTCTGC
GSC	FW	GAGGAGAAAGTGGAGGTCTGGTT
	REV	CTCTGATGAGGACCGCTTCTG
FOXA2	FW	GCATTCCCAATCTTGACACGGTGA
	REV	GCCCTTGCAGCCAGAATACACATT
DDIT4	FW	TGAGGATGAACACTTGTGTGC
	REV	CCAACTGGCTAGGCATCAGC
GADD45B	FW	CGGTGGAGGAGCTTTTGGTG
	REV	CACCCGCACGATGTTGATGT
NFKB1A	FW	CTCCGAGACTTTCGAGGAAATAC
	REV	GCCATTGTAGTTGGTAGCCTTCA
OCT4	FW	GAGAAGGAGAAGCTGGAGCA
	REV	CTTCTGCTTCAGGAGCTTGG
NANOG	FW	CAGAAGGCCTCAGCACCTAC

	REV	ATTGGAAGGTTCCCAGTCG
SOX2	FW	CATGTCCCAGCACTACCAG
	REV	CTCCCATTTCCCTCGTTTTT

Table 2.1 qRT-PCR Primers used in Chapter II.

2.2.4 BrdU Incorporation Assay and Immunofluorescence (IF) Microscopy

Cells were grown on Matrigel-coated coverslips for IF time points less than 24h and grown on Matrigel-coated 35mm MatTek glass bottom dishes (MatTek P35G-1.5-14-C, Ashland, MA) for BrdU incorporation and IF longer than 24h to allow for increased adhesion to the glass. For the BrdU incorporation assay, cells were incubated for 30 min at 37ºC with 10 μM 5-Bromo-2-deoxyuridine (Roche Kit No. 11 296 736 001, Basel, Switzerland) to allow for incorporation before fixation. Fixation was performed using 3.7% formaldehyde in phosphate buffered saline (PBS) for 10 min. Cells were then permeabilized in 0.1% Triton X-100 in PBS, and washed in 0.5% bovine serum albumin in PBS. For the BrdU incorporation assay, cells were treated with DNaseI (30 μg per million cells) (BD Biosciences, Franklin Lakes, NJ) for 1h at 37ºC after permeabilzation to expose the incorporated BrdU. Detection was performed using a rabbit polyclonal BRACHYURY antibody (H-210) (Santa Cruz Biotechnology Cat. No. sc-20109, Dallas, TX), a mouse monoclonal antibody (3B10) to SOX17 (Abcam ab84990, Cambridge, MA), a mouse monoclonal anti-BrdU antibody (clone MBG 6H8 igG1 from Roche), a rabbit polyclonal Ki67 antibody (Santa Cruz Cat. No. sc-15402), or a rabbit polyclonal WEE1 antibody (Cell Signaling #4936, Danvers, MA).

Staining was performed using fluorescent secondary antibodies; for rabbit polyclonal antibodies a goat anti-rabbit IgG (H+L) secondary antibody, Alexa Fluor® 568 conjugate (Life Technologies A-11011), was used and for mouse monoclonal a F(ab')2-goat anti-mouse IgG (H+L) secondary antibody, Alexa Fluor® 647 conjugate was used (Life Technologies A-21237).

2.2.5 Proliferation and Cell Viability

For growth curves, cells were plated in 12 well plates. The next day, cells were counted and this value was taken as D0, and differentiation was initiated in half of the wells. Counting was performed at the same time daily for five additional days until confluence was reached. Cell Viability was assessed using the LIVE/DEAD® Viability/Cytotoxicity Kit for mammalian cells (Life Technologies L3224) and was performed per manufacturer's instructions, with viable cells staining green and dead cells staining red.

2.2.6 Western Blot

Whole cell lysates were generated by incubating cells in RIPA buffer for 30 min on ice, followed by sonication using a Covaris S-220 Ultrasonic Processor for 5 min. Lysates were separated in a 12% polyacrylamide gel and transferred to PVDF membranes (Millipore, Billerica, MA) using an OWL semi-dry transfer apparatus. Membranes were blocked using 1% Blotting Grade Blocker Non-Fat Dry Milk (Bio-Rad) and incubated overnight at 4°C with the following primary

antibodies: a rabbit polyclonal WEE1 (Cell Signaling #4936, 1:1000); a rabbit polyclonal to CDK1(phospho Y15) (Abcam ab47594, 1:1000); a mouse monoclonal to CDK1/Cdc2 p34(17) (Santa Cruz sc-54, 1:1000); a rabbit polyclonal to CDK2 (M2) (Santa Cruz sc-163, 1:2000); a mouse monoclonal to GAPDH (0411) (Santa Cruz sc-47724). Secondary antibodies conjugated to HRP (Santa Cruz) were used for immunodetection, along with the Clarity Western ECL Substrate (Bio-Rad) on a Chemidoc XRS+ imaging system (Bio-Rad). Relative quantification was performed using the Image Lab Software (Bio-Rad) version 5.1.

2.2.7 WEE1 Inhibition

Inhibition of WEE1 was accomplished using MK-1775 (Selleck Chemicals S1525, Munich, Germany) diluted from 10 mM/1 mL DMSO to 100 nM or Wee1 Inhibitor II (Millipore 681641), also at 100 nM. Cells were treated from initiation of differentiation to 8h, 16h, or 24h of differentiation. For differentiation longer than 24h, the inhibitor was removed after 24h of treatment.

2.2.8 Flow Cytometry Analysis

Cells analyzed by flow cytometry were fixed for 10 min in 1% formaldehyde followed by 5 min of incubation with 0.125M glycine (Sigma-Aldrich, St. Louis, MO). Then cells were permeabilized for 10 min (BD Biosciences, 51-2091KZ) before being stained for 30 min with an antibody against H3S28P (Alexa fluor

647-conjugated, BD Biosciences, 558609). Cells were then re-suspended in 2% FBS in PBS and stained with 1 µg/ml DAPI (Life Technologies D1306) for at least 30 min to determine DNA content. Flow cytometric analysis was performed using the LSRII instrument (BD Biosciences) with 640 nm laser for Alexa Fluor-647 (670/30 BP) and 355 nm laser for DAPI (440/40 BP). Compensation for AF647-DAPI was not applicable. DNA cell cycle profiles were analyzed using ModFit LT v4.1.7 software (Verity Software House, Topsham, ME). FlowJo (Ashland, OR) version 10 was used to display DNA histograms and to determine the percent of cells positive for H3S28P within the cycling cell populations.

2.2.9 Statistical Analysis

Statistically significant differences were determined using unpaired Student's *t* tests with Welch's correction unless otherwise indicated with GraphPad Prism 6 software (GraphPad Software, La Jolla, CA). In order to determine the statistical significance associated with the measured percentage of a subset within the FACS data, the precision was calculated based on the Poisson statistical distribution. This confidence value takes into account the number of events measured and the number of events in the gated population.

2.3 Results

2.3.1 Human Embryonic Stem Cells Differentiated into Mesendodermal Lineages Pause in the G2 Phase of the Cell Cycle

We investigated the relationship between cell cycle progression and early lineage commitment of hESCs by initially comparing the proliferation rates of pluripotent cells with those of hESCs that were differentiated into mesendoderm (Nishikawa et al., 1998; Tada, 2005). As previously shown (Becker et al., 2006), hESCs grown under pluripotent conditions exhibited exponential growth with a doubling time of <17h, while differentiating hESCs had a biphasic growth curve (Figure 2.1A). Notably, hESCs exhibited a longer doubling time of ~47h from days 1-3 of differentiation that by days 3-5 was reduced to ~27h, comparable to somatic diploid cells. These findings are consistent with previous studies that show a lengthening of the G1 phase after 72h of differentiation (Becker et al., 2010).

To delineate mechanisms underlying the extended doubling time, we examined the cell cycle profile of hESCs during the first three days of mesendoderm differentiation. Cell populations stained with DAPI were assessed for DNA content by fluorescence activated cell analysis (Figure 2.1B and 2.2). Undifferentiated hESCs showed approximately 50% of cells in S phase, a typical cell cycle profile for hESCs. As early as 8h after induction of differentiation, cells began to accumulate in S/G2 phases, with a decrease in the G1 population (Figure 2.1B, 2.1C and 2.2). Accumulation in G2/M continued from 12-24 h, with

the greatest number of G2/M cells observed at 16h. By 72h of differentiation, cells were distributed throughout the cell cycle and by 96h, the percentage of cells in G2/M had decreased to nearly pre-pause levels (Figure 2.2). These findings indicate that cells pause in the late S, G2 or M phase of the cell cycle during the first cell cycle of mesendodermal differentiation.

To determine the specific phase of the cell cycle when differentiating hESCs pause, we first investigated whether pausing occurs in late S or G2 phases by measuring active DNA synthesis using BrdU incorporation and immunofluorescence (IF) microscopy (Figure 2.1D). Undifferentiated hESCs had approximately 70% BrdU positive cells, which was nearly unchanged at 8h. Consistent with the DNA content profiles obtained by flow cytometry (Figure 2.1B), the percentage of BrdU positive cells was significantly decreased at 16h of differentiation, indicating fewer cells were synthesizing DNA. Furthermore, fluorescence microscopy of DAPI stained cells indicated an increase in nuclear size, a hallmark of G2 cells (Figure 2.1D). To confirm the hESCs were alive and actively proliferating, cells were evaluated using a viability stain and an antibody against Ki67, a marker of active proliferation (Figure 2.1D and 2.3). Greater than 95% of cells were proliferating and viable, as determined by positive Ki67 staining and by the presence of ubiquitous intracellular esterase activity detected by green fluorescence, respectively (Figure 2.1D and 2.3). These results exclude the possibility that the cell cycle pause is in S phase. FACS analysis using the mitotic marker H3S28P (Goto et al., 1999), along with DNA content staining,

revealed no increase in mitotic cells during the cell cycle pause (Figure 2.1E). Rather, mitotic cells decreased from 2.3% to 1.9% by 16h, concomitant with an increase in cells with 4N DNA content. Taken together these findings indicate that hESCs exhibit a G2 cell cycle pause during early differentiation towards mesendodermal lineages.

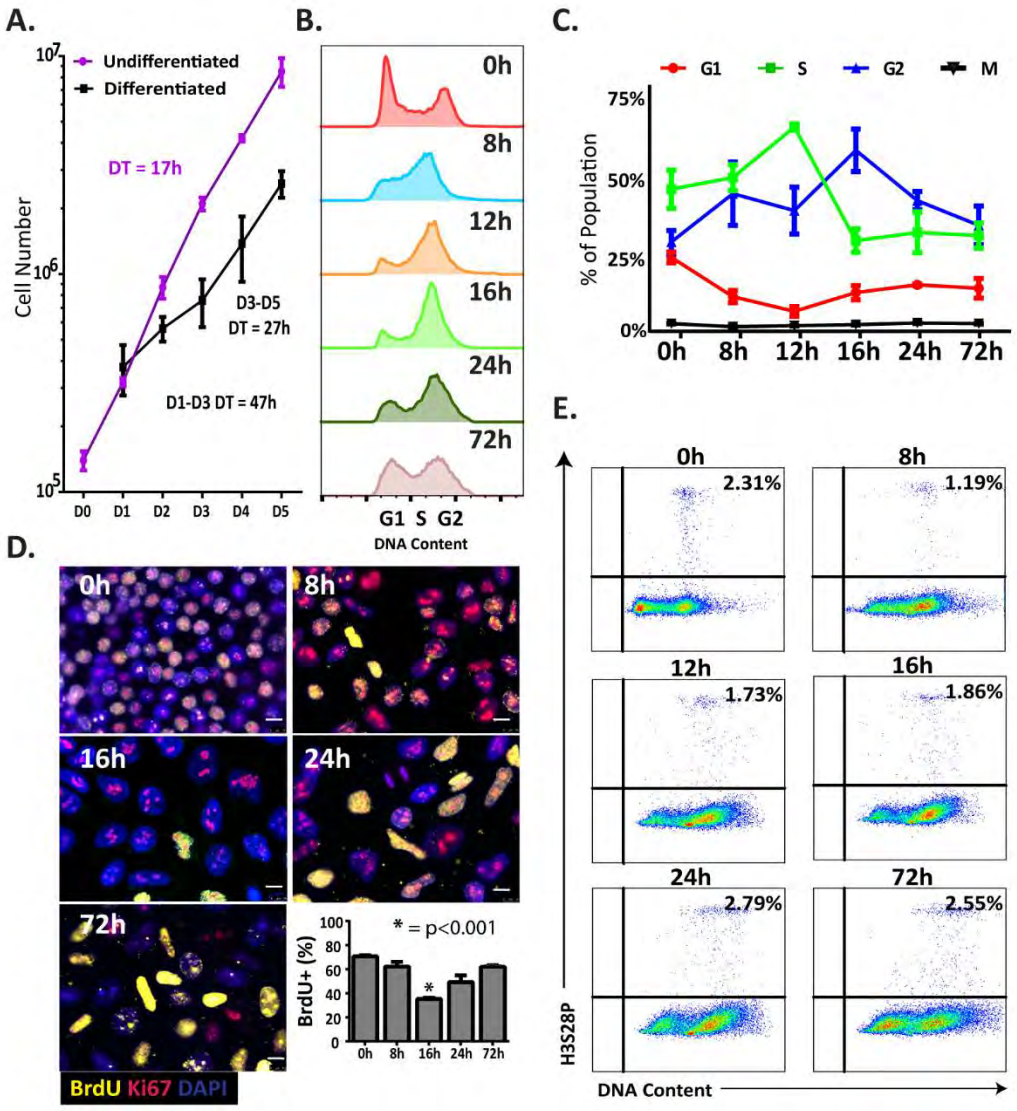

Figure 2.1. Human embryonic stem cells (hESCs) induced to differentiate into mesendoderm pause in G2. (A) Growth Curves for hESCs under pluripotent and differentiation conditions. Line graph represents mean±SD from three independent experiments each with a technical replicate (N= 6). (B) Representative flow cytometric analysis of DNA content by DAPI staining over a differentiation time course. Note the accumulation of cells in G2 between the 8h and 24h time points. (C) Percentages of cells in each phase (G1, S, G2, and Mitosis) at each time point during mesendoderm differentiation, as determined by cell cycle profile analysis using ModFit (G1, S, and G2 phases) and FlowJo (M phase, by determining the expression of H3S28P) software. Data represents mean±SD for three independent experiments (N=3). (D) Representative immunofluorescence images showing BrdU (yellow), and Ki67 (red) at time

points indicated. Nuclei are stained with DAPI (blue) (scale bars: 10 μm). Quantification of BrdU+ cells was performed using blind scoring in duplicate of 200 cells, data represents mean±SEM (*, $p < 0.001$). Significance was calculated by performing Student's *t* tests with Welch's correction between the undifferentiated state and the differentiated conditions. (E) Representative flow cytometric analysis during differentiation time course shown as H3S28P vs. DNA content with the percentage of mitotic cells indicated in the upper right corner.

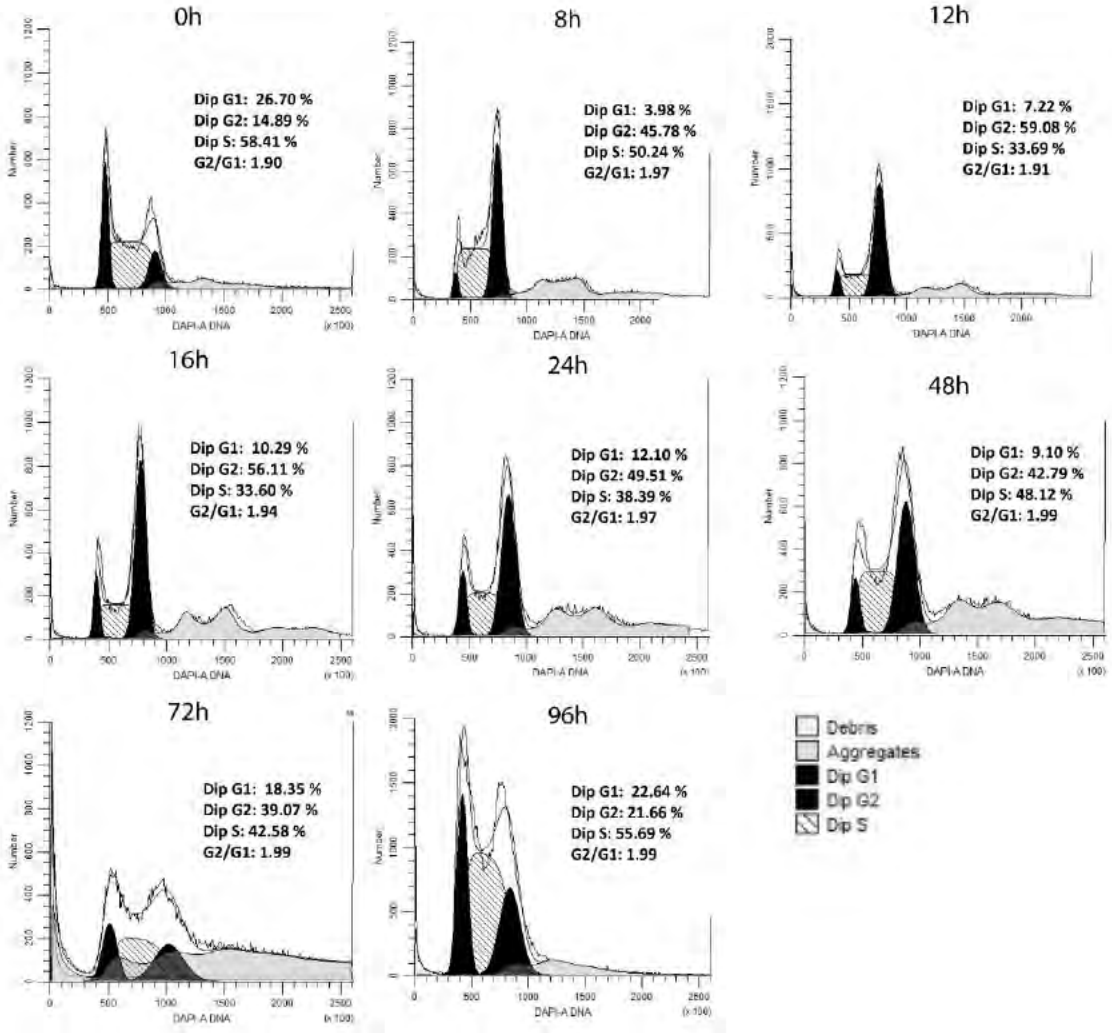

Figure 2.2. ModFit profiles across the mesendoderm differentiation time course labeled with the percentage of cells in each cell cycle phase. DNA profiles were fit using a model assuming a diploid ("Dip") cell cycle.

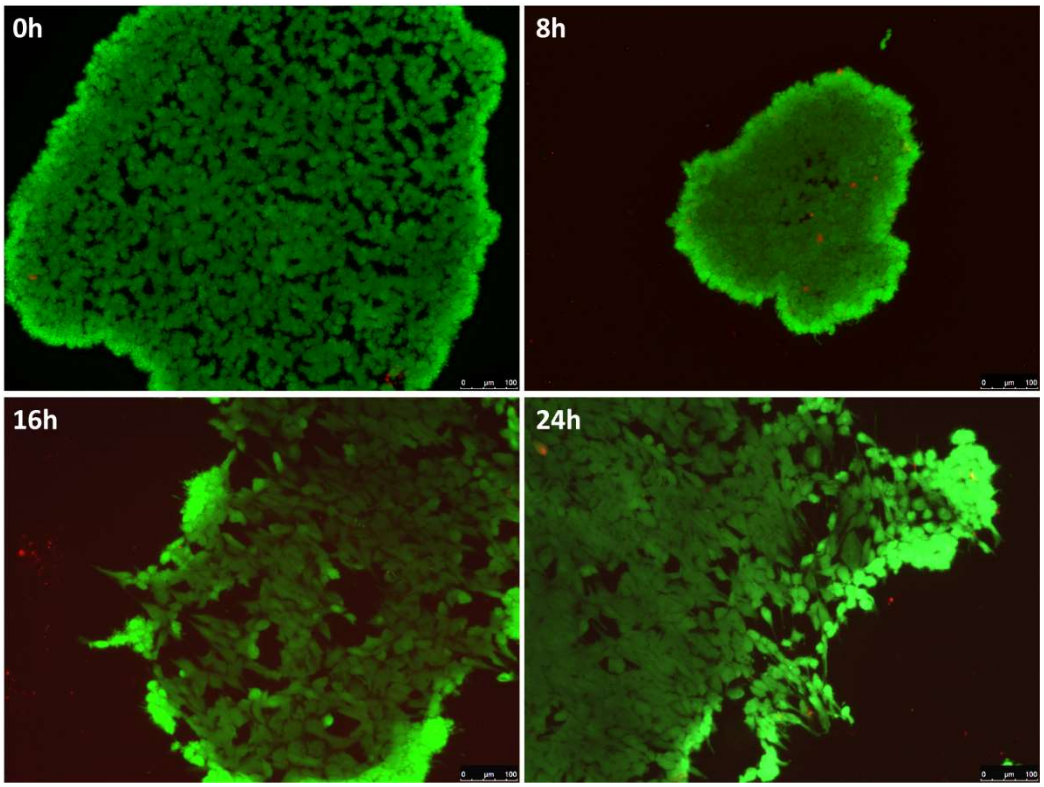

Figure 2.3. Analysis of viability during mesendoderm differentiation. LIVE/DEAD staining showing that the majority of cells attached to the plate are viable and living (scale bars indicate 100 μm).

2.3.2 Gene Expression Profiling of Early Mesendoderm Differentiation Identifies a Cluster of Differentially Expressed Genes Involved in the G2/M Transition

We examined global gene expression during early mesendoderm differentiation. Differentiation into mesendodermal lineages was confirmed by IF microscopy, and qRT-PCR for the mesoderm/primitive streak marker BRACHYURY and the endodermal marker SOX17, as well as the initiation of the decrease in pluripotency makers (Figure 2.4A, see Figure 2.5 for additional

lineage markers, and Figure 2.6 for pluripotency markers and an enlarged IF image of SOX17 staining at 72h). We performed microarray analysis at four time points (0h, 8h, 24h, 72h) with three independent biological replicates at each point. Reproducibility of the gene expression datasets is demonstrated by principal component analysis, which shows the undifferentiated hESC samples cluster away from the differentiated samples (Figure 2.4B). Bioinformatics analysis (see materials and methods for details) identified a large number of genes that were changed from 8h of differentiation onward (1080, ~27%), as well as from 24h onward (1016, ~25.5%), which indicates the progressive nature of the differentiation (Figure 2.4C).

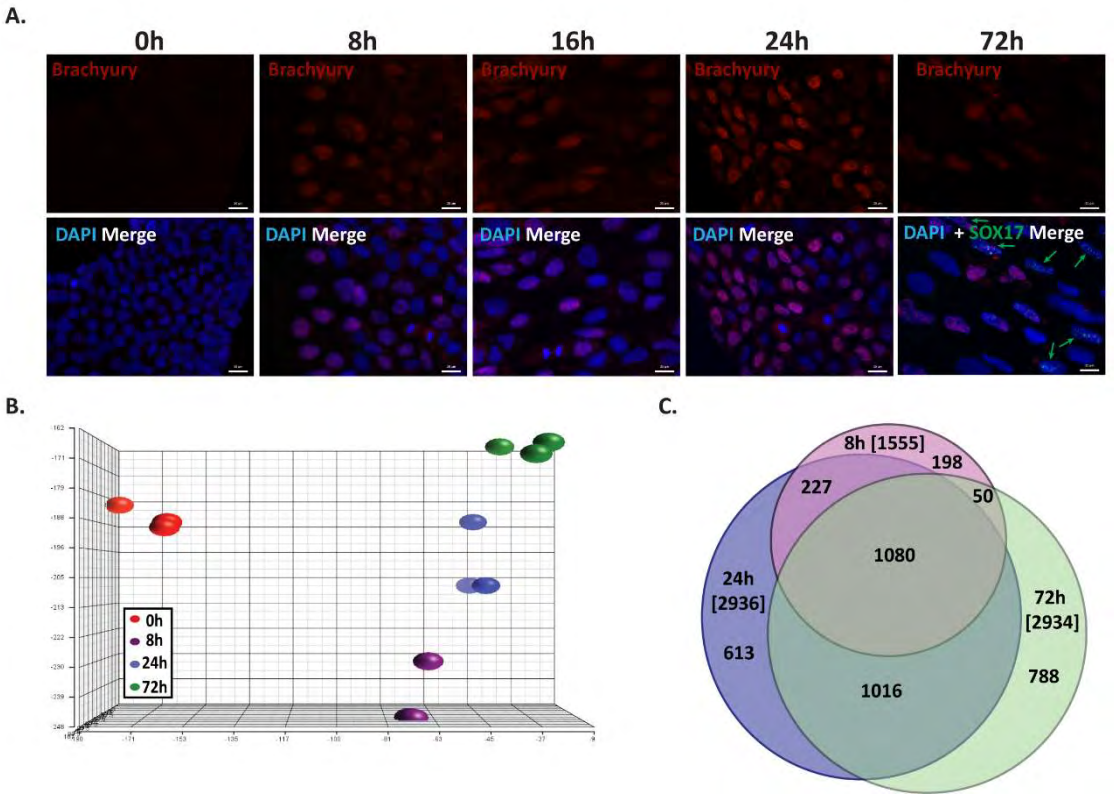

Figure 2.4. Transcriptome analysis of early differentiation into mesendoderm. (A) Representative immunofluorescence staining of BRACHYURY (red) and SOX17 (green) over a mesendodermal differentiation time course. Green arrows point to cells staining positive for SOX17, as expression is very low. Nuclei are stained with DAPI (blue) (scale bars: 20 μm). (B) Principal Component Analysis (PCA) of the time points and replicates for mesendodermal differentiation of hESCs from global expression profiling of four time points (Undifferentiated (0h), 8 hours (8h), 1 day (24h), and 3 days (72h)) (n=3) by microarray analysis. (C) Venn diagram of the number of genes with expression changes greater than 1.5 fold, and p value and FDR p values < 0.05, at each time point compared to undifferentiated hESCs. The total number of genes changed at each time point is in brackets.

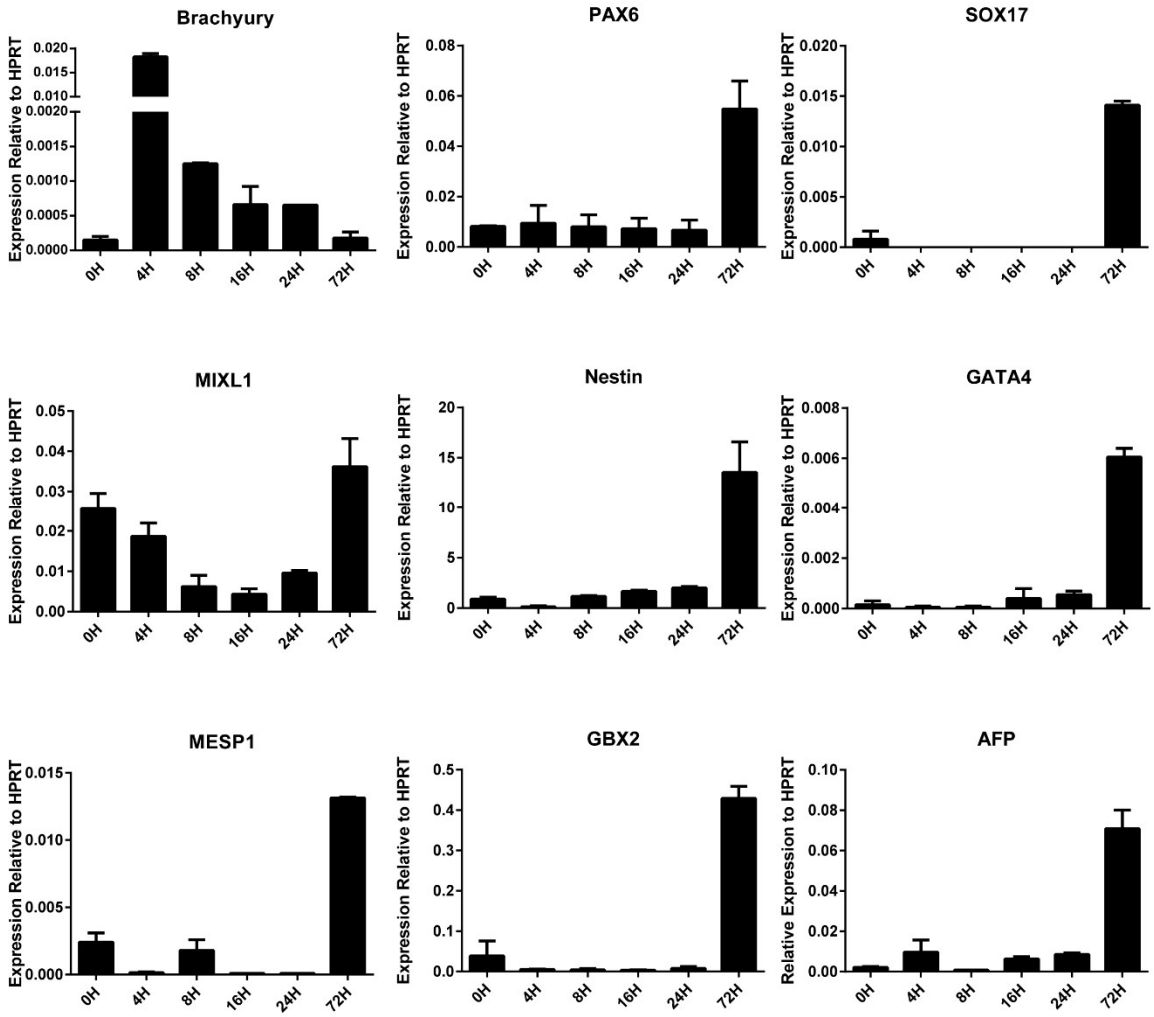

Figure 2.5. qRT-PCR panel of mesendodermal differentiation. Early mesoderm markers (BRACHYURY, MIXL1, and MESP1), early ectoderm markers (PAX6, NES, and GBX2) and early endoderm markers (SOX17, GATA4, and AFP) were used. Data represents mean±SD for four independent experiment each with a technical replicate (N=8).

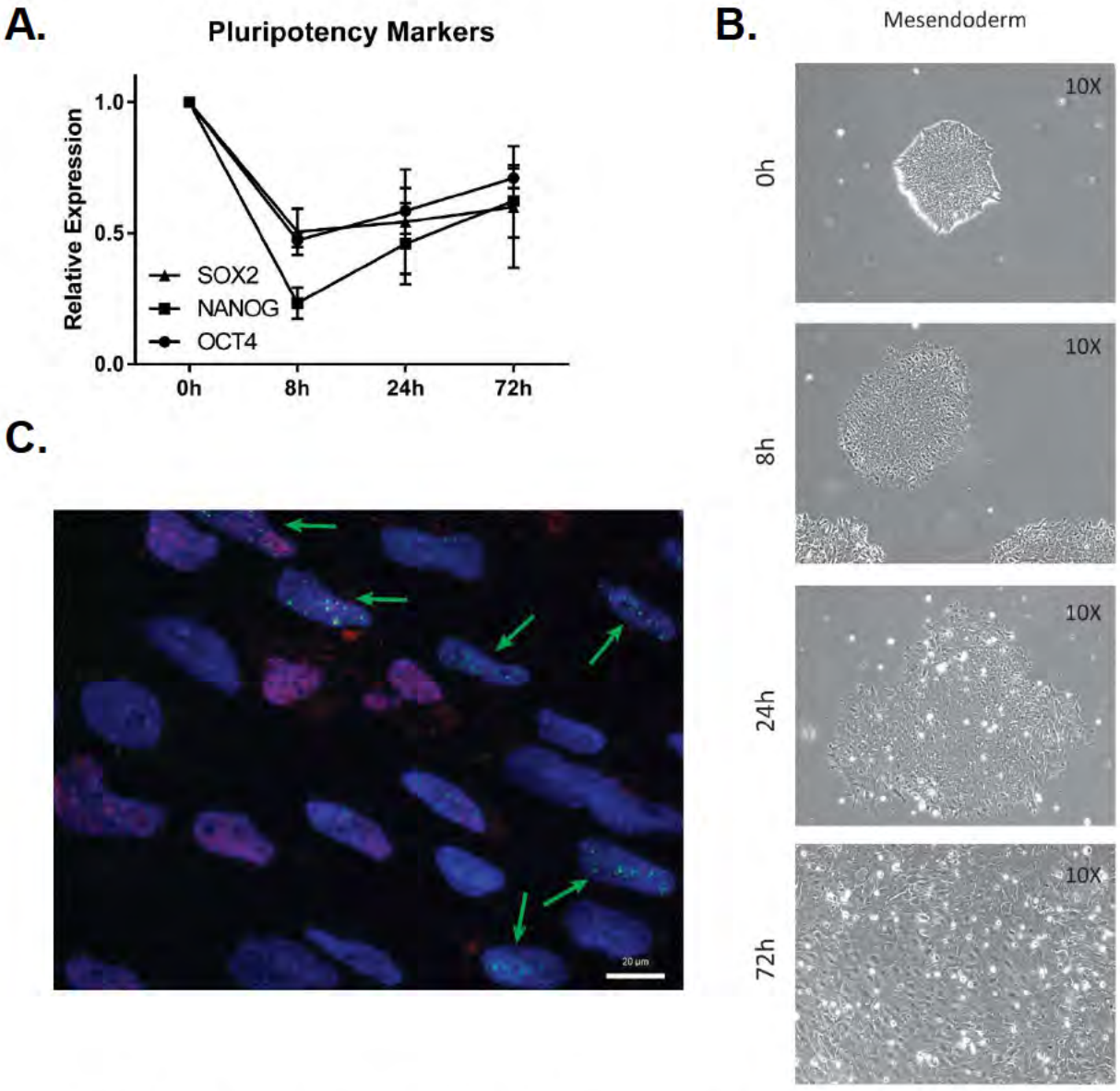

Figure 2.6. Establishment of Cell Differentiation. (A) qRT-panel of Pluripotency Markers (OCT4, NANOG, and SOX2). Line graph represents mean±SD from three independent experiments each with a technical replicate (N= 6). (B) Phase contrast images over a mesendodermal differentiation time course. (C) An enlarged immunofluorescence image of Brachyury (red) and SOX17 (green) staining at 72h from Figure 2.4. Nuclei are stained with DAPI (blue). Scale bar represents 20uM.

Hierarchical clustering revealed nine expression patterns for annotated genes that changed more than 1.5 fold and had a p value ≤ 0.05 and FDR p value ≤

0.05 at any time point relative to undifferentiated levels (Figure 2.7). We focused on gene clusters 2 and 9 that had peak expression at 8h of mesendoderm differentiation, which corresponds to the initiation of the cell cycle pause (Table 2.2). Cluster 9 contained only EGR1, an early response gene that is expressed but non-essential in early differentiation (Edwards et al., 1991; Lanoix et al., 1991; Lee et al., 1995). Reactome pathway analysis revealed that Cluster 2 had an enrichment of genes involved in the G2/M DNA replication checkpoint and in cyclin A/B1 associated events during G2/M (Table 2.3). These findings point to G2/M regulatory pathways as critical determinants of the observed G2 cell cycle pause during mesendodermal differentiation.

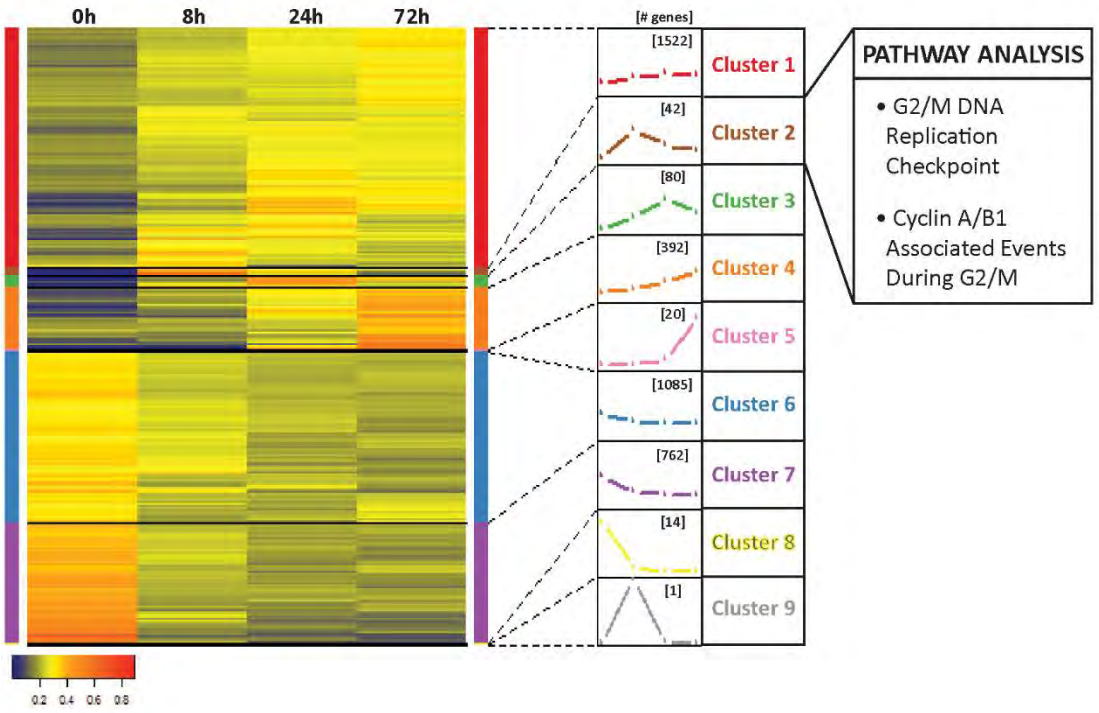

Figure 2.7. Hierarchical clustering identifies a cluster of genes involved with the G2/M transition that increases at the time of the cell cycle pause. Hierarchical clustering based on normalized expression values of four time points was performed on annotated genes whose expression levels changed greater than 1.5 fold and p value and p value FDR < 0.05 at any time point compared to undifferentiated hESCs. Nine clusters were generated with the number of genes in each cluster indicated in brackets over the trace of the expression pattern. Clusters were analyzed using Reactome and Cluster 2 was found to have enrichment in pathways involved in the G2/M transition.

ABTB2	ARAP2	CASP3	CER1	CNN1	CREB5
DDIT4	DNAJB5	EIF2AK3	ELL2	ETS2	FOSL2
ID1	IFFO2	KLF6	MIR21	MMP13	MT1A
MT1CP	MT1E	MT1F	MT1X	MT2A	NFKB1
NOG	NUAK2	PDGFB	PLAU	RHOB	SDC4
STMN4	THBS1	TNFAIP3	USP53	WEE1	ZFP36

Table 2.2. Genes in Cluster 2.

Cluster 2	
Pathway	**PValue**
G2/M DNA replication checkpoint	3.61E-04
IkBA variant leads to EDA-ID	7.04E-04
IKBKG deficiency causes anhidrotic EDA-ID	9.16E-04
NF-kB is activated and signals survival	2.38E-03
Extracellular matrix organization	3.50E-03
Polo-like kinase mediated events	3.56E-03
p75NTR signals via NF-kB	4.01E-03
Non-integrin membrane-ECM interactions	4.21E-03
Cytosolic sensors of pathogen-assoc. DNA	5.74E-03
RIP-mediated NFkB activation via ZBP1	6.03E-03
Cyclin A/B1 associated events during G2/M	6.60E-03

Table 2.3. Full pathway analysis from Reactome of Clusters 2.

2.3.3 WEE1, a G2/M Regulatory Kinase, is Up-regulated During the Cell Cycle Pause in Mesendoderm Differentiation

Ingenuity Pathway Analysis of Cluster 2 that exhibited peak expression at 8h after initiation of differentiation identified genes that are associated with cell cycle progression and the G2/M phase (Figure 2.8A). Many of these genes with known role(s) in regulating the G2 phase or the G2/M transition (*WEE1*, *GADD45B*, *DDIT4/REDD1*, and *NFKBIA/IKBA*) were highly expressed (Figure 2.8B and 2.9) (Ben Sahra et al., 2011; Mak and Kültz, 2004; McGowan and Russell, 1993; Patel et al., 2000; Vairapandi et al., 2002). The G2/M phase transition is

regulated by multiple activating and inhibitory phosphorylations of CDK1/CDC2 (Stark and Taylor, 2006; Vermeulen et al., 2003). *WEE1,* a kinase responsible for inhibitory phosphorylation of CDK1 at Y15 (McGowan and Russell, 1993), had the highest level of RNA expression during the cell cycle pause when compared to the other Cluster 2 genes (Figure 2.8B, and 2.9). WEE1 was also up-regulated on the protein level during the cell cycle pause (Figure 2.8C-D), and IF microscopy confirmed that the increased WEE1 protein was largely localized in the nucleus (Figure 2.8E), as expected (McGowan and Russell, 1995). Importantly, there was a corresponding increase in the inhibitory phosphorylation of CDK1 on Y15 during the cell cycle pause (Figure 2.8C, D). Together, these observations indicate that the increased WEE1 is functional and inhibiting progress into mitosis, and suggest a link between the cell cycle pause during early mesendoderm differentiation of hESCs and WEE1 activity.

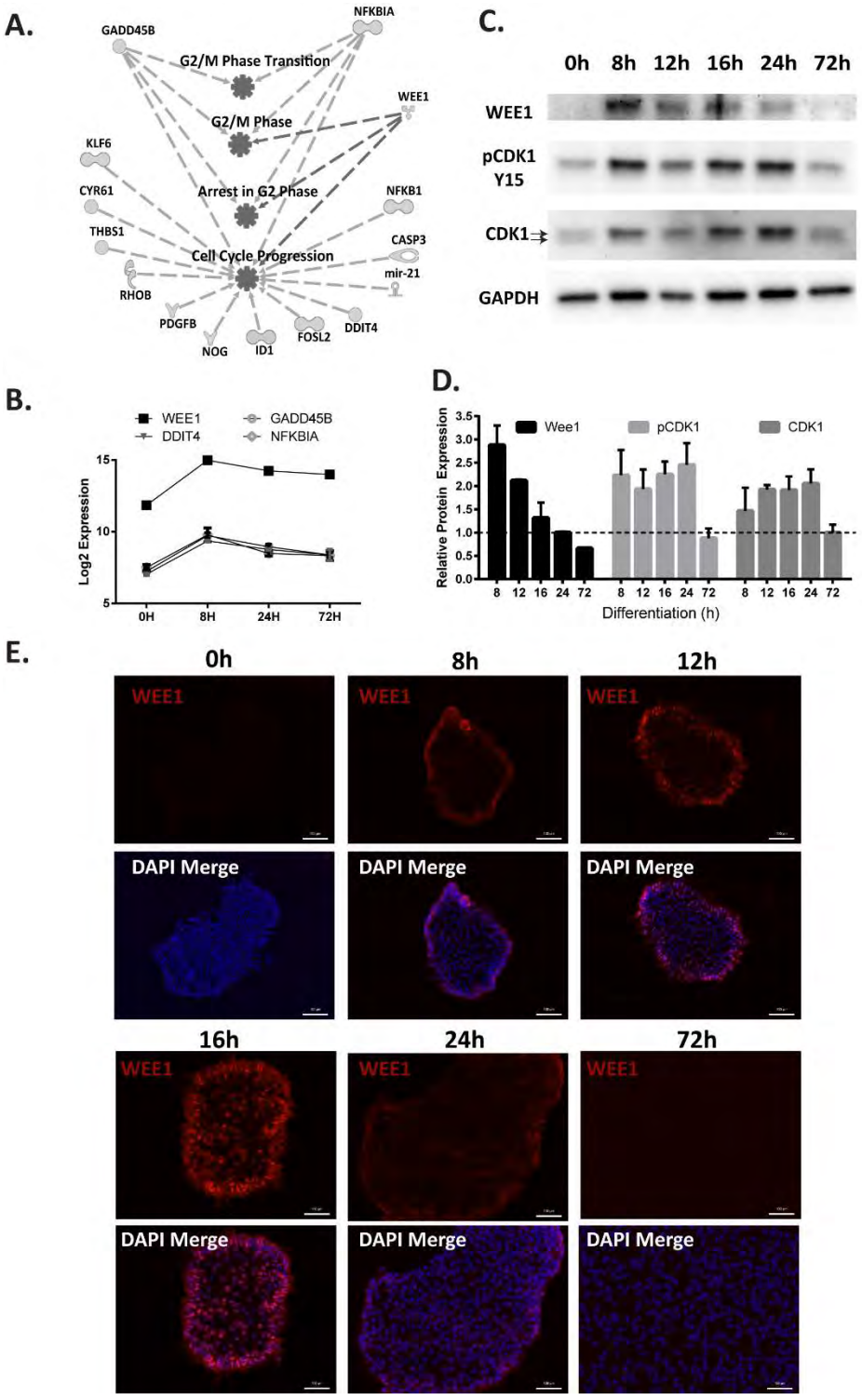

Figure 2.8. WEE1, a G2/M regulator, is up-regulated during the G2 cell cycle pause. (A) Using Ingenuity to analyze Cluster 2, genes were selected that

related to cell cycle progression/ regulation, and G2/M associated genes were mapped. (B) Expression profiles of the four known regulators of G2 phase progression. The graph shows microarray expression levels as log2 values. Data represents mean±SD from three independent experiments (N=3). (C) Representative Western blot showing the levels of WEE1, pCDK1 Y15, and CDK1 in hESCs induced to differentiate to mesendoderm. GAPDH is used as a loading control. The two arrows indicate the separation between the phosphorylated and unphosphorylated states of CDK1. (D) Quantification of Western blots represented in (C). Quantification data is the mean±SD from two independent experiments with a technical replicate of each (N=4). The dotted line is set at one, which is the initial normalized value for the undifferentiated stae. (E) Representative immunofluorescence images with WEE1 (red). Nuclei are stained with DAPI (blue) (scale bars: 100 μm).

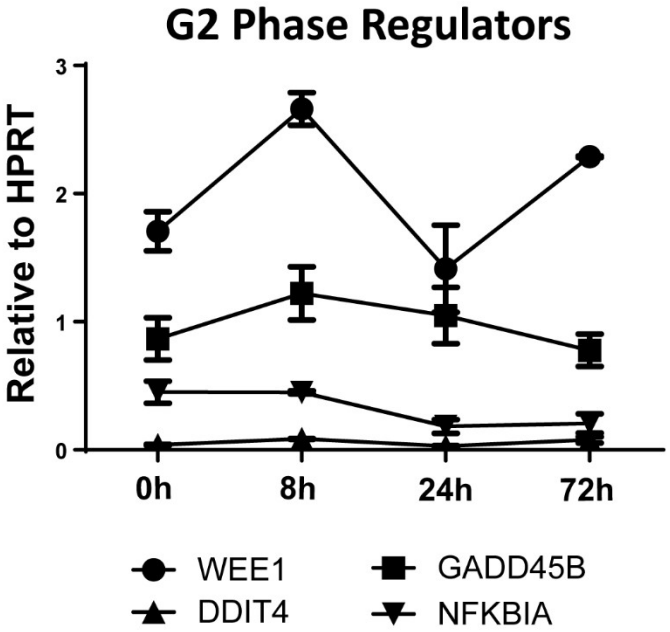

Figure 2.9. qRT-panel of G2 regulators. Confirmation of overall microarray expression levels for WEE1, DDIT4, GADD45B, and NFKBIA by qRT-PCR. Data is the mean±SD from three independent experiments with a technical replicate of each (N=6).

2.3.4 Induction of WEE1 Expression and the G2 Cell Cycle Pause Are Lineage-Specific

We investigated whether the G2 cell cycle pause is a general feature of early differentiation, or is lineage specific. Human ESCs were differentiated into

ectoderm, mesoderm, or endoderm and evaluated at 0h (undifferentiated), 8h, 16h, and 24h after induction of differentiation. Commitment to the desired lineages was confirmed by qRT-PCR on a panel of lineage-restrictive transcription factors RNAs (Figure 2.10, and see Figure 2.11 for phase contrast images of differentiation). The cell cycle distribution for each differentiation time course was quantified using flow cytometric analyses of H3S28P mitotic staining, along with DNA content (Figure 2.12A-F and 2.13). Similar to mesendodermal differentiation, we observed an accumulation of cells in G2 during endodermal differentiation, which became prominent at 16h and continued through 24h (Figure 2.12A, D). Although an enrichment of cells in G2 was seen at 16h of mesodermal differentiation, it did not extend to 24h, and involved a smaller percentage of the cells (Figure 2.12B, E). Of note, there was an increase in the percent of cells in S phase at 8h during both endodermal and mesodermal differentiation (Figure 2.12D, E). Consistent with the G2 cell cycle pause, *WEE1* RNA levels were increased at 8h in both mesodermal and endodermal differentiation (Figure 2.12G). No cell cycle stage specific accumulation or *WEE1* up-regulation was detected during ectodermal differentiation (Figure 2.12C, F, G). These findings establish that the G2 pause is lineage restricted and also reveal a correlation between *WEE1* up-regulation and the G2 cell cycle pause.

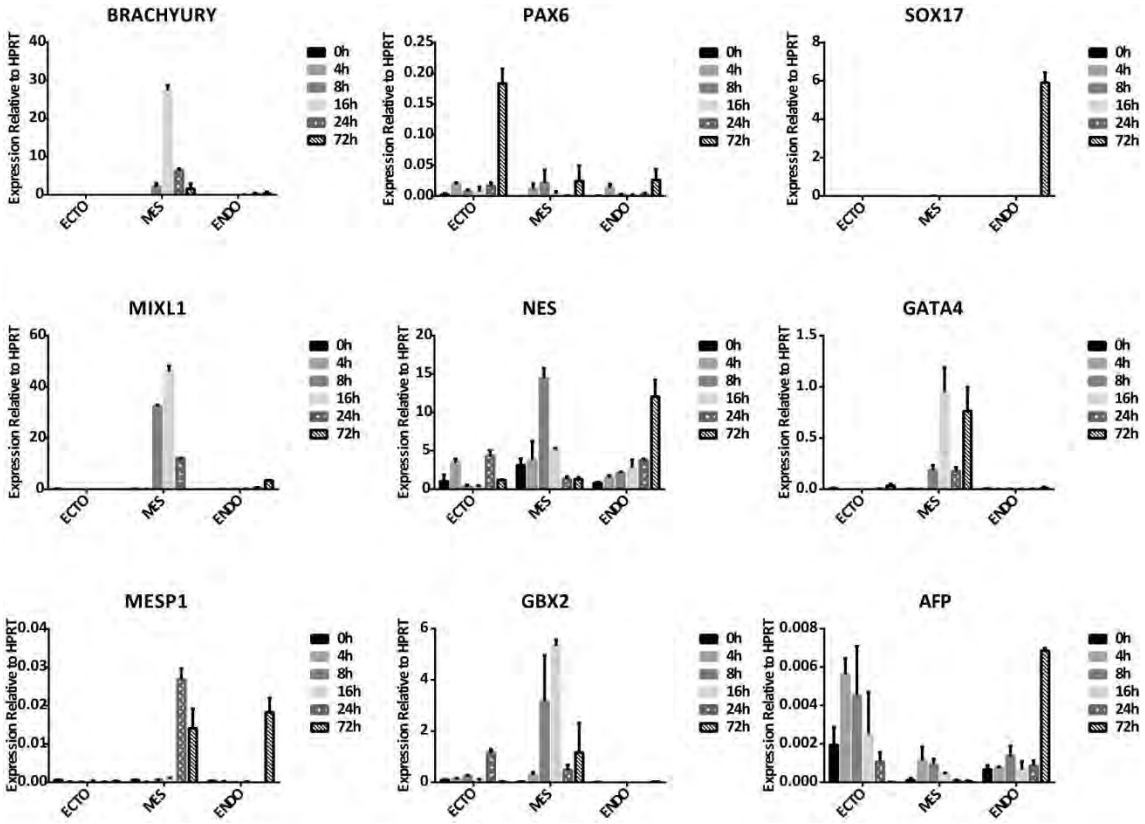

Figure 2.10. qRT-panel of differentiation directed to ectoderm, mesoderm, and endoderm. Early markers for mesoderm (BRACHYURY, MIXL1, and MESP1), ectoderm (PAX6, NES, GBX2) and endoderm (SOX17, GATA4, AFP) were examined. Data is the mean±SD from three independent experiments with a technical replicate of each (N=6).

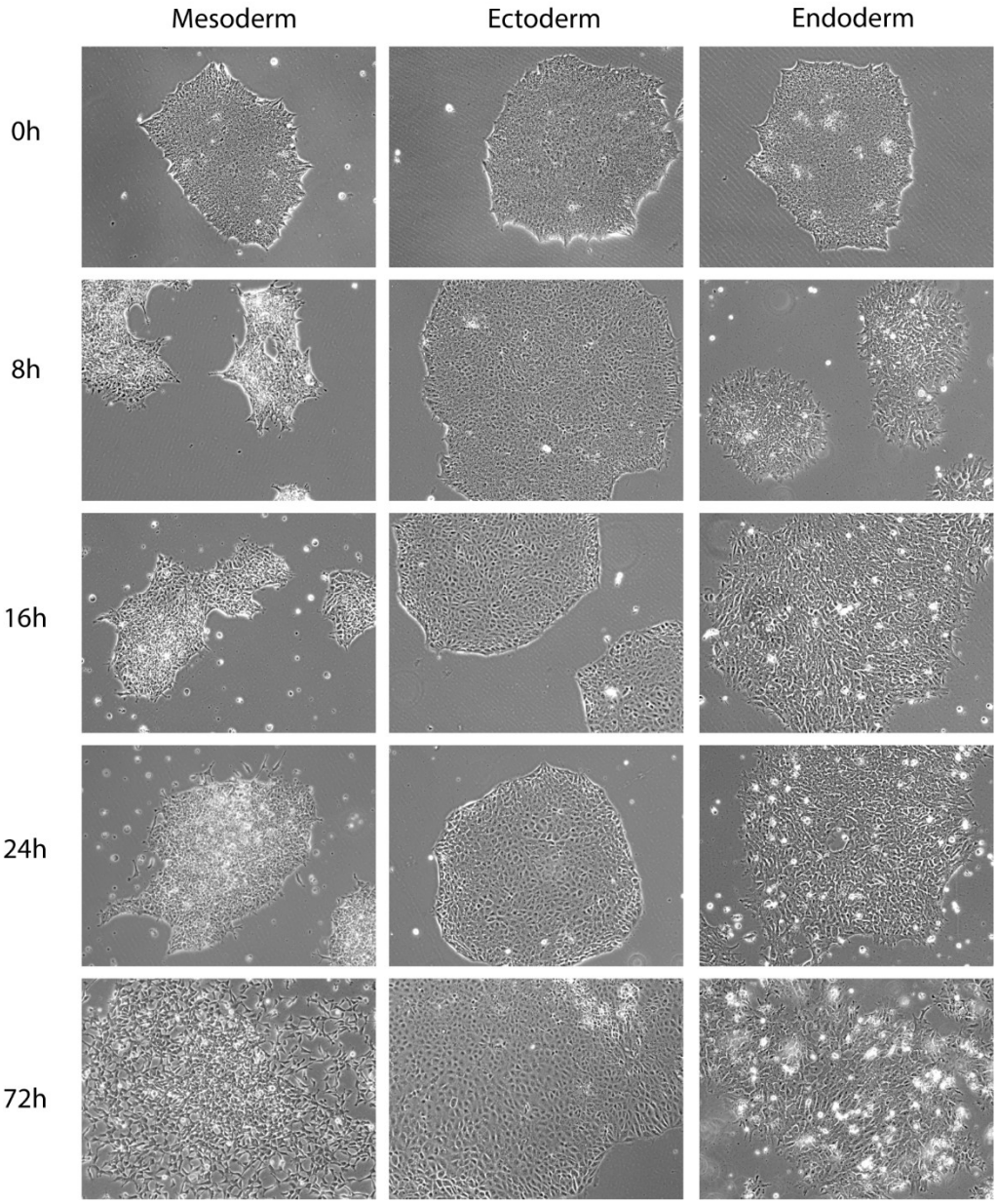

Figure 2.11. Phase Contrast images across mesoderm, ectoderm, and endoderm differentiation time courses. All images were taken at 10x magnification.

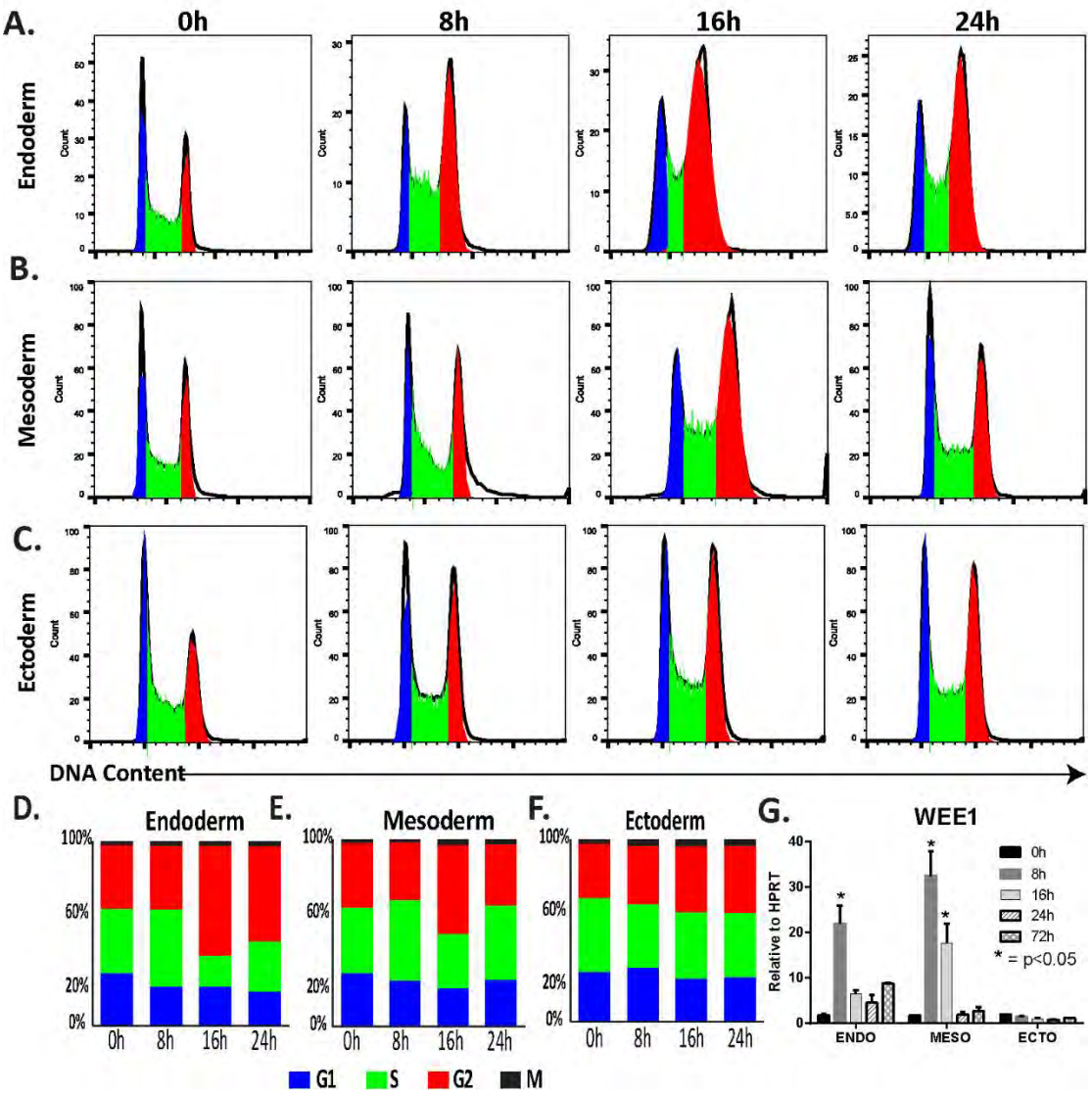

Figure 2.12. Differentiation to endoderm and mesoderm induces a cell cycle pause and expression of WEE1. (A-C) Representative flow cytometric DNA content analysis by DAPI staining across differentiation time courses to (A) Endoderm (B) Mesoderm and (C) Ectoderm. (D-F) Quantification of flow cytometric DNA content analysis by DAPI staining for differentiation to (D) Endoderm (E) Mesoderm and (F) Ectoderm, showing enrichment in the G2 population in both mesoderm and endoderm differentiation. The percentage of cells in each phase (G1, S, G2, and Mitosis) at each time point during differentiation was determined by cell cycle profile analysis using Flow Jo and ModFit. Data represents the mean of three independent experiments normalized to 100%. (G) The levels of *WEE1* normalized to HPRT, during endoderm, mesoderm, and ectoderm differentiation by qRT-PCR. A significant increase in

WEE1 expression is seen during mesoderm and endoderm differentiation. Data represented as mean±SD from three independent experiments, with a technical replicate each (N=6) (*, $p < 0.05$).

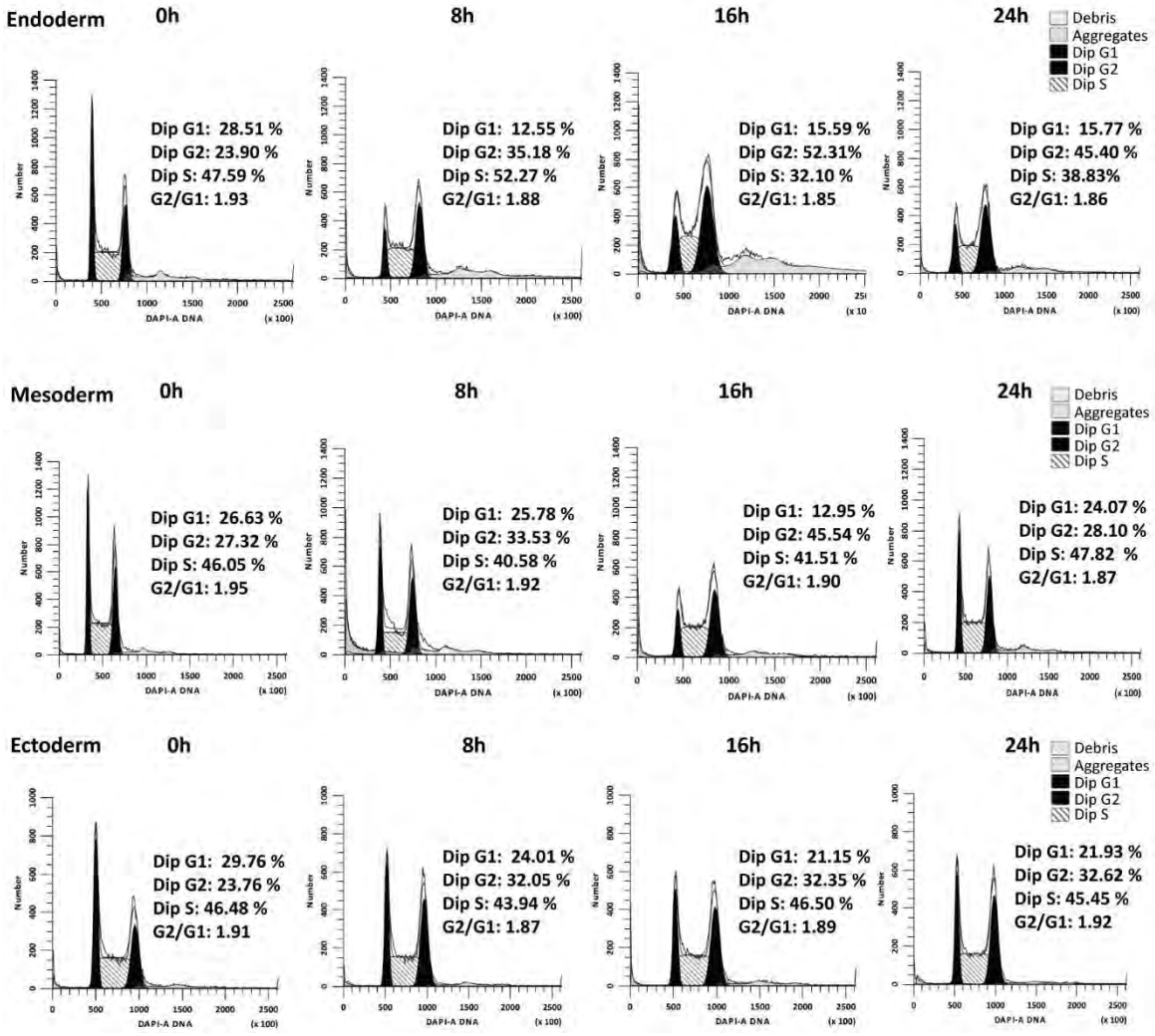

Figure 2.13. ModFit profiles across mesoderm, ectoderm, and endoderm differentiation time courses with the percentage of cells in each cell cycle phase.

2.3.5 Inhibition of WEE1-Mediated CDK1 Phosphorylation Compromises Endodermal Differentiation

To experimentally test whether WEE1 plays a functional role in the G2 cell cycle pause, we blocked the ability of WEE1 to phosphorylate Y15 of CDK1 using the WEE1 selective inhibitor MK-1775 (Guertin et al., 2013; Krajewska et al., 2013; Kreahling et al., 2012) or Wee1 Inhibitor II (Palmer et al., 2006). Inhibition of WEE1 activity by MK-1775 in cells differentiating into mesendoderm significantly increased the percentage of mitotic cells at 16h (3.69±0.15% with MK-1775 vs. 2.33±0.11% in uninhibited cells) and 24h (3.29±0.14% with MK-1775 vs. without treatment 2.31±0.11%) (Figure 2.14A). Similar results were seen with treatment with Wee1 Inhibitor II, though a larger, significant increase in mitotic cells was observed at 8h (Figure 2.15A). Importantly, in the presence of MK-1775, there was no observable enrichment of cells in G2, indicating that the cell cycle pause was prevented (Figure 2.14A and 2.16). Western blot analysis confirmed that inhibition of WEE1 activity decreased CDK1 Y15 phosphorylation (Figure 2.14B). These results demonstrate that WEE1-mediated inhibitory phosphorylation of CDK1 is a key regulatory event in the G2 cell cycle pause.

We investigated whether the WEE1-mediated cell cycle pause was necessary for lineage commitment to either mesodermal or endodermal lineages. Differentiating cells were treated with the WEE1 inhibitor and expression of lineage restrictive transcription factors was measured by qRT-PCR. During endodermal differentiation, inhibition of WEE1 activity significantly decreased the

levels of the key lineage determinants SOX17 and FOXA2 (D'Amour et al., 2005; Sulzbacher et al., 2009) by 72h (Figure 2.14C). In contrast, MK-1775 did not significantly affect expression of lineage markers during mesodermal differentiation (Figure 2.14D). These findings indicate that the cell cycle pause mediated by the WEE1-CDK1 pathway is necessary for endodermal, but not mesodermal differentiation.

Wee1 Inhibitor II had less efficacy in inhibiting WEE1, evidenced by the substantial number of cells still paused in the G2 phase at 16h and 24h (Figure 2.15A and 2.16) and the smaller decrease in CDK1 Y15 phosphorylation with treatment with inhibitor when compared with MK-1775 treatment (Figure 2.15B). However, even with this decreased efficacy, treatment with Wee1 Inhibitor II exhibited similar results to treatment with MK-1775. During directed differentiation treatment with Wee1 Inhibitor II decreased the levels of endodermal markers (though not statistically significant) and had no significant effect on mesodermal differentiation lineage marker expression (Figure 2.15C and 2.15D). These results obtained using the second WEE1 inhibitor reinforce the conclusion that the cell cycle pause mediated by the WEE1-CDK1 pathway is necessary for endodermal, but not mesodermal differentiation.

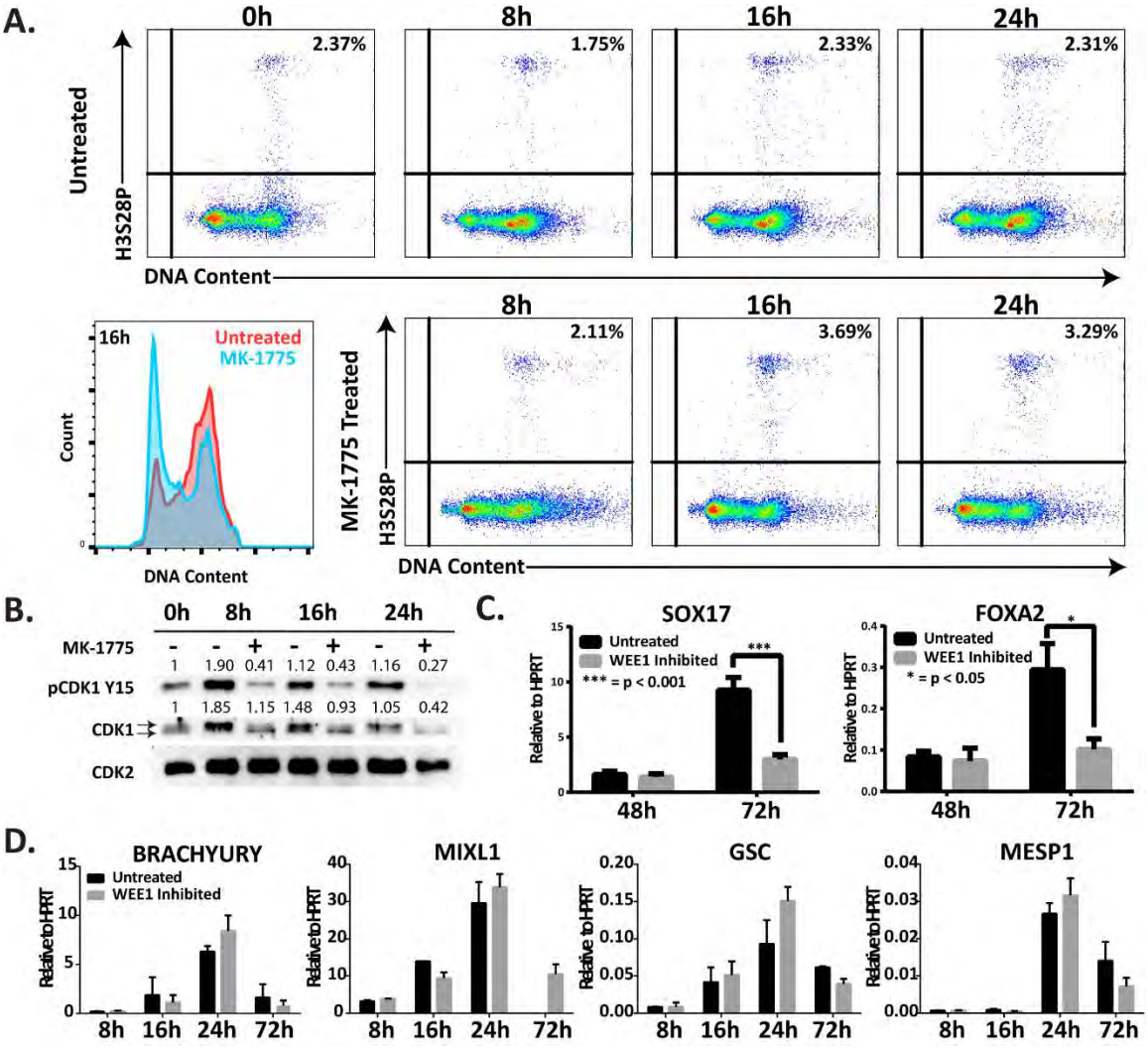

Figure 2.14. WEE1 inhibition compromises endodermal differentiation. (A) Representative flow cytometric analysis of hESCs undergoing mesendodermal differentiation treated with WEE1 inhibitor, MK-1775, shown as H3S28P vs. DNA content with the percentage of mitotic cells indicated in the upper right corner. This panel shows an increase in mitotic population with treatment with the WEE1 inhibitor at 16h and 24h. (B) Representative Western blot showing the levels of pCDK1 Y15, and CDK1 in hESCs induced to differentiate to mesendoderm with and without treatment with MK-1775. CDK2 is used as a loading control. The two arrows indicate the separation between the phosphorylated and unphosphorylated states of CDK1. The numbers above each band of the Western blot indicate the relative quantification of that band normalized to the loading control. (C) After 48h and 72h of differentiation directed to endoderm, with and without 24h treatment with MK-1775, the levels of endoderm markers *SOX17* and *FOXA2* were measured by qRT-PCR. Data represented as

mean±SD from three independent experiments, with a technical replicate each (N=6) (D) A time course of differentiation directed to mesoderm, with and without treatment with the WEE1 inhibitor MK-1775, the levels of mesoderm markers *BRACHYURY*, *MIXL1*, *GSC*, and *MESP1* were measured by qRT-PCR. qRT-PCR data shown as mean±SD from three independent experiments with a technical replicate each (N=6) (***, p < 0.001; *, p<0.05).

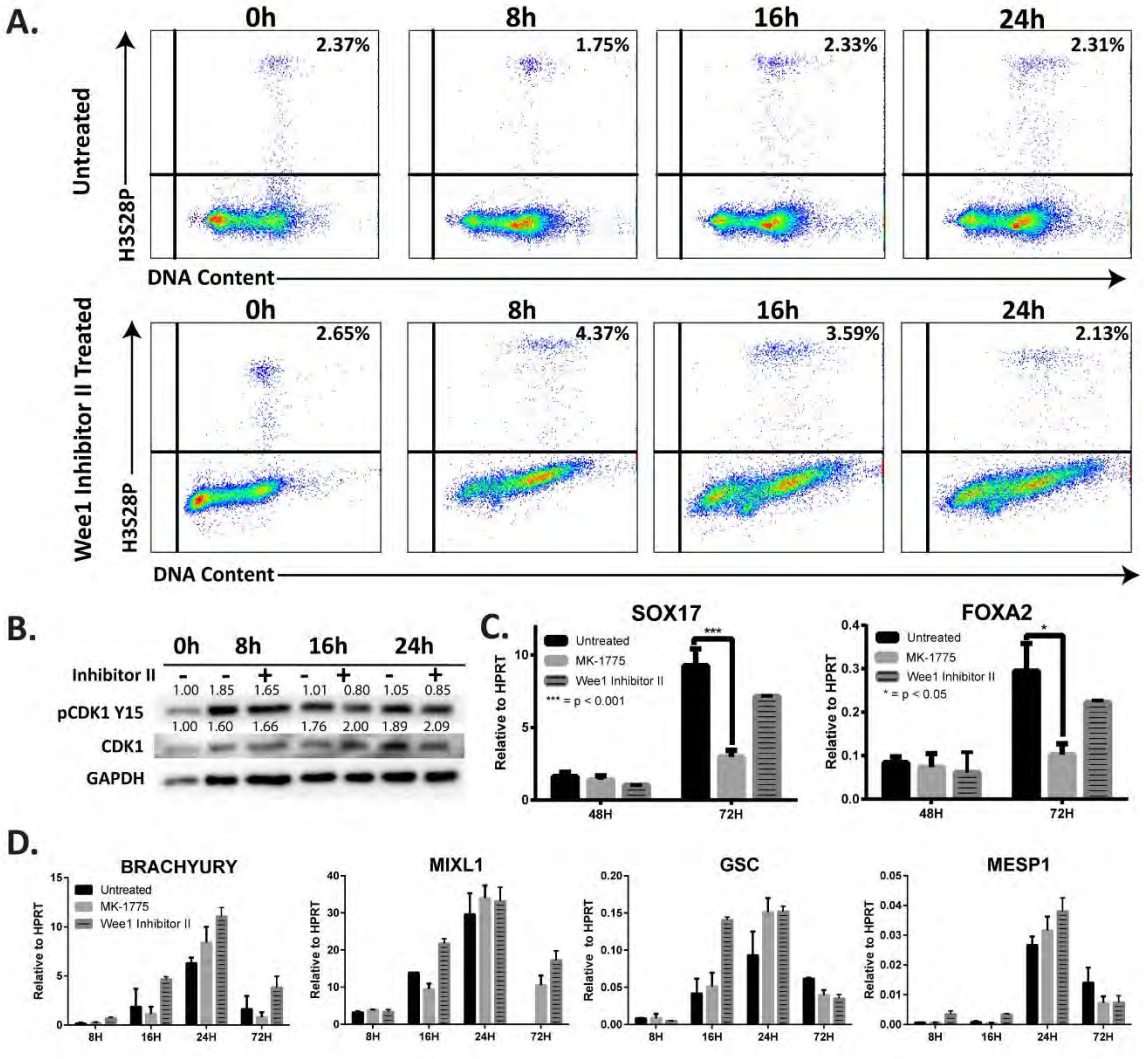

Figure 2.15. A second WEE1 inhibitor with lower efficacy show similar effects to use of MK-1775. (A) Representative flow cytometric analysis of hESCs undergoing mesendodermal differentiation either untreated or treated with WEE1 inhibitor II, shown as H3S28P vs. DNA content with the percentage of mitotic cells indicated in the upper right corner. This panel shows an increase in mitotic population with treatment with the WEE1 inhibitor at 8h and 16h. (B) Representative Western blot showing the levels of pCDK1 Y15, and CDK1 in

hESCs induced to differentiate to mesendoderm with and without treatment with Wee1 Inhibitor II. GAPDH is used as a loading control. The numbers above each band of the Western blot indicate the relative quantification of that band normalized to the loading control. (C) After 48h and 72h of differentiation directed to endoderm, with and without 24h treatment with MK-1775 or Wee1 Inhibitor II, the levels of endoderm markers *SOX17* and *FOXA2* were measured by qRT-PCR. Data represented as mean±SD from three independent experiments, with a technical replicate each (N=6) (D) A time course of differentiation directed to mesoderm, with and without treatment with the MK-1775 or WEE1 inhibitor II, the levels of mesoderm markers *BRACHYURY*, *MIXL1*, *GSC*, and *MESP1* were measured by qRT-PCR. qRT-PCR data shown as mean±SD from three independent experiments with a technical replicate each (N=6) (***, $p < 0.001$; *, $p<0.05$).

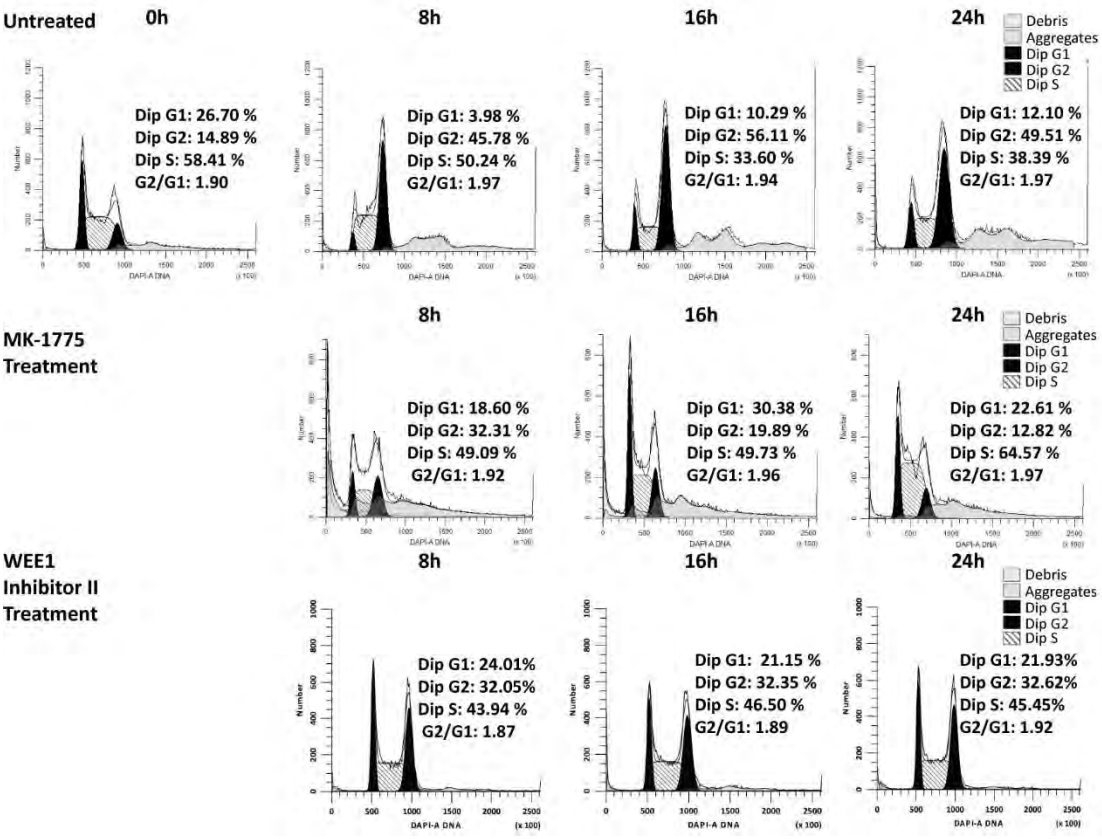

Figure 2.16. ModFit profiles across mesendoderm differentiation time courses with and without treatment of MK-1775 or the Wee1 Inhibitor II with the percentage of cells in each cell cycle phase.

2.4 Discussion for Chapter II

In this chapter we have discovered mechanistic underpinnings linking the cell cycle and early events during human embryonic stem cell differentiation. Our findings identify a novel G2 cell cycle pause in early differentiation of human embryonic stem cells. This G2 pause is mediated by Y15 CDK1 phosphorylation due to an increase in the WEE1 kinase. Up-regulation of WEE1 and the cell cycle pause are observed during differentiation to both endodermal and mesodermal lineages, but only endoderm specification is compromised upon WEE inhibition (Figure 2.17). By 72 hours of differentiation the levels of WEE1 begin to decrease, as does the amount of inactivating phosphorylation on CDK1 Y15 (Figure 2.8C-E), and the number of cells paused in G2 (Figure 2.1). This allows the balance between the opposing forces of the inactivating phosphorylation of WEE1 and the activing de-phosphorylation by CDC25 to return to normal, and allows cells to begin to progress more regularly through the cell cycle. We conclude that there is a WEE1-mediated cell cycle pause in G2 that when disrupted, selectively compromises lineage commitment to endoderm.

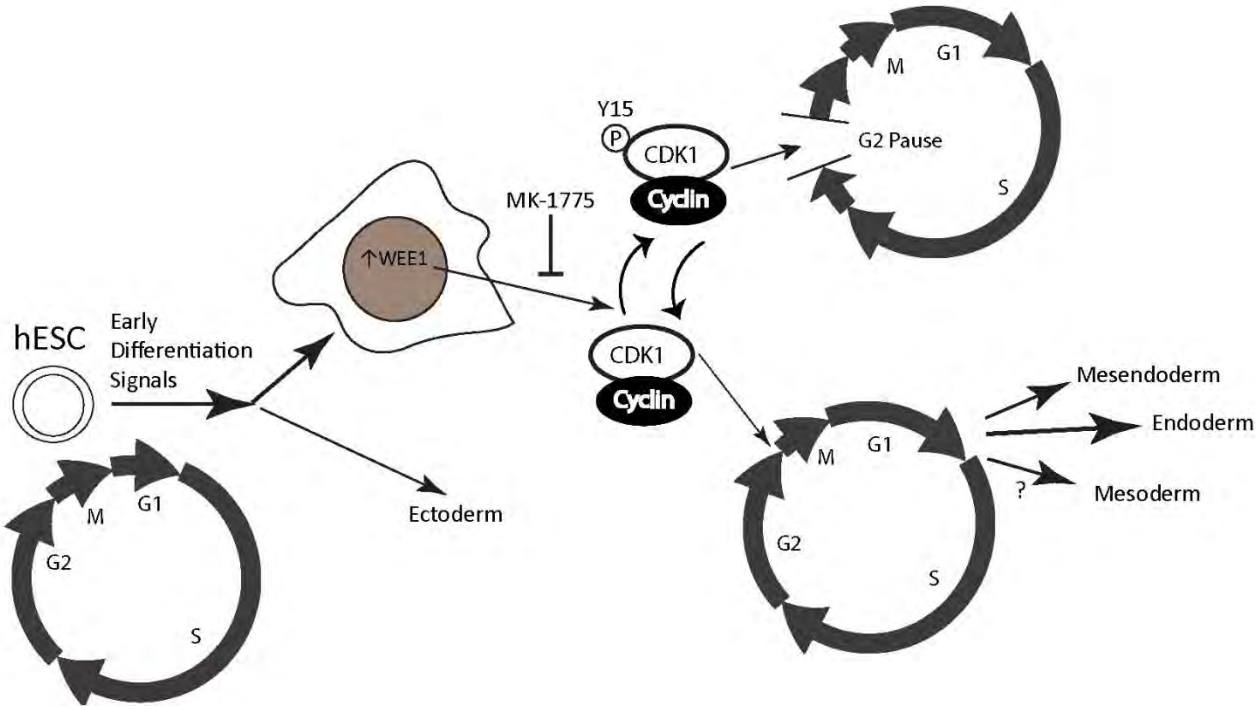

Figure 2.17. A summary model showing our finding of a novel G2 cell cycle pause.

Recent studies have focused on the role of the G1 phase in promoting differentiation of hESC (Pauklin and Vallier, 2013; Sela et al., 2012). Gonzalez et al examined pluripotent state dissolution and retinoic acid induced differentiation and found that the S and G2 phases of the cell cycle have intrinsic functions in pluripotent state maintenance (Gonzales et al., 2015). Our results have uncovered a previously unknown role for G2 events in regulating cell fate determination during the first cell cycle after induction of differentiation, and reveal that multiple mechanisms link cell cycle control to differentiation. The very early G2 pause we observed may function as a transition point between active maintenance of pluripotency and the incorporation of differentiation cues before

commitment to lineage determination. This could be beneficial to the cells to prevent premature or unintended differentiation. At a cellular mechanistic level, this G2 cell cycle pause could also be required to establish competency for chromatin rearrangement or movement of nuclear factors necessary for mediating differentiation. This could be tested by looking at the accessibility of chromatin, histone modifications, and binding of factors around the promoters of SOX17 and FOXA2 after directed differentiation to each of three germ layers in the presence and absence of a WEE1 inhibitor to see if there is a requirement for the G2 pause to obtain a certain permissive chromatin state.

Fifteen of the 42 genes that were up-regulated during the early stages of the cell cycle pause are involved in regulation of G2 or cell cycle progression. *WEE1*, the most highly up-regulated of these genes, and its phosphorylation of CDK1 Y15 provide compelling functional linkage between the cell cycle and competency for lineage commitment. Our findings that additional genes are up-regulated at the cell cycle pause suggest that other mechanisms may be operative at the G2/M transition during early differentiation. It remains to be determined whether these genes are upstream of WEE1 or function coordinately with WEE1.

The conclusions reached in this chapter regarding WEE1 inhibition preventing the G2 cell cycle pause that compromised endodermal differentiation could be strengthened by use of another WEE1 inhibitor that efficiently prevented the phosphorylation of CDK1 at Y15. Unfortunately, beyond MK-1775, there are not

well published selective inhibitors of WEE1 that are commercially available. An alternate strategy to further strengthen the evidence for the role of WEE1 in the G2 cell pause would be to knock down the WEE1 protein. One concern with knocking down the WEE1 protein would be that it would be more disruptive than only inhibiting the specific Y15 phosphorylation of CDK1. WEE1 may have additional roles in the cell, as the defects in WEE1 deficient cells were more serious than in cells with other defects in the G2/M checkpoint (Tominaga et al., 2006). A second concern would be that in order to have WEE1 levels reduced before the 8h point of differentiation, WEE1 would have to be knocked down in pluripotent hESCs; however, when pluripotent hESCs were treated with MK-1775 an extremely high level of cell death was observed. Additionally, RNAi approaches carry inherent limitations that include transfection efficiency (especially in hESCs) and off target effects. Similarly, mutating the Y15 residue of CDK1 to prevent phosphorylation with gene editing technology would have to be done in undifferentiated cells, prior to differentiation and by the time differentiation could be initiated, effects would be already accumulating.

From a physiological standpoint, the up-regulation of WEE1 and the G2 cell cycle pause are lineage restricted. Although WEE1 up-regulation occurs during commitment to both endodermal and mesodermal lineages, only differentiation to endoderm was compromised when WEE1 activity was inhibited. Neither the G2 pause nor increased WEE1 was observed in ectodermal differentiation. This lineage restricted cell cycle pause could reflect a decision point for cell fate

determination of a bipotent progenitor with the ability to differentiate to either mesoderm or endoderm. Mesodermal differentiation may be the default pathway, because WEE1 inhibition compromises endodermal but not mesodermal differentiation.

In a broader biological context, our results may provide mechanistic insight into early events for lineage commitment that are mediated by crosstalk between regulatory components of the cell cycle and competency for initiation of phenotype. This crosstalk may be governed by selective expression of genes that control the cell cycle and those that sustain pluripotency or are permissive for the transition to developmental progression. We postulate that a G2 cell cycle pause in pluripotent cells provides a window of opportunity to reconfigure genomic and epigenetic regulatory machinery. These regulatory events permit a transition from unrestrained proliferation and suppression of lineage specific genes to restricted proliferation with physiologically responsive cell and tissue specific gene expression.

CHAPTER III. Transient RUNX1 Expression during Early Mesendodermal Differentiation of hESCs Promotes Epithelial to Mesenchymal Transition through TGFβ2 Signaling

3.1 Introduction

In this chapter, we investigated whether phenotype associated transcription factors may play an initial role in differentiation prior to their established function in specifying lineage identity. A candidate screen of phenotypic transcription factors identified RUNX1 as selectively and transiently upregulated as early as 8h during mesendodermal differentiation of hESCs. We investigated what role the early expressed phenotypic transcription factor RUNX1 might play during differentiation in addition to its known role in association with hematopoietic lineage identity.

A large portion of this chapter has been submitted for publication as:

VanOudenhove JJ, Medina, R, Ghule PN, Lian JB, Stein JL, Zaidi SK, Stein, GS. Transient RUNX1 Expression during Early Mesendodermal Differentiation of hESCs Promotes Epithelial to Mesenchymal Transition through TGFβ2 Signaling. *Submitted to Stem Cell Reports*.

All experiments were performed by Jennifer VanOudenhove, with the exception of the initially phenotypic transcription factor screen, which was performed by Ricardo Medina. All figures were created by Jennifer VanOudenhove, with the exception of 3.1A, which was created by Dr. Zaidi.

3.2 Materials and Methods

3.2.1 Stem Cell Culture

The female H9 (WA09) line and the male H1 (WA01) of hESCs were maintained on Matrigel and differentiated as previously reported (VanOudenhove et al., 2016). In short, mesendoderm differentiation was induced with Knockout DMEM, containing 20% heat inactivated Defined Fetal Bovine Serum (FBS), 1mM L-glutamine with 1% v/v 2-mercaptoethanol, and 0.1 mM nonessential amino acids. Retinoic acid (RA)-induced ectodermal differentiation was induced by the addition of 1 μM all-trans retinoic acid (Sigma-Aldrich, St. Louis, MO). The mesodermal differentiation protocol induces differentiation by introducing medium containing RPMI 1640 with B-27 supplement without insulin (Life Technologies), which is a serum free growth supporting supplement and 12 μM CHIR99021 (Selleck Chemicals S2924, Houston, TX), a GSK-3 inhibitor that activates WNT signaling. To produce endoderm, undifferentiated hESC cultures were switched to RPMI 1640 containing 1X Glutamax and 100 ng/mL Activin A (R&D Systems, Minneapolis, MN). For treatments past 24h, 0.2% FBS was added.

3.2.2 Lentiviral RNAi

H9 hESCs plated on Matrigel were transduced in 6-well plates with lentivirus carrying shRNA designed to knockdown RUNX1 (clone V2LHS_150257) or be non-silencing (Cat No. RHS4346) using the GIPZ Lentiviral RNAi System (GE, Lafayette, CO) in the presence of polybrene. After introduction of lentivirus, cells

were spun at 2000 rpm at 37ºC for 45 minutes. Selection with 1 µg/ml puromycin (Sigma-Aldrich P7255-100MG) was performed for the first three passages after infection.

3.2.3 Microarray Expression Analysis

RNA was extracted using Trizol and prepared for microarray analysis as described previously (VanOudenhove et al., 2016). All target preparation and microarray hybridization/ scanning was performed in the VGN Microarray Facility at UVM. The datasets generated have been deposited in the NCBI Gene Expression Omnibus database according to MIAME guidelines with accession numbers **GSE74004 and GSE79598.**

Due to evident fold change compression, Affymetrix (Santa Clara, CA) used a GC content leveling and signal space transformation to reduce background levels. Analysis of data was performed using Affymetrix Expression Console Build 1.3.1.187 and the Affymetrix Transcriptome Analysis Console Version 1.0.0.234. Differential gene expression was defined as a fold change greater than 1.5, an ANOVA *p* value less than 0.05, and a False Discovery Rate *p* value less than 0.05. Partek Genomic Suite software (St. Louis, MO) was used to generate the principal component analysis (PCA). EulerAPE version 3.0.0 was used to generate the proportional Venn Diagram and then recolored (Micallef and Rodgers, 2014). Pathway analysis was performed using QIAGEN's Ingenuity Pathways Analysis (Qiagen, Valencia, CA, www.qiagen/com/ingenuity). GO term

analysis was performed using DAVID (Version 6.7) (Huang et al., 2009a, 2009b). The ClueGO plug-in for Cytoscape 2.8 (Version 1.8) was used for functional grouping GO analysis (Bindea et al., 2009).

3.2.4 Quantitative Real-Time PCR Analysis

RNA was isolated as described for microarray analysis, and cDNA was synthesized with random hexamer primers using Super Script III First Strand Synthesis System (Life Technologies Cat No. 18080-051). QRT-PCR was performed using SYBR Green PCR Master Mix (Bio-Rad, Hercules, CA) and samples were normalized to HPRT and fold change was determined using the ΔΔCt method. Primers used are as specified in Table 3.1.

Gene for qPCR	Primer	Sequence
PanRUNX1	FW	AGCATGGTGGAGGTGCTG
	REV	GATGGGCAGGGTCTTGTTG
PanRUNX2	FW	ACTTCCTGTGCTCGGTGCT
	REV	CCGGAGCTCAGCAGAATAAT
PanRUNX3	FW	GAGGCTCACTCAGCACCAC
	REV	TCGGAGAATGGGTTCAGTTC
OCT4	FW	GAGAAGGAGAAGCTGGAGCA
	REV	CTTCTGCTTCAGGAGCTTGG
NANOG	FW	CAGAAGGCCTCAGCACCTAC
	REV	ATTGGAAGGTTCCCAGTCG
Brachyury (T)	FW	TGCTTCCCTGAGACCCAGTT
	REV	GATCACTTCTTTCCTTTGCATCAAG
SOX17	FW	AGCAGAATCCAGACCTGCAC
	REV	CTTGTAGTTGGGGTGGTCCT
PAX6	FW	AGACACAGCCCTCACAAACA
	REV	GCAGCATGCAGGAGTATGAG
AFP	FW	AAATGCGTTTCTCGTTGCTT
	REV	GCCACAGGCCAATAGTTTGT
MIXL1	FW	TCCAGGATCCAGGTATGGTT
	REV	AGCCAAAGGTTGGAAGGATT

MYOD	FW	CCAGGATATGGAGCTACTGTC
	REV	AACACGGGTCGTCATAGAAG
PPARγ	FW	CCTATTGACCCAGAAAGCGATT
	REV	CATTACGGAGAGATCCACGGA
HPRT1	FW	GACCAGTCAACAGGGGACAT
	REV	CCTGACCAAGGAAAGCAAAG
RUNX1a	FW	CACATGGGACAATTGTGAGG
	REV	GTACCGGGATCCATGCTAAA
RUNX1b	FW	GGCATGACAACCCTCTCTGC
	REV	GCGTCGGGGAGTAGGTGAA
RUNX1c	FW	GTTTCGCAGCGTGGTAAAAG
	REV	AAGCACTGTGGGTACGAAGG
TGFβ1	FW	CGCGTGCTAATGGTGGAAAC
	REV	GTTCAGGTACCGCTTCTCGG
TGFβ2	FW	CTTTGGATGCGGCCTATTGC
	REV	TCCAGCACAGAAGTTGGCAT
TGFβ3	FW	GGGTCCATGAACCTAAGGGC
	REV	AGGCAGATGCTTCAGGGTTC
E-Cadherin (CDH1)	FW	GGAAGTCAGTTCAGACTCCAGCC
	REV	AGGCCTTTTGACTGTAATCACACC
Occludin	FW	GCAAAGTGAATGACAAGCGGT
	REV	CTGTAACGAGGCTGCCTGAA
CLD7	FW	CCGAGGAGAGAGCACTTTGG
	REV	TGGATTTCCCTCGAACACCG
VIM	FW	AGGAAATGGCTCGTCACCTTCGTGAATA
	REV	GGAGTGTCGGTTGTTAAGAACTAGAGCT
TWIST1	FW	TGAGCAAGATTCAGACCCTCA
	REV	ATCCTCCAGACCGAGAAGG
ZEB2	FW	AAGCCAGGGACAGATCAGC
	REV	CCACACTCTGTGCATTTGAACT
SNAI 1	FW	CCAATCGGAAGCCTAACTACAG
	REV	GACAGAGTCCCAGATGAGCATT
SNAI2	FW	ACAGCGAACTGGACACACATAC
	REV	GTATCCGGAAAGAGGAGAGAGG
CD44	FW	CCATTTTGCCCTTCCATAGC
	REV	CAACCCCCAACCTCAGTGG

Table 3.1. qRT-PCR Primers used in Chapter III.

3.2.5 Immunofluorescence (IF) Microscopy and RNA FISH

Cells were grown on Matrigel-coated coverslips for IF and RNA FISH. Detection of RUNX1 protein was performed using a rabbit polyclonal RUNX1 antibody (Cell Signaling #4336, Danvers, MA). Staining was performed using a fluorescent secondary antibody to rabbit polyclonal antibodies; a goat anti-rabbit IgG (H+L) secondary antibody, Alexa Fluor® 488 conjugate (ThermoFisher Scientific Cat No. A-11001) (Waltham, MA). For RNA FISH, a RUNX1 probe was created using a BAC clone (RP11-299D9) spanning the RUNX1 gene locus, obtained from the BAC/PAC Resources at the Children's Hospital Oakland Research Institute from the RPCI-11 Human Male BAC Library (Osoegawa et al., 2001, 1998) (See Figure 3.0). The BAC clone was amplified and isolated using the QIAGEN® Large-Construct Kit, and labeled by nick translation using the DIG-Nick Translation Mix (Roche Cat No. 11745816910, Basel, Switzerland). Hybridization and detection were carried out as previously reported (Byron et al., 2013), with the addition of a pepsin digest (5 mg/ml pepsin in a 1:2000 dilution in 0.01N HCl) to allow full penetrance of probe. Hybridization occurred overnight at 37ºC. A Rhodamine anti-digoxygenin secondary antibody (Roche 11207750910) was used for signal detection. Images were taken on a Zeiss AxioImager microscope equipped with a Hamamatsu CCD camera and Metamorph imaging software.

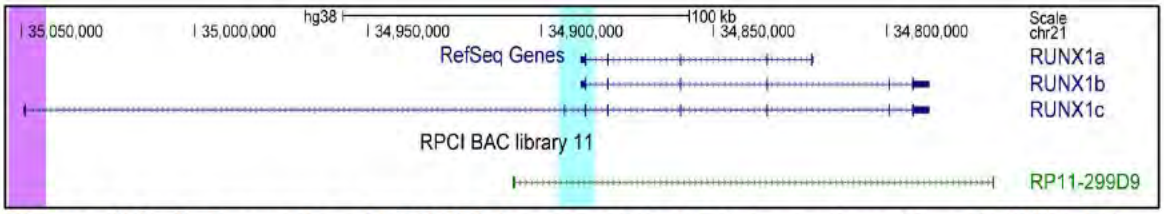

Figure 3.0. Schematic of RUNX1 Locus with BAC Location. The RUNX1 P1 promoter is highlighted in purple, where the P2 promoter is in cyan.

3.2.6 Proliferation Assays

For growth curves, cells were plated in 12 well plates. The next day, cells were counted and this value was taken as 0h, and differentiation was initiated in half the plates. Counting was performed at the same time daily for up to 120h until confluence was reached. For the BrdU incorporation assay, cells were incubated for 30 min at 37ºC with 10 µM 5-Bromo-2-deoxyuridine (Roche Kit No. 11 296 736 001) to allow for incorporation before fixation. Fixation was performed using 3.7% formaldehyde in phosphate buffered saline (PBS) for 10 min. Cells were then permeabilized in 0.1% Triton X-100 in PBS, and washed in 0.5% bovine serum albumin in PBS. For the BrdU incorporation assay, cells were treated with DNaseI (30 µg per million cells) (BD Biosciences, Franklin Lakes, NJ) for 1h at 37ºC after permeabilzation to expose the incorporated BrdU. Detection was performed using a mouse monoclonal anti-BrdU antibody (clone MBG 6H8 igG1 from Roche) and staining was performed using a mouse monoclonal F(ab')2-goat anti-mouse IgG (H+L) secondary antibody, Alexa Fluor® 647 conjugate was used (Life Technologies A-21237).

3.2.7 Western Blot

Whole cell lysates were generated by incubating cells in RIPA buffer for 30 min on ice, followed by sonication using a Covaris S-220 Ultrasonic Processor for 5 min. Lysates were separated in an 8% polyacrylamide gel and transferred to PVDF membranes (Millipore, Billerica, MA) using an OWL semi-dry transfer apparatus. Membranes were blocked using 1% Blotting Grade Blocker Non-Fat Dry Milk (Bio-Rad) and incubated overnight at 4°C with the following primary antibodies: a rabbit polyclonal RUNX1 (Cell Signaling #4334, 1:1000); a goat polyclonal to OCT3/4 (Santa Cruz sc-8628, 1:1000); a rabbit polyclonal to CDK2 (M2) (Santa Cruz sc-163, 1:2000); a mouse monoclonal to GAPDH (0411) (Santa Cruz sc-47724); a rabbit monoclonal to Smad2 (D43B4) (Cell Signaling #5339); a rabbit monoclonal to pSmad2 (Ser465/467) (138D4) (Cell Signaling #3108). Secondary antibodies conjugated to HRP (Santa Cruz) were used for immunodetection, along with the Clarity Western ECL Substrate (Bio-Rad) on a Chemidoc XRS+ imaging system (Bio-Rad).

3.2.8 TGFβ Rescues

Reintroduction of TGFβ1 (R&D Systems, 240-B) and TGFβ2 (R&D Systems, 302-B2) reconstituted in 4 mM HCl was performed at 5.0 ng/ml.

3.2.9 Scratch Assays

hESCs were plated and, 24h later, were induced to differentiate. Thirty hours into differentiation, Mitomycin C at 10 µg/ml was introduced to inhibit cell proliferation. After 48h of differentiation colonies were scratched down the center using a sterile 10µl pipette tip. Scratches were imaged by phase-contrast microscopy directly in the center of the colony, after being washed twice with medium, and marked. The scratch was imaged 18h later in the marked location. The scratch area was calculated using the Scratch Assay Analyzer plugin from MiToBo toolbox for ImageJ (Glaß et al., 2012).

3.2.10 Chromatin Immunoprecipitation

Cells after two days of mesendodermal differentiation, were cross-linked with 0.8% formaldehyde (Sigma-Aldrich) in PBS for 10 min. The cells were washed twice, and lysed in a buffer containing 0.1% sodium deoxycholate, 0.5% N-Lauroylsarcosine,1 mM EDTA, 1mM EGTA, 10 mM Tris-HCl (pH 8), and 1× protease inhibitor mixture. Lysates were sonicated to fragment chromatin DNA into ~200-800 bp pieces using a Covaris S220 Sonicator (Covaris, Woburn, MA). Lysates were switched into a buffer containing 0.1% SDS,1 mM EDTA, 50 mM HEPES (pH 7.9), 140 mM NaCl, 1% Triton X-100, and 1× protease inhibitor mixture. Sheared chromatin was used for immunoprecipitation with RUNX1 antibody (Cell Signaling #4334) or immunoglobulin G (IgG) (12-370, Millipore)

overnight at 4 °C. Subsequently, the immunoprecipitation mixture was incubated with Protein-G Dynabeads (ThermoFisher #10003D) for an additional 3h at 4 °C. Precipitated chromatin was washed with salt solutions of increasing concentration, and eluted into a buffer containing 1% SDS, and 0.1 M $NaHCO_3$. The cross-linking was reversed and DNA was recovered using the QiaQuick PCR purification kit (Qiagen #28104). Primers targeting the promoters of the listed genes that were used for qPCR are in Table 3.2.

Genes for ChIP	**Primer**	**Sequence**
TGFβ1	FW	TCTGGGGTTGCCTTCATCTA
	REV	CAGCATTTGGGAAAGGAGAG
TGFβ2	FW	AACATAGTGGATCCTGACTGCAA
	REV	TCTGGCAGATGAGGAGACTGA
RUNX1	FW	CTCCCGGGGCCTCTCATC
	REV	CGCCGGGGAGCTTAATTG

Table 3.2. ChIP qPCR Primers.

3.2.11 Statistical Analysis

Statistically significant differences were determined using unpaired Student's *t* tests with Welch's correction with GraphPad Prism 6 software (GraphPad Software, La Jolla, CA).

3.3 Results

3.3.1 RUNX1 is Transiently and Selectively Upregulated During Early Mesendodermal Differentiation of Human Embryonic Stem Cells

To investigate whether phenotype associated transcription factors play a role in early hESC differentiation prior to their established role in control of lineage identity, we screened expression of candidate transcription factors using qRT-PCR analysis. We induced mesendodermal differentiation as described in the experimental procedures, and ensured mesendodermal commitment of hESCs by evaluating the expression of known markers of mesendoderm (Mahmood and Aldahmash, 2015; Tada, 2005; VanOudenhove et al., 2016). As expected *BRACHYURY*, *MIXL1*, and *MESP1* were upregulated (Figure 3.1A). In our screen of candidate transcription factors we looked at over twenty candidates that included among others: *TDGF1, GATA4, AFP, PDGFRA, CDX2, PAX6, FGF5, SOX17, GATA6, GATA2, RUNX1, RUNX2, RUNX3, PPARγ, MYH6, MYOD, OCT4, NANOG, SOX2* (a selection are included in Figure 3.1B). We discovered *RUNX1* was the only candidate factor selectively and transiently upregulated as early as 4-8hrs following induction of differentiation (Figure 3.1B).

Different *RUNX1* isoforms (Figure 3.1C) are linked to distinct biological processes (Brady et al., 2013; Challen and Goodell, 2010; Ran et al., 2013). Importantly, the *RUNX1c* isoform, transcribed from the P1 promoter, is expressed at the time of emergence of definitive hematopoietic precursors, while *RUNX1b*, transcribed from the P2 promoter, is more widely expressed

(Sroczynska et al., 2009). Therefore, we used specific primers to examine relative levels of each RUNX1 isoform. We discovered that the *RUNX1b* isoform was the predominantly expressed transcript in two different hESC lines, the female (H9) and male (H1), during mesendodermal differentiation (Figure 3.1C).

We next examined the levels of total *RUNX1* transcripts during endodermal (D'Amour et al., 2005), mesodermal (Lian et al., 2013), and ectodermal (Tonge and Andrews, 2010) differentiation of hESCs to determine whether expression is lineage specific (Figure 3.1D). RUNX1 was expressed during both endodermal and mesodermal, but not ectodermal differentiation, confirming the mesendodermal specificity. Furthermore, RNA FISH (fluorescence in situ hybridization) revealed that >98% of colonies and >95% of cells exhibited *RUNX1* expression during mesendodermal differentiation (Figure 3.1E). The majority of cells had two nuclear foci, consistent with two sites of transcription. In agreement with the RNA expression data, there was a complete lack of *RUNX1* foci in undifferentiated hESCs (Figure 3.1E). These findings establish that *RUNX1* transcripts are transiently and selectively expressed in mesendodermal lineage commitment.

Because several post transcriptional mechanisms can prevent translation (R. J. Jackson et al., 2010), we investigated whether the *RUNX1* RNA was translated into protein. Both H1 and H9 hESC lines were subjected to early mesendodermal differentiation. Western blot analysis showed that RUNX1 protein was detectable by 12h, peaked at 48h, and decreased by 96h (Figure

3.1F). As expected, levels of the pluripotency marker OCT4 decrease during differentiation (Figure 3.1F). Since RUNX1 protein is functionally organized in punctate nuclear foci (Zeng et al., 1998, 1997), we investigated its localization using immunofluorescence (IF) microscopy (Figure 3.1G). Undifferentiated hESCs were devoid of RUNX1 protein, but robust nuclear staining was detected in >90% of cells by 48h, which corroborates the RNA expression and FISH results. Taken together, these findings demonstrate that RUNX1 upregulation is specific for early differentiation towards mesendodermal lineages.

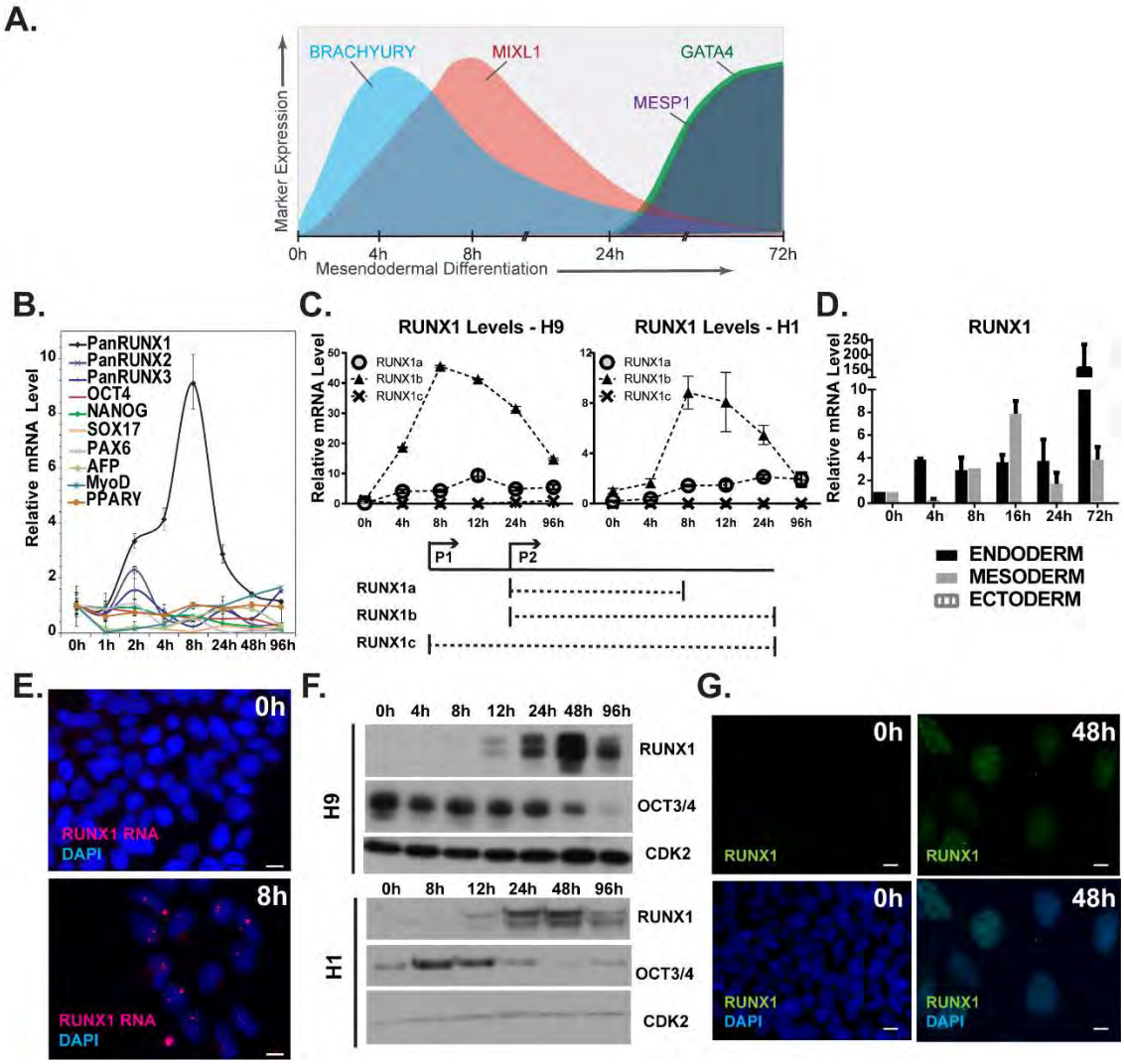

Figure 3.1. RUNX1 is transiently upregulated during early differentiation of human embryonic stem cells (hESCs) to mesendodermal lineages. (A) Diagram of gene expression profile of early mesendodermal differentiation of hESCs. (B) Relative transcript levels of select transcription factors, including the RUNX family, during early mesendodermal differentiation of hESCs. Graph represents mean±SEM from three independent experiments with a technical replicate each (N=6). (C) Relative levels of the RUNX1 isoforms in both the female (H9) and male (H1) hESCs with a schematic of different RUNX1 transcript isoforms. Graph represents mean±SEM from three independent experiments with a technical replicate each (N=6). (D) Relative levels of total RUNX1 transcript during directed differentiation to the three germ layers. No RUNX1 transcript was detected during ectoderm differentiation. Data represents the mean±SEM for three independent experiments with a technical replicate each (N=6). (E) Representative RNA FISH images showing RUNX1 RNA (red) at time

points indicated. Nuclei are stained with DAPI (blue). All images taken at 63X magnification. (F) Representative Western blot showing the transient increase in levels of RUNX1, and the decrease in OCT3/4 in the H1 and H9 hESCs during a mesendoderm differentiation time course with CDK2 used as the loading control. (G) Representative immunofluorescence images showing RUNX1 (green) nuclear staining at the time points indicated. Nuclei are stained with DAPI (blue). All images taken at 63X magnification.

3.3.2 RUNX1 Regulates Cell Motility and EMT in Differentiating hESCs

To determine the functional role of RUNX1, we performed global gene expression profiling during early mesendodermal differentiation of hESCs in which RUNX1 had been depleted (Figure 3.2A). Knockdown of RUNX1 was confirmed by Western blot (Figure 3.2B), and microarray analysis was performed on total cellular RNA from uninfected, non-silencing (shNS), and RUNX1 depleted (shRUNX1) hESCs at four time points (0h, 8h, 24h, 72h) (Figure 3.2A). Reproducibility of gene expression datasets from three independent experiments was demonstrated by principal component analysis, which shows the undifferentiated and differentiated hESC samples in distinct clusters. As differentiation progresses, shRUNX1 samples separate away from the control samples (uninfected and shNS) indicating that the depletion of RUNX1 has an effect on the differentiation, though the effect may be subtle (Figure 3.2A). Bioinformatics analyses determined that the non-silencing shRNA had very little effect on the differentiation time course. Upon RUNX1 knockdown, only a small number of genes were significantly changed (1.5-fold change with a p value ≤ 0.05 and FDR p value ≤ 0.05) by 8h of differentiation (31). The number of genes

that were changed continued to increase by 24h (334) and 72h (435) (Figure 3.2C). These observations indicate that the depletion of RUNX1 affects gene expression, and suggest a functional role for RUNX1 in early hESC differentiation.

We investigated which biological processes were altered by RUNX1 knockdown during mesendodermal differentiation. Functional grouping of Gene Ontology (GO) annotations showed that three biological processes were potentially affected: regulation of endothelial cell proliferation, smooth muscle cell migration and cell adhesion (Figure 3.2D). We experimentally addressed contributions of RUNX1 in the regulation of these processes. Proliferation was assessed by measuring growth curves of pluripotent or differentiating uninfected, shNS, or shRUNX1 hESCs (Figure 3.2E). RUNX1 depletion had no net effect on proliferation when compared with the two controls. This observation was further confirmed by measuring active DNA synthesis using BrdU incorporation (Figure 3.2F), which showed no effect of RUNX1 knockdown on the percentage of BrdU positive cells in pluripotent or differentiating hESCs.

The effect of RUNX1 on the migration of differentiating hESCs was examined by scratch closure assays (Figure 3.2G and 3.2H). The extent of scratch closure was measured 18h after scratch initiation (Figure 3.2G). Uninfected and shRNA control cells achieved ~70% closure, while the shRUNX1 cells achieved only ~40% closure (Figure 3.2H), indicating impaired migration upon RUNX1 depletion. Taken together with the lack of RUNX1 effect on proliferation, these

findings establish a role for RUNX1 in regulating migration during early mesendodermal differentiation.

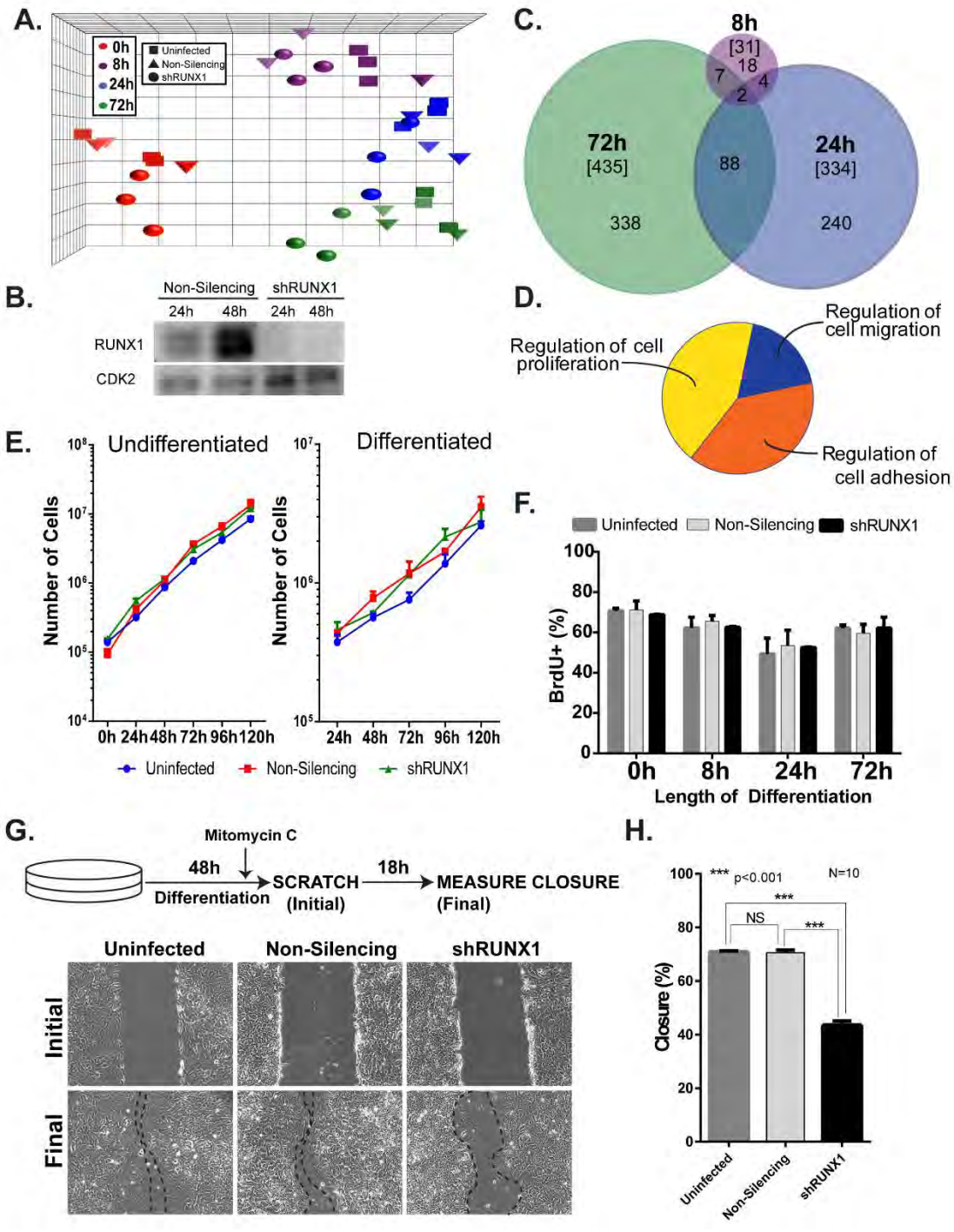

Figure 3.2. Knockdown of RUNX1 impairs the migration ability, but not the proliferation rate, of hESCs during mesendoderm differentiation. (A) Principal Component Analysis (PCA) of the time points, replicates, and treatments for mesendodermal differentiation of hESCs from transcriptome

profiling. Four time points (Undifferentiated (0h) [red], 8 hours (8h) [purple], 1 day (24h) [blue], and 3 days (72h) [green]) (n=3 replicates from independent experiments) were analyzed by microarray analysis under three different treatments (Uninfected (squares), Non-Silencing infected (triangles), and shRUNX1 (circles)). (B) Representative Western blot comparing the levels of RUNX1 in hESCs treated either with non-silencing shRNA or RUNX1 shRNA differentiating to mesendoderm, confirming that RUNX1 is knocked down in shRUNX1 hESCs. (C) Venn diagram of the number of gene with expression changes greater than 1.5 fold, and p value and FDR p values < 0.05, at each differentiation time point under shRUNX1 treatment as compared to non-silencing infected hESCs. The total number of genes changed at each time point is in brackets. (D) ClueGO analysis of genes with significant expression changes reveals three biological processes that might effected by RUNX1 knockdown. The pie represents the total genes that were grouped into all three biological process, and each slice represents the percentage of the total genes grouped to each biological process. (E) Growth curves for hESCs either uninfected(blue), non-silencing infected (red), or with shRUNX1 (green) under pluripotent and mesendoderm differentiation conditions. Line graph represents mean±SEM from three independent experiments with a technical replicate each (N=6). No statistically significant differences were found (*, $p<0.05$). (F) Percent of cells staining positive for BrdU with a 30-minute pulse of labeling. Quantification of BrdU+ cells was performed using blind scoring in duplicate of 200 cells from immunofluorescent images, data represents mean±SEM from three independent experiments. No statistically significant differences were found (*, $p<0.05$). (G) Representative phase contrast images from a scratch closure assay. Cells were plated, differentiated for 48h, after 46h of differentiation cells were treated with Mitomycin C (to inhibit proliferation) and then a scratch was made. Closure was measured 18h later. All phase contrast images were taken at 10X magnification. (H) Percentage of scratch closure for hESCs uninfected, non-silencing infected, and infected with shRUNX1, as quantitated by Image J plugin. Ten scratches were measured for each condition, and data is represented as mean±SD, (*, $p<0.001$).

Consistent with these results, GO term analysis using DAVID revealed that knockdown of RUNX1 upregulated genes involved in cell-cell adhesion and junction interactions (Figure 3.3A). Additionally, many of the top genes that are increased upon RUNX1 depletion during differentiation are associated with an epithelial-like phenotype (Figure 3.3B). These findings led us to experimentally test whether the epithelial to mesenchymal transition (EMT) was affected by loss

of RUNX1. We evaluated the expression of several epithelial (*CDH1/E-Cadherin*, *OCLN*, and *CLD7*) and mesenchymal (*VIM*, *TWIST1*, *ZEB2*, *SNAI1*, *SNAI2*, and *CD44*) marker genes across early mesendodermal differentiation in either shNS or shRUNX1 hESCs (Figure 3.4). A typical profile of cells undergoing EMT is observed in shNS hESCs, where all epithelial markers decreased and all mesenchymal markers increased during differentiation (Figure 3.4, light gray bars). However, in the absence of RUNX1, the epithelial markers decreased initially but were restored to undifferentiated levels by 72h (Figure 3.4, black bars). In contrast, the majority of mesenchymal markers were unaffected with the exception of *ZEB2*, which was not induced (Figure 3.4, black bars). Collectively these findings show that RUNX1 contributes modestly to regulation of a physiological EMT that occurs during early mesendodermal differentiation.

A.

Pathway Analysis of Up-regulated Genes

Pathway name	pValue
Cell-cell junction organization	1.30E-04
Adherens junctions interactions	3.72E-04
Cell junction organization	4.83E-04
Cell-Cell communication	2.50E-03
Conversion from APC/C:Cdc20 to APC/C:Cdh1 in late anaphase	2.62E-03
POU5F1 (OCT4), SOX2, NANOG activate genes related to proliferation	5.57E-03
RHO GTPases activate IQGAPs	5.96E-03
O-linked glycosylation	9.64E-03
Transcriptional regulation of pluripotent stem cells	1.80E-02
SCF-beta-TrCP mediated degradation of Emi1	1.94E-02

Pathway Analysis of Down-regulated Genes

Pathway name	pValue
Smooth Muscle Contraction	3.44E-08
Muscle contraction	3.10E-07
GRB7 events in ERBB2 signaling	7.89E-04
Recycling of eIF2:GDP	1.39E-03
Role of Abl in Robo-Slit signaling	1.75E-03
Downregulation of ERBB2:ERBB3 signaling	4.15E-03
RHO GTPases Activate ROCKs	6.04E-03
RHO GTPases activate CIT	6.04E-03
TALDO1 deficiency: failed conversion of SH7P, GA3P to Fru(6)P, E4P	6.74E-03
Axon guidance	6.74E-03

B.

E-Cadherin
Epithelial Splicing Regulatory Protein 1
Protocadherin gamma subfamily A, 10
Protocadherin alpha 11
Occludin
Claudin7
Protocadherin beta 5
Cadherin 9, type 2 (T1-cadherin)

Figure 3.3. GO Term Analysis. (A) Using DAVID (version 6.7) for GO term analysis the top terms upregulated are involved in cell-cell adhesion and junction interactions. (B) A majority of the top upregulated genes are directly related to maintaining an epithelial phenotype.

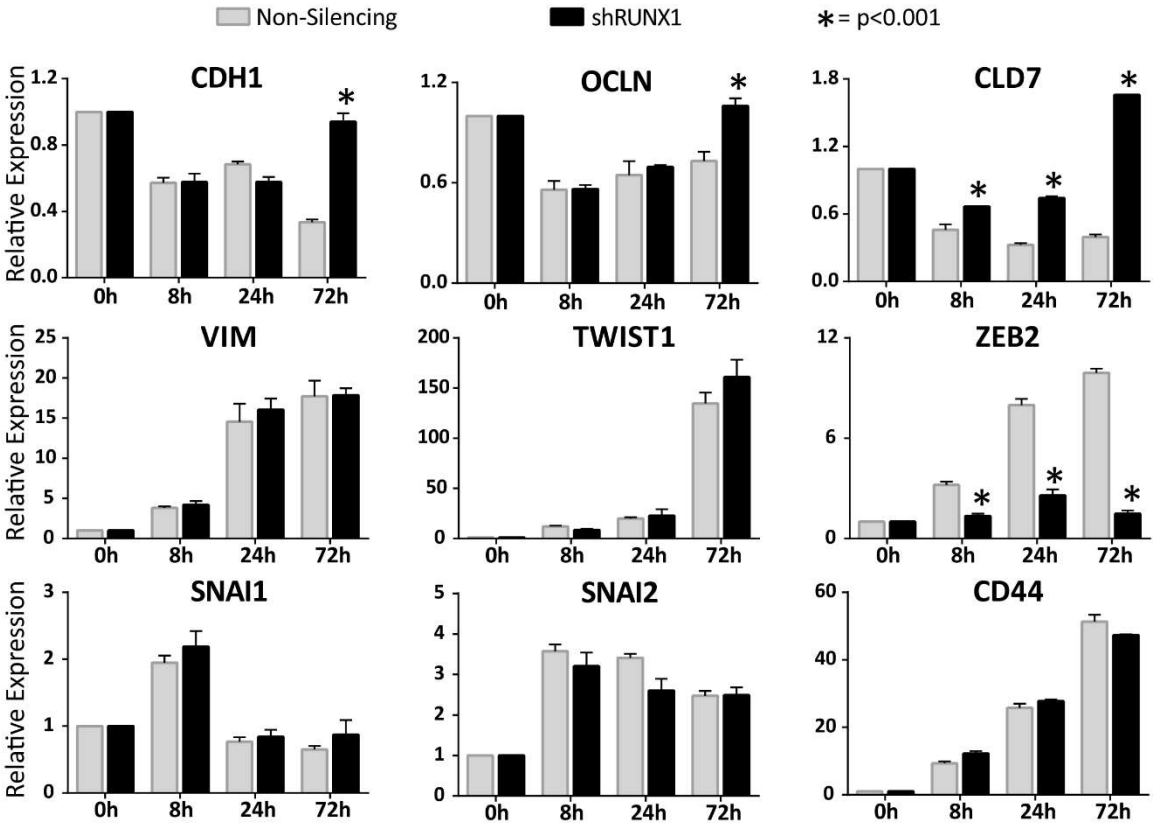

Figure 3.4. Genes that regulate the epithelial to mesenchymal transition (EMT) are effected by RUNX1 knockdown. During mesendoderm differentiation of hESCs the levels of multiple effectors of EMT (epithelial associated [*CDH1*, *OCLN*, and *CLD7*] and mesenchymal associated [*VIM, TWIST1, ZEB2, SNAI1, SNAI2, and CD44*]) were measured by qRT-PCR under treatment by non-silencing infection, or shRUNX1. During the control (Non-Silencing) differentiation epithelial marker expression decreases and mesenchymal gene expression increases. However, with shRUNX1 treatment, the epithelial marker genes fail to be suppressed and *ZEB2* is not induced. Data shown as mean±SEM from three independent experiments with a technical replicate each (N=6). P values were determined by Student's *t* tests with Welch's correction between non-silencing infected and shRUNX1 treatment at each corresponding time point (*, $p < 0.0001$).

3.3.3 RUNX1 Depletion Inhibits TGFβ2 Signaling

Because EMT is a complex process regulated by multiple signaling pathways (Derynck et al., 2014; Zhang et al., 2016), we performed signaling pathway analysis on annotated genes that changed significantly upon RUNX1 depletion (Figure 3.5A, and Table 3.3). Distinct pathways were activated by RUNX1 knockdown at each time point, although no single pathway was activated at all time points. Conversely, the TGFβ pathway was the most inhibited across the differentiation time course (Figure 3.5A, and Table 3.3), suggesting that RUNX1 activates TGFβ signaling during mesendodermal differentiation.

To directly investigate how RUNX1 regulates the TGFβ signaling pathway, we examined expression of the TGFβ ligands upon RUNX1 depletion (Figure 3.5B). *TGFβ1* and *TGFβ2* exhibited sequential and significant upregulation (>15 fold) during hESC differentiation, while *TGFβ3*, which is expressed at relatively low levels, remained unchanged. Importantly, only *TGFβ2* expression was significantly affected by RUNX1 depletion (Figure 3.5B). We also found that both *TGFβ1* and *TGFβ2*, but not *TGFβ3*, promoters contain RUNX1 consensus sites within 1 kb of the transcription start site. We tested whether RUNX1 binds to the *TGFβ* promoters using ChIP-qPCR (Figure 3.5C). Our results show that RUNX1 selectively occupies the *TGFβ2*, but not the *TGFβ1*, promoter (Figure 3.5C), which is consistent with the effect of RUNX1 depletion on *TGFβ2* expression (Figure 3.5B). As expected, RUNX1 occupied its own promoter, which was

included as a positive control (Knezevic et al., 2011). These results show that RUNX1 selectively occupies and regulates expression of the *TGFβ2* gene.

We next examined whether downstream effectors of the canonical TGFβ2 pathway were changed in the absence of RUNX1. Western blot analysis was carried out for both phospho- and total SMAD2 during mesendodermal differentiation (Figure 3.5D and Figure 3.6). In the control (non-silencing) time course, there was an increase in phospho-SMAD2 at 8h and 24h that decreased by 72h relative to total SMAD2 (Figure 3.5D, 3.6A, and 3.6B). This increase coincides with the expression of *TGFβ1 and TGFβ2* ligands (Figures 3.5B, 3.5D and 3.6). Quantitation of the ratio of phospho- to total SMAD2 revealed a decrease at 24h and 72h upon RUNX1 knockdown (Figures 3.5D, 3.5E, and 3.6B). Together, these findings show that RUNX1 is an upstream activator of TGFβ2 signaling during early mesendodermal differentiation.

A. Top Signaling Pathways Inhibited By RUNX1 Knockdown

8h			24h			72h		
Regulator	Activation z-score	p-value	Regulator	Activation z-score	p-value	Regulator	Activation z-score	p-value
TGFB1	-3.896	6.77E-06	TGFB1	-4.422	8.00E-20	TGFB1	-3.721	4.25E-06
OSM	-2.911	8.47E-05	TGFB	-3.270	6.72E-08	NF-κβ	-3.222	1.49E-01
VEGF	-2.553	5.08E-05	NF-κβ	-3.238	3.29E-05	NFE2L2	-3.010	1.11E-02
ESR2	-2.401	7.97E-04	NUPR1	-3.207	8.04E-03	IL1	-3.000	1.52E-02
beta-estradiol	-2.265	1.97E-04	TGFB3	-3.091	5.54E-07	TNF	-2.923	6.13E-03

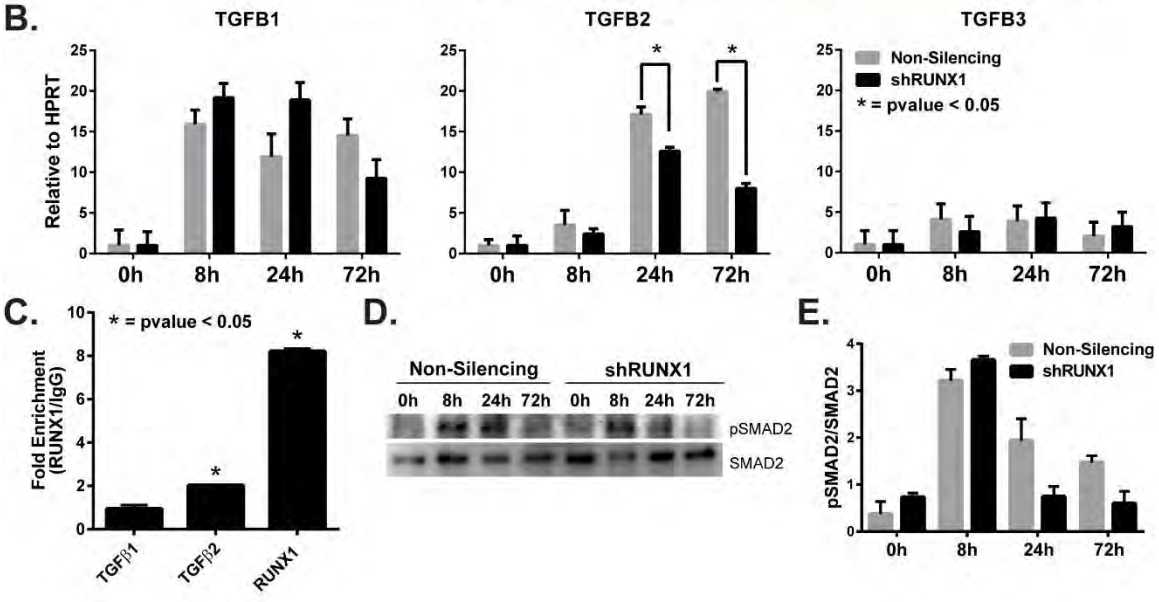

Figure 3.5. Knockdown of RUNX1 inhibits the TGFβ signaling pathway, specifically through TGFβ2. (A) Top signaling pathways inhibited by RUNX1 knockdown as determined by Ingenuity Pathway analysis. (B) Relative expression of the three TGFβ ligands under non-silencing and shRUNX1 treatment by RT-qPCR. Data represented as mean±SEM from three independent experiments with a technical replicate each and a p value determined by T-test (*, $p < 0.05$). (C) ChIP-qPCR analysis for RUNX1 binding sites in the promoters of the TGFβ1, TGFβ2, and RUNX1 promoters. Experiments were carried out at the peak of RUNX1 protein expression at 48h of differentiation. Data represented as mean±SEM of fold enrichment from four independent experiments with a p value determined by T-test comparing specific signaling to signal obtained from the IgG control (*, $p < 0.05$). (D) Representative Western blot showing a decrease in levels of pSMAD2 at 24h and 72h, with an increase in total SMAD2 levels with shRUNX1 treatment during mesendoderm differentiation. (E) Quantitation of Western blots from three independent experiments. Data is represented as the mean±SEM of the ratio of pSMAD2 over total SMAD2, and though not statistically significant, there is a decrease in the ratio of pSMAD2 to total SMAD2 at 24h and 72h of differentiation.

	Upstream Regulator	Molecule Type	Predicted State	Activation z-score
8hr	TGFB1	growth factor	Inhibited	-3.896
	OSM	cytokine	Inhibited	-2.911
	Vegf	group	Inhibited	-2.553
	ESR2	ligand-dependent nuclear receptor	Inhibited	-2.401
	beta-estradiol	chemical - endogenous	Inhibited	-2.265
	SP1	transcription regulator	Inhibited	-2.216
	F2	peptidase	Inhibited	-2.158
	TREM1	transmembrane receptor	Inhibited	-2.000
	GLI1	transcription regulator	Inhibited	-2.000
	ADCYAP1	other	Inhibited	-2.000
	SPDEF	transcription regulator	Activated	2.000
	butyric acid	chemical - endogenous	Activated	2.019
	Alpha catenin	group	Activated	2.401
	MYCN	transcription regulator	Activated	2.762
24hr	TGFB1	growth factor	Inhibited	-4.422
	Tgf beta	group	Inhibited	-3.270
	NFkB (complex)	complex	Inhibited	-3.238
	NUPR1	transcription regulator	Inhibited	-3.207
	TGFB3	growth factor	Inhibited	-3.091
	CTNNB1	transcription regulator	Inhibited	-2.940
	Cg	complex	Inhibited	-2.873
	MAP2K1	kinase	Inhibited	-2.760
	dihydrotestosterone	chemical - endogenous	Inhibited	-2.748
	P38 MAPK	group	Inhibited	-2.746
	PI3K (complex)	complex	Inhibited	-2.641
	EDN1	cytokine	Inhibited	-2.627
	HIF1A	transcription regulator	Inhibited	-2.618
	RELA	transcription regulator	Inhibited	-2.612
	FOXO1	transcription regulator	Inhibited	-2.600
	CTGF	growth factor	Inhibited	-2.566
	WNT3A	cytokine	Inhibited	-2.548
	Pkc(s)	group	Inhibited	-2.510
	NFE2L2	transcription regulator	Inhibited	-2.505
	CREB1	transcription regulator	Inhibited	-2.481
	F2	peptidase	Inhibited	-2.474
	TNF	cytokine	Inhibited	-2.429
	GATA4	transcription regulator	Inhibited	-2.425
	MTPN	transcription regulator	Inhibited	-2.415
	RHOA	enzyme	Inhibited	-2.412
	FOXC2	transcription regulator	Inhibited	-2.401

FOSL1	transcription regulator	Inhibited	-2.400
aldosterone	chemical - endogenous	Inhibited	-2.328
hydrogen peroxide	chemical - endogenous	Inhibited	-2.322
EGF	growth factor	Inhibited	-2.291
FN1	enzyme	Inhibited	-2.257
LDL	complex	Inhibited	-2.243
SYVN1	transporter	Inhibited	-2.236
NFATC2	transcription regulator	Inhibited	-2.236
IL1B	cytokine	Inhibited	-2.232
YBX1	transcription regulator	Inhibited	-2.219
PI3K (family)	group	Inhibited	-2.216
TWIST1	transcription regulator	Inhibited	-2.213
IL1	group	Inhibited	-2.211
TBX5	transcription regulator	Inhibited	-2.207
MEF2C	transcription regulator	Inhibited	-2.207
IL1A	cytokine	Inhibited	-2.190
MYOCD	transcription regulator	Inhibited	-2.185
Ap1	complex	Inhibited	-2.183
INHBA	growth factor	Inhibited	-2.180
ATF2	transcription regulator	Inhibited	-2.174
VEGFA	growth factor	Inhibited	-2.170
EP300	transcription regulator	Inhibited	-2.157
Vegf	group	Inhibited	-2.129
STAT6	transcription regulator	Inhibited	-2.093
SNAI2	transcription regulator	Inhibited	-2.090
ERK	group	Inhibited	-2.053
BMP2	growth factor	Inhibited	-2.035
SNAI1	transcription regulator	Inhibited	-2.010
RAC1	enzyme	Inhibited	-2.008
EGFR	kinase	Inhibited	-2.002
Rock	group	Inhibited	-2.000
CCL5	cytokine	Inhibited	-2.000
APC	enzyme	Activated	2.106
miR-30c-5p (and other miRNAs w/seed GUAAACA)	mature microrna	Activated	2.153
let-7a-5p (and other miRNAs w/seed GAGGUAG)	mature microrna	Activated	2.170
ADIPOQ	other	Activated	2.190
KLF2	transcription regulator	Activated	2.219
miR-1-3p (and other miRNAs w/seed GGAAUGU)	mature microrna	Activated	2.223

	ACOX1	enzyme	Activated	2.236
	MEOX2	transcription regulator	Activated	2.236
	let-7	microrna	Activated	2.353
	COL18A1	other	Activated	2.380
	TAF4	transcription regulator	Activated	2.415
	ZNF217	transcription regulator	Activated	2.828
72hr	TGFB1	growth factor	Inhibited	-3.721
	NFkB (complex)	complex	Inhibited	-3.222
	NFE2L2	transcription regulator	Inhibited	-3.010
	IL1	group	Inhibited	-3.000
	TNF	cytokine	Inhibited	-2.923
	EGFR	kinase	Inhibited	-2.867
	F2	peptidase	Inhibited	-2.804
	XBP1	transcription regulator	Inhibited	-2.785
	WNT3A	cytokine	Inhibited	-2.639
	TLR4	transmembrane receptor	Inhibited	-2.621
	IL4	cytokine	Inhibited	-2.613
	Mek	group	Inhibited	-2.588
	TGFB3	growth factor	Inhibited	-2.573
	hydrogen peroxide	chemical - endogenous	Inhibited	-2.446
	leukotriene D4	chemical - endogenous	Inhibited	-2.433
	dihydrotestosterone	chemical - endogenous	Inhibited	-2.409
	CXCL12	cytokine	Inhibited	-2.396
	CD38	enzyme	Inhibited	-2.376
	AGT	growth factor	Inhibited	-2.301
	JUN	transcription regulator	Inhibited	-2.272
	HGF	growth factor	Inhibited	-2.237
	HDAC1	transcription regulator	Inhibited	-2.236
	TWIST1	transcription regulator	Inhibited	-2.219
	PGR	ligand-dependent nuclear receptor	Inhibited	-2.199
	EGR1	transcription regulator	Inhibited	-2.177
	RELA	transcription regulator	Inhibited	-2.176
	TGM2	enzyme	Inhibited	-2.121
	INHBA	growth factor	Inhibited	-2.103
	DNMT3B	enzyme	Inhibited	-2.000
	glutamine	chemical - endogenous	Activated	2.000
	RICTOR	other	Activated	2.000
	estrogen receptor	group	Activated	2.170

Table 3.3. Complete pathway analysis from Ingenuity Pathway Analysis Software at 8h, 24h, and 72h.

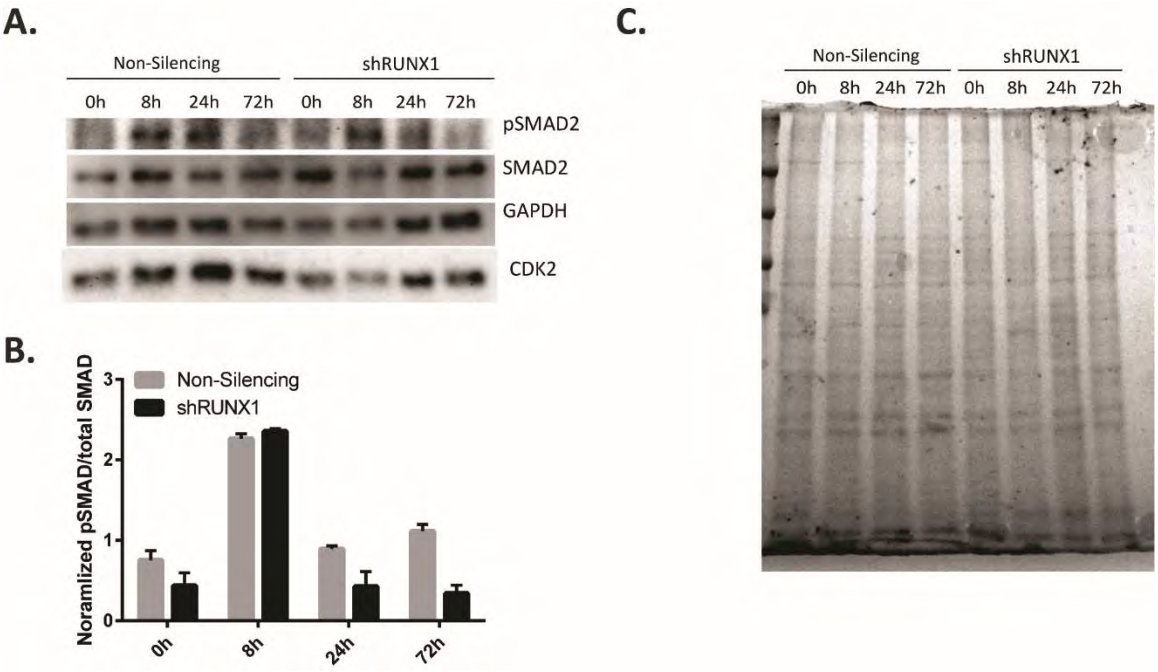

Figure 3.6. Further Analysis of pSMAD/SMAD2 Western Blot.
(A)Representative Western blot showing a decrease in levels of pSMAD2 at 24h and 72h, with an increase in total SMAD2 levels with shRUNX1 treatment during mesendoderm differentiation. Loading controls of GAPDH and CDK2 are included. (B) Quantitation of Western blots from three independent experiments. Data is represented as the mean±SEM of the ratio of pSMAD2 over total SMAD, both normalized using the loading control CDK2. Normalizing to the loading control does not affect the overall result, as there is still a decrease in the ratio of pSMAD to total SMAD at 24h and 72h of differentiation. (C) Coomassie stained gel for Western blot showing no gross total difference in protein loading.

3.3.4 TGFβ2 Rescues Impaired Cell Motility and Epithelial Gene Expression Caused by RUNX1 Depletion

The TGFβ pathway is known to regulate cell migration and adhesion (Xu et al., 2009). Our findings reveal that RUNX1 affects cell motility (Figure 3.2G) and specifically regulates *TGFβ2* expression (Figure 3.5B). We directly tested whether there is a connection between the defect in motility and EMT gene expression resulting from RUNX1 depletion and TGFβ2 signaling. Scratch

closure assays were performed to determine whether the effect of RUNX1 depletion on hESC migration can be rescued by TGFβ2 (Figure 3.7). We found that addition of TGFβ2 significantly increased the scratch closure of the shRUNX1 hESCs from ~40% to ~60%; TGFβ1, which was included as a control, had no effect (Figure 3.7B). These findings are consistent with our discovery that RUNX1 occupies and transcriptionally activates the *TGFβ2* gene (Figure 3.5B and 3.5C), and establish that RUNX1 regulation of hESC migration is mediated through TGFβ2.

TGFβ signaling can regulate EMT and the associated changes in cell adhesion and migration (Nieto, 2013; Thiery et al., 2009). Because RUNX1 knockdown inhibits TGFβ signaling (Figure 3.5), we evaluated whether supplementation of the shRUNX1 cultures with exogenous TGFβ1 or TGFβ2 could rescue the altered expression of EMT genes (Figure 3.7C). While TGFβ2 caused significant repression of the epithelial markers to levels similar to those in shNS hESCs, TGFβ1 was unable to repress most of these genes (Figure 3.7C). TGFβ2 failed to induce expression of *ZEB2*, the only mesenchymal marker that was not upregulated during differentiation of shRUNX1 hESCs, suggesting that the effect of TGFβ2 is primarily epithelial (Figure 3.7C). These findings indicate that knockdown of RUNX1 alleviates repression of epithelial genes (Figure 3.4), and addition of TGFβ2 decreases the expression of these epithelial genes (Figure 3.7C). Taken together, our results show that the selective and transient

RUNX1 expression during early mesendodermal differentiation of hESCs regulates cell motility and EMT gene expression through TGFβ2.

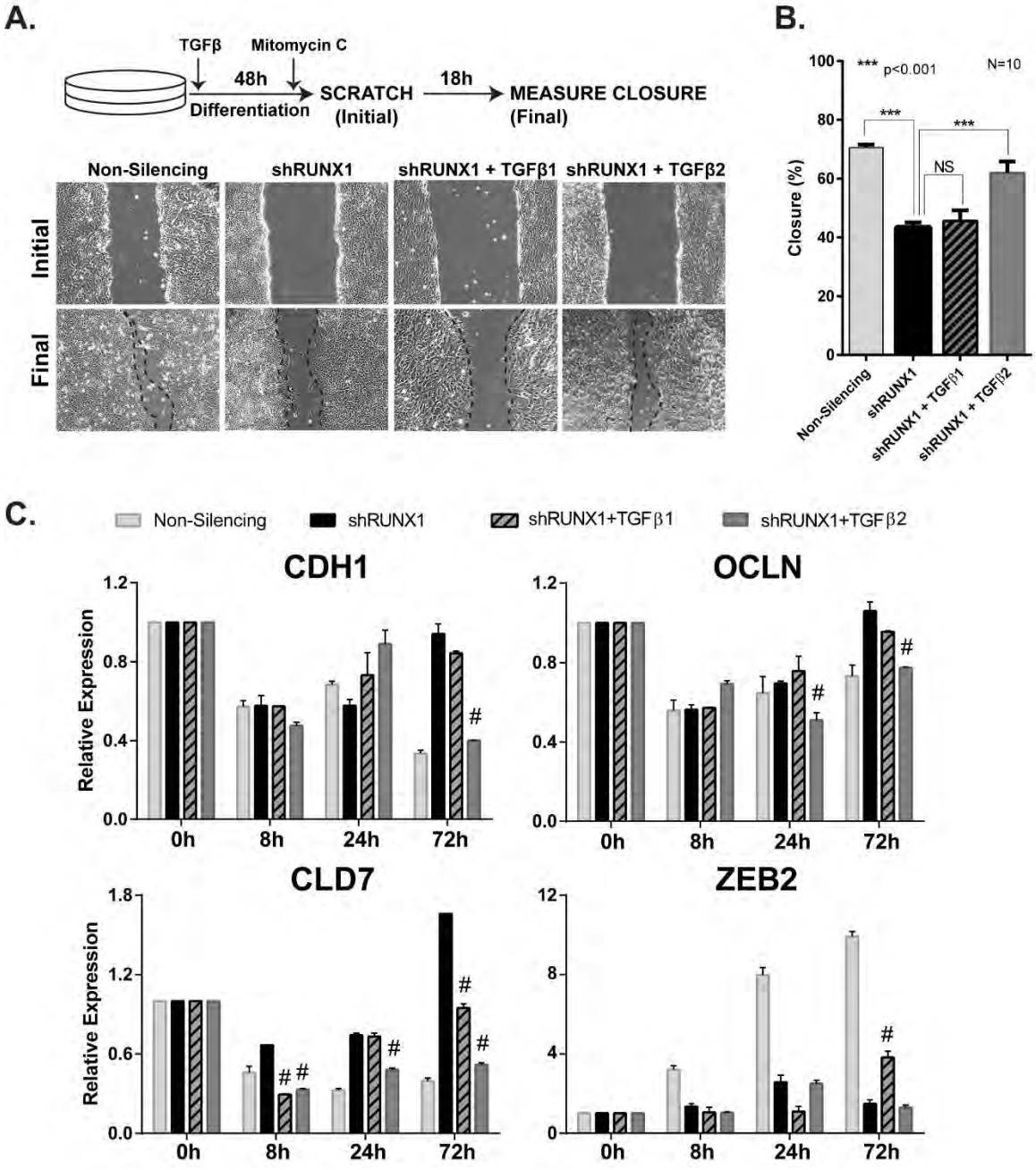

Figure 3.7. Defects in cell motility and EMT gene expression caused by RUNX1 depletion are rescued by reintroduction of TGFβ2, but not TGFβ1. (A) Representative phase contrast images from a scratch closure assay. Assays were carried out as in Figure 2G, with the addition of TGFβ ligand. All phase contrast images were taken at 10X magnification. (B) Percentage of scratch closure for hESCs with non-silencing infection, and shRUNX1 infection, as wells as shRUNX1 cells supplemented with exogenous TGFβ1 or TGFβ2, as

quantitated by Image J plugin. Ten scratches were measured for each condition, and data is represented as mean±SD, (***, $p<0.001$). (C) The expression of the four genes that were found to be affected by RUNX1 knockdown (CDH1, OCLN, CLD7, and ZEB2) with Non-Silencing, shRUNX1, shRUNX1+TGFβ2, and shRUNX1+TGFβ1 over a mesendoderm differentiation time course. Data shown as mean±SEM from three independent experiments with a technical replicate each (N=6). P values were determined by t-test between shRUNX1 and either shRUNX1 cells supplemented with TGFβ2, or TGFβ1 (#, $p < 0.0001$).

3.4 Discussion for Chapter III

In this chapter, we discovered unexpected, transient expression of the phenotypic transcription factor RUNX1 during early mesendodermal differentiation of hESCs, which suggested that RUNX1 contributes to differentiation in addition to its established role in hematopoietic lineage identity. Our findings showed that RUNX1 regulates cell motility and gene expression during mesendodermal differentiation specifically through *TGFβ2* signaling (Figure 3.8). These results suggest a novel role for RUNX1 in early development.

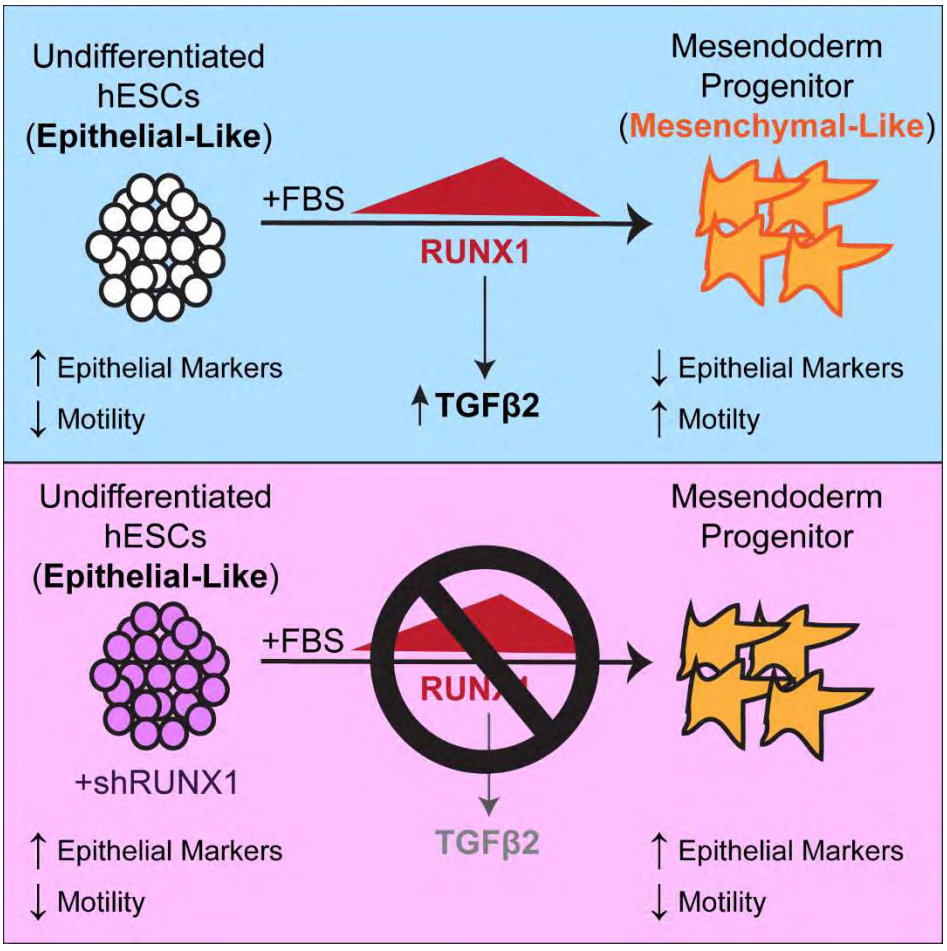

Figure 3.8 Graphical Summary of Chapter III.

The discovery of a burst of RUNX1 expression was both selective and specific because none of the other examined phenotypic transcription factors showed increased expression. *RUNX1* expression from the distal P1 promoter is linked with the emergence of definitive hematopoietic stem cells (Chen et al., 2009; Lacaud et al., 2002; Okuda et al., 1996), but little work has been done on the role of transcripts from the more ubiquitous proximal P2 promoter (Challen and Goodell, 2010; Fujita et al., 2001; Sroczynska et al., 2009). In this study, the *RUNX1* transcript that we found during early mesendodermal differentiation is the *RUNX1b* isoform from the P2 promoter. Interestingly, the RUNX1 P2 promoter from which the RUNX1b transcript originates is poised for expression, being bivalently marked with H3K27me^3 and H3K4me^3, in undifferentiated hESC, while the P1 promoter is not (Figure 1.2) (Mikkelsen et al., 2007). Additionally, the transcripts from the two promoters are translated through different primary mechanisms with the P1 transcript translated through a cap-mediated mechanism, and the P2 transcripts translated though an IRES mediated mechanism (Pozner et al., 2000), which is often used in times of cellular stress, mitosis, and during differentiation (Komar and Hatzoglou, 2011). This supports the idea that the RUNX1 expression from the P2 promoter has evolved specifically to be expressed early under differentiating conditions, indicating it could have an important role in early development.

Our discovery of a rapid, substantial increase in RUNX1 expression early in differentiation to mesendoderm suggests a potential role for RUNX1 that is

unrelated to hematopoiesis. We provide evidence that RUNX1 has a role in early mesendodermal differentiation of hESCs through regulation of cell migration and adhesion, as indicated by impairment of these processes upon RUNX1 depletion. These findings are consistent with the emerging role of RUNX1 in controlling cell motility and migration in other biological systems. We have previously shown that RUNX1 depletion in breast cancer cells results in a decreased migration and invasion phenotype (Browne et al., 2015); similar results were found in ovarian cancer cells (Keita et al., 2013). Likewise, RUNX1b is responsible for inducing a cell adhesion and migration program prior to release of mouse hematopoietic stem cells from hemogenic endothelium (Lie-A-Ling et al., 2014).

One notable result was that upon RUNX1 depletion there was decrease in cell motility and a de-repression of epithelial markers, which suggests that there is a requirement for RUNX1 to produce proper EMT. However, when the morphology of the differentiating cells was examined, there were not any differences between control and knockdown cells, which is unexpected because of the connection between EMT and cell morphological changes. Interestingly, one study has shown that the cell morphological changes associated with EMT precede down-regulation of E-Cadherin, and forced expression of E-Cadherin did not affect cell morphology (Maeda et al., 2005). This study indicates that it is possible that the deregulation of the epithelial markers could not have an effect on cell morphology, while still influencing cell adhesion or migration in the EMT process.

Gene expression profiling of early mesendodermal differentiation revealed that RUNX1 regulates TGFβ signaling, which has known roles in maintenance of pluripotency of hESCs (James et al., 2005; Wei et al., 2005), differentiation (Itoh et al., 2014; Watabe and Miyazono, 2009) and EMT (Xu et al., 2009). The inhibition of motility and de-repression of epithelial genes observed upon RUNX1 depletion indicates that RUNX1 is upstream of the TGFβ pathway. Moreover, we found that RUNX1 specifically occupies and regulates the expression of the *TGFβ2* gene, which encodes one of the three TGFβ ligands. Though the TGFβ ligands share greater than 70% homology (Kingsley, 1994), studies of knockout mice show non-overlapping phenotypes, indicating that each ligand has specific functions in development (Sanford et al., 1997). TGFβ2 knockout mice have cardiac, lung, craniofacial, limb, spinal column, eye, inner ear and urogenital defects (Sanford et al., 1997), whereas the TGFβ1 mice exhibit an autoimmune-like inflammatory disease or embryonic lethality due to defective yolk sac hematopoiesis and vasculogenesis depending on the genetic background (Dickson et al., 1995; Kulkarni et al., 1993; Shull et al., 1992). Consistent with the results from these mouse models, we found a specific requirement for TGFβ2, but not TGFβ1, to rescue the phenotype of RUNX1 depletion.

In addition to a decrease in TGFβ2 ligand expression upon RUNX1 depletion, we also found a decrease in phosphorylation of the downstream effector SMAD2. SMAD2 is required for proper gastrulation, as well as primitive streak/mesendoderm and mesoderm formation, with SMAD2 knockout being

embryonic lethal before E8.5 (Nomura and Li, 1998; Weinstein et al., 1998). This is consistent with the idea that RUNX1 has a role in mesendodermal regulation upstream of TGFβ2-SMAD2 signaling.

One result that did not fit well into our model of RUNX1 regulating TGFβ2 signaling, motility, and epithelial marker gene expression was that when RUNX1 was depleted, the expression of the mesenchymal associated transcription factor *ZEB2* was not induced. *ZEB2* was the only mesenchymal associated gene whose expression was found to be altered by RUNX1 knockdown, as the primary effect of RUNX1 depletion was on epithelial marker genes. ZEB2 is an important regulator of EMT, responsible for down-regulating epithelial markers (Kalluri and Weinberg, 2009; Vandewalle et al., 2005). One hypothesis was that the effect on epithelial marker genes was mediated through ZEB2. *ZEB2* expression was not rescued by introduction of exogenous TGFβ2, and was only very slightly induced upon exposure to TGFβ1, while the expression of epithelial genes was re-repressed to levels similar to what is observed in control cells. This suggests that the effect on epithelial gene expression was not mediated through ZEB2. However, while introduction of exogenous TGFβ2 did not rescue RNA expression levels, there is the possibility that TGFβ2 post transcriptionally increased the levels of ZEB2, which was then responsible for decreasing the level of epithelial marker genes.

Interestingly, when ZEB2 is conditionally knocked out in mice, the phenotype was noted as similar to the RUNX1 knockout mouse with embryonic lethality by

E12.5, however ZEB2 is not necessary for hematopoietic stem cell formation, but rather to establish hematopoietic lineage differentiation potential (Goossens et al., 2011). This could indicate that *ZEB2* is a downstream target of RUNX1. We tested whether there was direct binding of RUNX1 to the *ZEB2* promoter, and did not find any, though this does not rule out that RUNX1 regulates *ZEB2* expression through an enhancer or other distal site.

Were this work to be continued, one thing that could be investigated in more detail is the effect of RUNX1 depletion on TGFβ2 signaling. The current work has been limited to examining the transcript levels of the TGFβ ligands and the phosphorylation levels of SMAD2. However, there is a long process between transcription of a ligand and presentation of active ligand to the cell surface receptor. Therefore, it might be informative to assay by ELISA the amount of active human and bovine (supplied in the media) TGFβ1 and TGFβ2 present in the media. This result might be more meaningful since it would measure ligands in the forms that can directly affect the cells and would eliminate the possibility that the transcriptional differences in ligand expression are nullified in either the translational processing or in the activation step.

In conclusion, our discovery of Runx1-mediated regulation of TGFβ2 signaling provides mechanistic insights into early mesendodermal differentiation. These results also establish RUNX1 as a selective and specific regulator of cell motility and EMT-associated gene expression.

CHAPTER IV. Discussion

The overarching goal of this body of work was to examine some of the early mechanisms that control the development of a whole organism from a single cell. Using human embryonic stem cells (hESCs), which can recapitulate *in vivo* developmental events, we tested the hypothesis that key regulatory events take place at very early stages of human embryonic stem cell (hESC) differentiation that accommodate their ability to differentiate into specific lineages. The studies in this dissertation focused mainly on the regulation of differentiation to mesendodermal lineages. Of note, the progression of differentiation of hESC to mesendodermal lineages was very reproducible, which made obtaining consistent results possible.

In Chapter II of this dissertation, we investigated mechanisms that connect alterations in the cell cycle to early lineage commitment. We discovered a cell cycle pause that occurred concurrently with an increase in expression of genes that regulate the G2/M transition, including WEE1, which when inhibited prevented this G2 pause. This pause was only observed during commitment to the endo- and mesodermal, but not ectodermal, lineages. WEE1 inhibition during meso- and endodermal differentiation selectively compromised differentiation to endoderm. Taken together these findings revealed a novel G2 cell cycle pause required for endodermal differentiation.

In Chapter III of this dissertation, we examined whether phenotypic transcription factors have a role in very early differentiation to mesendodermal

lineages prior to their known role in establishing lineage identity. We performed a screen of candidate transcription factors and found that RUNX1 is selectively and transiently up-regulated. In order to determine if RUNX1 has a role in early differentiation, we carried out transcriptome profiling and functional analyses upon RUNX1 depletion. These approaches established a role for RUNX1 in promoting cell motility and repressing several epithelial genes, which are required to complete the epithelial to mesenchymal transition during differentiation. Cell biological and biochemical assays revealed that RUNX1 depletion inhibited TGFβ2 signaling. Both the decrease in motility and deregulated epithelial marker expression in the absence of RUNX1 were rescued by reintroduction of TGFβ2, but not TGFβ1. These findings identify novel roles for a RUNX1-TGFβ2 signaling axis during mesendodermal lineage commitment.

Though both of the regulatory processes examined in this dissertation are active during the same period of early mesendodermal differentiation, there does not appear to be a direct connection between the two mechanisms. When the G2 cell cycle pause caused by WEE1 was inhibited, it had no effect on RUNX1 expression levels during differentiation to any lineage. The reverse situation is true as well; when RUNX1 was depleted in hESCs differentiated to mesendodermal lineages there was no effect on the cell cycle pause or net proliferation in general. It was important to show that RUNX1 depletion had no effect on the cell cycle profile or proliferation since previous studies have shown

RUNX1 can regulate cell cycle progress and proliferation in other systems (Bernardin and Friedman, 2002; Chimge et al., 2016; Friedman, 2009).

One limitation of the studies in both chapters of this dissertation is that all the experiments focused on studying the downstream effects/effectors of the regulatory mechanism/regulator. An interesting direction for future research would be to try to figure out what was upstream of either WEE1 or RUNX1 in the regulatory pathway. It would be interesting to find out what was initiating these regulatory mechanisms as it could give insight into how their lineage specificity was determined/maintained. Unfortunately, there were no transcriptome profiling time points collected earlier than 8 hours of differentiation (by which time WEE1 and RUNX1 had already been induced), as it was unexpected how early these regulatory mechanisms started. This data could give a clue as to what is being expressed earlier and possibly functioning as an inducer. However, having the transcriptome data would not necessarily be able to answer the question of what is inducting WEE1 or RUNX1, as there are many varieties of post-transcriptional mechanisms that could be involved. Additionally, if we were able to determine what was inducing the expression of WEE1 and/or RUNX1, this might also indicate what is responsible for the subsequent down regulation of these factors. This information is important because the “off” switch of a regulatory mechanism is as important as the “on” switch, since each early event is very tightly coordinated and timed with the other events necessary for proper development.

We had hypothesized that RUNX1 was being induced by TGFβ1, as it has

been shown that TGFβ1 can induce RUNX expression (Jin et al., 2004; Klunker et al., 2009; Miyazono et al., 2004), that TGFβ1 is a regulator of EMT, and that TGFβ1 is already highly expressed by 8 hours of mesendodermal differentiation with an expression pattern that mirrors *RUNX1* expression. However, since TGFβ1 is a key signal required to maintain pluripotency as well as promote differentiation, any alteration in TGFβ1 signaling altered multiple properties of the differentiation. Also, TGFβ1 is both expressed by the cell and contributed by the medium, making it technically challenging to alter the levels of TGFβ1 signaling. Therefore, connecting the expression of RUNX1 directly back to TGFβ1 was not possible from a technical perspective.

A challenge associated with studying early mechanisms of differentiation is defining the lineages that develop. One reason that this is a challenge is that there are very few markers for lineages that are expressed within the first few days of differentiation. Many markers of early lineages were first discovered in studies of development in early mouse embryos, where in addition to marker expression, there is the advantage of three dimensional positioning to aid in cell type/lineage identification. In hESC culture, where there is no three dimensional positioning, many markers that have been put forward as being specific for a specific early cell type or lineage are not in fact very specific, and there are multiple conflicting reports as to what lineages are marked by certain genes. For example, GBX2 is listed in several papers as a marker of early ectoderm (Pazhanisamy, 2015; Vallier et al., 2009), but another paper reveals that GBX2 is

also expressed in early presomitic mesoderm (Carapuço et al., 2005). In Figure 2.10, GBX2 was expressed during ectodermal differentiation, but there was also expression during mesodermal differentiation. This was initially unexpected based on GBX2 being considered a marker of ectoderm, but now is explainable after learning about the role of GBX2 in presomitic mesoderm.

Additionally, when maintaining pluripotent stem cells, there is always a certain amount of heterogeneity in level of pluripotency, with spontaneous differentiation occurring as well, which can result in high levels of unexpected markers depending on the amount and type of spontaneous differentiation (Laslett et al., 2007; Nair et al., 2015). This could explain why there are levels of ectodermal markers observed late during differentiation toward the mesendodermal lineages, and why markers of other lineages are observed during lineage specific differentiation, since a certain percentage of cells had already begun to spontaneously differentiate to other lineages before differentiation had been induced.

The discovery of these two novel regulatory mechanisms detailed in this dissertation indicate that there are many undiscovered regulatory mechanisms controlling early development and differentiation. If this research were to be continued there are several areas of investigation that may prove interesting. One interesting result from the analysis of the microarray data is that there is an enrichment of genes related to the positive regulation of smooth muscle and heart contraction among the genes that had increased expression during

mesendodermal differentiation. GO TERM analysis of genes that decreased upon depletion of RUNX1 revealed an enrichment in genes associated with smooth muscle and muscle contraction (Figure 3.3). It would be interesting to take the RUNX1 knockdown cells and perform directed differentiation toward the smooth muscle lineage and compare their lineage marker expression and ability to contract to that of control cells. This might provide evidence that early RUNX1 expression has functional consequence on later differentiation events.

A further study of interest would be to perform the same screen of candidate transcription factors or transcriptome profiling during very early differentiation to ectodermal lineages, as the present studies were performed during mesendodermal differentiation. This might reveal a novel role for an unexpected transcription factor in ectodermal differentiation.

In conclusion, this dissertation has examined two separate regulatory mechanisms that act very early in hESC differentiation and accommodate differentiation into specific lineages. One of these mechanisms is a novel G2 cell cycle pause required for endodermal differentiation, the other is early RUNX1 expression during mesendodermal differentiation that is necessary to properly regulate cell motility and EMT gene expression. The understanding of these processes has expanded our knowledge of the complex series of events that are required at every step of development to create the intricate creature that is a human being.

Bibliography

Acloque, H., Adams, M.S., Fishwick, K., Bronner-Fraser, M., Nieto, M.A., 2009. Epithelial-mesenchymal transitions: the importance of changing cell state in development and disease. J. Clin. Invest. 119, 1438–49. doi:10.1172/JCI38019

Alcaraz, L.B., Exposito, J.-Y., Chuvin, N., Pommier, R.M., Cluzel, C., Martel, S., Sentis, S., Bartholin, L., Lethias, C., Valcourt, U., 2014. Tenascin-X promotes epithelial-to-mesenchymal transition by activating latent TGF-β. J. Cell Biol. 205, 409–428. doi:10.1083/jcb.201308031

Amit, M., Carpenter, M.K., Inokuma, M.S., Chiu, C.P., Harris, C.P., Waknitz, M.A., Itskovitz-Eldor, J., Thomson, J.A., 2000. Clonally derived human embryonic stem cell lines maintain pluripotency and proliferative potential for prolonged periods of culture. Dev. Biol. 227, 271–8. doi:10.1006/dbio.2000.9912

Annes, J.P., 2003. Making sense of latent TGFbeta activation. J. Cell Sci. 116, 217–224. doi:10.1242/jcs.00229

Aronson, B.D., Fisher, A.L., Blechman, K., Caudy, M., Gergen, J.P., 1997. Groucho-dependent and -independent repression activities of Runt domain proteins. Mol. Cell. Biol. 17, 5581–7.

Atherton-Fessler, S., Parker, L.L., Geahlen, R.L., Piwnica-Worms, H., 1993. Mechanisms of p34cdc2 regulation. Mol. Cell. Biol. 13, 1675–1685. doi:10.1128/MCB.13.3.1675

Avilion, A.A., Nicolis, S.K., Pevny, L.H., Perez, L., Vivian, N., Lovell-Badge, R., 2003. Multipotent cell lineages in early mouse development depend on SOX2 function. Genes Dev. 17, 126–40. doi:10.1101/gad.224503

Bangsow, C., Rubins, N., Glusman, G., Bernstein, Y., Negreanu, V., Goldenberg, D., Lotem, J., Ben-Asher, E., Lancet, D., Levanon, D., Groner, Y., 2001. The RUNX3 gene – sequence, structure and regulated expression. Gene 279, 221–232. doi:10.1016/S0378-1119(01)00760-0

Becker, K.A., Ghule, P.N., Therrien, J.A., Lian, J.B., Stein, J.L., van Wijnen, A.J., Stein, G.S., 2006. Self-renewal of human embryonic stem cells is supported by a shortened G1 cell cycle phase. J. Cell. Physiol. 209, 883–93. doi:10.1002/jcp.20776

Becker, K.A., Stein, J.L., Lian, J.B., van Wijnen, A.J., Stein, G.S., 2010. Human embryonic stem cells are pre-mitotically committed to self-renewal and acquire a lengthened G1 phase upon lineage programming. J. Cell. Physiol. 222, 103–10. doi:10.1002/jcp.21925

Bee, T., Liddiard, K., Swiers, G., Bickley, S.R.B., Vink, C.S., Jarratt, A., Hughes, J.R., Medvinsky, A., de Bruijn, M.F.T.R., 2009. Alternative Runx1 promoter usage in mouse developmental hematopoiesis. Blood Cells. Mol. Dis. 43, 35–42. doi:10.1016/j.bcmd.2009.03.011

Bee, T., Swiers, G., Muroi, S., Pozner, A., Nottingham, W., Santos, A.C., Li, P.S., Taniuchi, I., De Bruijn, M.F.T.R., 2010. Nonredundant roles for Runx1 alternative promoters reflect their activity at discrete stages of developmental hematopoiesis. Blood 115, 3042–3050. doi:10.1182/blood-2009-08-238626

Ben Sahra, I., Regazzetti, C., Robert, G., Laurent, K., Le Marchand-Brustel, Y., Auberger, P., Tanti, J.-F., Giorgetti-Peraldi, S., Bost, F., 2011. Metformin, independent of AMPK, induces mTOR inhibition and cell-cycle arrest through REDD1. Cancer Res. 71, 4366–72. doi:10.1158/0008-5472.CAN-10-1769

Bernardin, F., Friedman, A.D., 2002. AML1 stimulates G1 to S progression via its transactivation domain. Oncogene 21, 3247–52. doi:10.1038/sj.onc.1205447

Bernstein, B.E., Mikkelsen, T.S., Xie, X., Kamal, M., Huebert, D.J., Cuff, J., Fry, B., Meissner, A., Wernig, M., Plath, K., Jaenisch, R., Wagschal, A., Feil, R., Schreiber, S.L., Lander, E.S., 2006. A bivalent chromatin structure marks key developmental genes in embryonic stem cells. Cell 125, 315–26. doi:10.1016/j.cell.2006.02.041

Bindea, G., Mlecnik, B., Hackl, H., Charoentong, P., Tosolini, M., Kirilovsky, A., Fridman, W.H., Pagès, F., Trajanoski, Z., Galon, J., 2009. ClueGO: A Cytoscape plug-in to decipher functionally grouped gene ontology and pathway annotation networks. Bioinformatics 25, 1091–1093. doi:10.1093/bioinformatics/btp101

Blyth, K., Cameron, E.R., Neil, J.C., 2005. The RUNX genes: gain or loss of function in cancer. Nat. Rev. Cancer 5, 376–87. doi:10.1038/nrc1607

Booher, R.N., Holman, P.S., Fattaey, A., 1997. Human Myt1 Is a Cell Cycle-regulated Kinase That Inhibits Cdc2 but Not Cdk2 Activity. J. Biol. Chem. 272, 22300–22306. doi:10.1074/jbc.272.35.22300

Boward, B., Wu, T., Dalton, S., 2016. Control of cell fate through cell cycle and pluripotency networks. Stem Cells. doi:10.1002/stem.2345

Boyer, L.A., Lee, T.I., Cole, M.F., Johnstone, S.E., Levine, S.S., Zucker, J.P., Guenther, M.G., Kumar, R.M., Murray, H.L., Jenner, R.G., Gifford, D.K., Melton, D.A., Jaenisch, R., Young, R.A., 2005. Core transcriptional regulatory circuitry in human embryonic stem cells. Cell 122, 947–56. doi:10.1016/j.cell.2005.08.020

Brady, G., Elgueta Karstegl, C., Farrell, P.J., 2013. Novel function of the unique

N-terminal region of RUNX1c in B cell growth regulation. Nucleic Acids Res. 41, 1555–68. doi:10.1093/nar/gks1273

Brandeis, M., Rosewell, I., Carrington, M., Crompton, T., Jacobs, M.A., Kirk, J., Gannon, J., Hunt, T., 1998. Cyclin B2-null mice develop normally and are fertile whereas cyclin B1-null mice die in utero. Proc. Natl. Acad. Sci. U. S. A. 95, 4344–9.

Browne, G., Taipaleenmäki, H., Bishop, N.M., Madasu, S.C., Shaw, L.M., van Wijnen, A.J., Stein, J.L., Stein, G.S., Lian, J.B., 2015. Runx1 is associated with breast cancer progression in MMTV-PyMT transgenic mice and its depletion in vitro inhibits migration and invasion. J. Cell. Physiol. 230, 2522–32. doi:10.1002/jcp.24989

Byron, M., Hall, L.L., Lawrence, J.B., 2013. A multifaceted FISH approach to study endogenous RNAs and DNAs in native nuclear and cell structures. Curr. Protoc. Hum. Genet. Chapter 4, Unit 4.15. doi:10.1002/0471142905.hg0415s76

Calder, A., Roth-Albin, I., Bhatia, S., Pilquil, C., Lee, J.H., Bhatia, M., Levadoux-Martin, M., McNicol, J., Russell, J., Collins, T., Draper, J.S., 2013. Lengthened G1 phase indicates differentiation status in human embryonic stem cells. Stem Cells Dev. 22, 279–95. doi:10.1089/scd.2012.0168

Cano, A., Pérez-Moreno, M.A., Rodrigo, I., Locascio, A., Blanco, M.J., del Barrio, M.G., Portillo, F., Nieto, M.A., 2000. The transcription factor snail controls epithelial-mesenchymal transitions by repressing E-cadherin expression. Nat. Cell Biol. 2, 76–83. doi:10.1038/35000025

Carapuço, M., Nóvoa, A., Bobola, N., Mallo, M., 2005. Hox genes specify vertebral types in the presomitic mesoderm. Genes Dev. 19, 2116–21. doi:10.1101/gad.338705

Challen, G.A., Goodell, M.A., 2010. Runx1 isoforms show differential expression patterns during hematopoietic development but have similar functional effects in adult hematopoietic stem cells. Exp. Hematol. 38, 403–16. doi:10.1016/j.exphem.2010.02.011

Chambers, I., Colby, D., Robertson, M., Nichols, J., Lee, S., Tweedie, S., Smith, A., 2003. Functional expression cloning of Nanog, a pluripotency sustaining factor in embryonic stem cells. Cell 113, 643–55.

Chen, B., Mao, B., Huang, S., Zhou, Y., Tsuji, K., Ma, F., 2014. Human Embryonic Stem Cell-Derived Primitive and Definitive Hematopoiesis, in: Pluripotent Stem Cell Biology - Advances in Mechanisms, Methods and Models. InTech. doi:10.5772/58628

Chen, G., Gulbranson, D.R., Hou, Z., Bolin, J.M., Ruotti, V., Probasco, M.D.,

Smuga-Otto, K., Howden, S.E., Diol, N.R., Propson, N.E., Wagner, R., Lee, G.O., Antosiewicz-Bourget, J., Teng, J.M.C., Thomson, J.A., 2011. Chemically defined conditions for human iPSC derivation and culture. Nat. Methods 8, 424–9. doi:10.1038/nmeth.1593

Chen, M.J., Yokomizo, T., Zeigler, B.M., Dzierzak, E., Speck, N.A., 2009. Runx1 is required for the endothelial to haematopoietic cell transition but not thereafter. Nature 457, 887–91. doi:10.1038/nature07619

Chimge, N.-O., Little, G.H., Baniwal, S.K., Adisetiyo, H., Xie, Y., Zhang, T., O'Laughlin, A., Liu, Z.Y., Ulrich, P., Martin, A., Mhawech-Fauceglia, P., Ellis, M.J., Tripathy, D., Groshen, S., Liang, C., Li, Z., Schones, D.E., Frenkel, B., 2016. RUNX1 prevents oestrogen-mediated AXIN1 suppression and β-catenin activation in ER-positive breast cancer. Nat. Commun. 7, 10751. doi:10.1038/ncomms10751

Chuang, L.S.H., Ito, K., Ito, Y., 2013. RUNX family: Regulation and diversification of roles through interacting proteins. Int. J. Cancer 132, 1260–71. doi:10.1002/ijc.27964

Comijn, J., Berx, G., Vermassen, P., Verschueren, K., van Grunsven, L., Bruyneel, E., Mareel, M., Huylebroeck, D., van Roy, F., 2001. The Two-Handed E Box Binding Zinc Finger Protein SIP1 Downregulates E-Cadherin and Induces Invasion. Mol. Cell 7, 1267–1278. doi:10.1016/S1097-2765(01)00260-X

Croft, D., Mundo, A.F., Haw, R., Milacic, M., Weiser, J., Wu, G., Caudy, M., Garapati, P., Gillespie, M., Kamdar, M.R., Jassal, B., Jupe, S., Matthews, L., May, B., Palatnik, S., Rothfels, K., Shamovsky, V., Song, H., Williams, M., Birney, E., Hermjakob, H., Stein, L., D'Eustachio, P., 2014. The Reactome pathway knowledgebase. Nucleic Acids Res. 42, D472–7. doi:10.1093/nar/gkt1102

D'Amour, K.A., Agulnick, A.D., Eliazer, S., Kelly, O.G., Kroon, E., Baetge, E.E., 2005. Efficient differentiation of human embryonic stem cells to definitive endoderm. Nat. Biotechnol. 23, 1534–41. doi:10.1038/nbt1163

Davidson, K.C., Adams, A.M., Goodson, J.M., McDonald, C.E., Potter, J.C., Berndt, J.D., Biechele, T.L., Taylor, R.J., Moon, R.T., 2012. Wnt/ -catenin signaling promotes differentiation, not self-renewal, of human embryonic stem cells and is repressed by Oct4. Proc. Natl. Acad. Sci. 109, 4485–4490. doi:10.1073/pnas.1118777109

Derynck, R., Muthusamy, B.P., Saeteurn, K.Y., 2014. Signaling pathway cooperation in TGF-β-induced epithelial-mesenchymal transition. Curr. Opin. Cell Biol. 31, 56–66. doi:10.1016/j.ceb.2014.09.001

Dickson, M.C., Martin, J.S., Cousins, F.M., Kulkarni, A.B., Karlsson, S., Akhurst,

R.J., 1995. Defective haematopoiesis and vasculogenesis in transforming growth factor-beta 1 knock out mice. Development 121, 1845–54.

Drissi, H., Luc, Q., Shakoori, R., Chuva De Sousa Lopes, S., Choi, J.Y., Terry, A., Hu, M., Jones, S., Neil, J.C., Lian, J.B., Stein, J.L., Van Wijnen, A.J., Stein, G.S., 2000. Transcriptional autoregulation of the bone related CBFA1/RUNX2 gene. J. Cell. Physiol. 184, 341–50. doi:10.1002/1097-4652(200009)184:3<341::AID-JCP8>3.0.CO;2-Z

Duband, J.L., Monier, F., Delannet, M., Newgreen, D., 1995. Epithelium-Mesenchyme Transition during Neural Crest Development. Cells Tissues Organs 154, 63–78. doi:10.1159/000147752

Dubois, C.M., Laprise, M.-H. l n., Blanchette, F., Gentry, L.E., Leduc, R., 1995. Processing of Transforming Growth Factor [IMAGE]1 Precursor by Human Furin Convertase. J. Biol. Chem. 270, 10618–10624. doi:10.1074/jbc.270.18.10618

Eastham, A.M., Spencer, H., Soncin, F., Ritson, S., Merry, C.L.R., Stern, P.L., Ward, C.M., 2007. Epithelial-mesenchymal transition events during human embryonic stem cell differentiation. Cancer Res. 67, 11254–62. doi:10.1158/0008-5472.CAN-07-2253

Ebisawa, T., Fukuchi, M., Murakami, G., Chiba, T., Tanaka, K., Imamura, T., Miyazono, K., 2001. Smurf1 interacts with transforming growth factor-beta type I receptor through Smad7 and induces receptor degradation. J. Biol. Chem. 276, 12477–80. doi:10.1074/jbc.C100008200

Edwards, S.A., Darland, T., Sosnowski, R., Samuels, M., Adamson, E.D., 1991. The transcription factor, Egr-1, is rapidly modulated in response to retinoic acid in P19 embryonal carcinoma cells. Dev. Biol. 148, 165–73.

Eger, A., Aigner, K., Sonderegger, S., Dampier, B., Oehler, S., Schreiber, M., Berx, G., Cano, A., Beug, H., Foisner, R., 2005. DeltaEF1 is a transcriptional repressor of E-cadherin and regulates epithelial plasticity in breast cancer cells. Oncogene 24, 2375–85. doi:10.1038/sj.onc.1208429

Egozi, D., Shapira, M., Paor, G., Ben-Izhak, O., Skorecki, K., Hershko, D.D., 2007. Regulation of the cell cycle inhibitor p27 and its ubiquitin ligase Skp2 in differentiation of human embryonic stem cells. FASEB J. 21, 2807–2817. doi:10.1096/fj.06-7758com

Endicott, J.A., Nurse, P., Johnson, L.N., 1994. Mutational analysis supports a structural model for the cell cycle protein kinase p34. Protein Eng. 7, 243–53.

Evseenko, D., 2010. Mapping the first stages of mesoderm commitment during differentiation of human embryonic stem cells. Proc. ….

doi:10.1073/pnas.1002077107/-/DCSupplemental.www.pnas.org/cgi/doi/10.1073/pnas.1002077107

Filipczyk, A.A., Laslett, A.L., Mummery, C., Pera, M.F., 2007. Differentiation is coupled to changes in the cell cycle regulatory apparatus of human embryonic stem cells. Stem Cell Res. 1, 45–60. doi:10.1016/j.scr.2007.09.002

Fong, H., Hohenstein, K.A., Donovan, P.J., 2008. Regulation of self-renewal and pluripotency by Sox2 in human embryonic stem cells. Stem Cells 26, 1931–8. doi:10.1634/stemcells.2007-1002

Friedman, A.D., 2009. Cell cycle and developmental control of hematopoiesis by Runx1. J. Cell. Physiol. 219, 520–4. doi:10.1002/jcp.21738

Fujita, Y., Nishimura, M., Taniwaki, M., Abe, T., Okuda, T., 2001. Identification of an alternatively spliced form of the mouse AML1/RUNX1 gene transcript AML1c and its expression in early hematopoietic development. Biochem. Biophys. Res. Commun. 281, 1248–55. doi:10.1006/bbrc.2001.4513

Fujiwara, M., Tagashira, S., Harada, H., Ogawa, S., Katsumata, T., Nakatsuka, M., Komori, T., Takada, H., 1999. Isolation and characterization of the distal promoter region of mouse Cbfa1. Biochim. Biophys. Acta 1446, 265–72.

Gautier, J., Solomon, M.J., Booher, R.N., Bazan, J.F., Kirschner, M.W., 1991. cdc25 is a specific tyrosine phosphatase that directly activates p34cdc2. Cell 67, 197–211. doi:10.1016/0092-8674(91)90583-K

Gerrard, L., Rodgers, L., Cui, W., 2005. Differentiation of human embryonic stem cells to neural lineages in adherent culture by blocking bone morphogenetic protein signaling. Stem Cells 23, 1234–41. doi:10.1634/stemcells.2005-0110

Ghozi, M.C., Bernstein, Y., Negreanu, V., Levanon, D., Groner, Y., 1996. Expression of the human acute myeloid leukemia gene AML1 is regulated by two promoter regions. Proc. Natl. Acad. Sci. U. S. A. 93, 1935–40.

Giacomini, M.M., Travis, M.A., Kudo, M., Sheppard, D., 2012. Epithelial cells utilize cortical actin/myosin to activate latent TGF-β through integrin αvβ6-dependent physical force. Exp. Cell Res. 318, 716–722. doi:10.1016/j.yexcr.2012.01.020

Glaß, M., Möller, B., Zirkel, A., Wächter, K., Hüttelmaier, S., Posch, S., 2012. Cell migration analysis: Segmenting scratch assay images with level sets and support vector machines. Pattern Recognit. 45, 3154–3165. doi:10.1016/j.patcog.2012.03.001

Gong, D., Ferrell, J.E., 2010. The roles of cyclin A2, B1, and B2 in early and late mitotic events. Mol. Biol. Cell 21, 3149–61. doi:10.1091/mbc.E10-05-0393

Gong, D., Pomerening, J.R., Myers, J.W., Gustavsson, C., Jones, J.T., Hahn, A.T., Meyer, T., Ferrell, J.E., 2007. Cyclin A2 regulates nuclear-envelope breakdown and the nuclear accumulation of cyclin B1. Curr. Biol. 17, 85–91. doi:10.1016/j.cub.2006.11.066

Gonzales, K.A.U., Liang, H., Lim, Y.-S., Chan, Y.-S., Yeo, J.-C., Tan, C.-P., Gao, B., Le, B., Tan, Z.-Y., Low, K.-Y., Liou, Y.-C., Bard, F., Ng, H.-H., 2015. Deterministic Restriction on Pluripotent State Dissolution by Cell-Cycle Pathways. Cell 162, 564–579. doi:10.1016/j.cell.2015.07.001

Gonzalez, D.M., Medici, D., 2014. Signaling mechanisms of the epithelial-mesenchymal transition. Sci. Signal. 7, re8. doi:10.1126/scisignal.2005189

Goossens, S., Janzen, V., Bartunkova, S., Yokomizo, T., Drogat, B., Crisan, M., Haigh, K., Seuntjens, E., Umans, L., Riedt, T., Bogaert, P., Haenebalcke, L., Berx, G., Dzierzak, E., Huylebroeck, D., Haigh, J.J., 2011. The EMT regulator Zeb2/Sip1 is essential for murine embryonic hematopoietic stem/progenitor cell differentiation and mobilization. Blood 117, 5620–30. doi:10.1182/blood-2010-08-300236

Goto, H., Tomono, Y., Ajiro, K., Kosako, H., Fujita, M., Sakurai, M., Okawa, K., Iwamatsu, A., Okigaki, T., Takahashi, T., Inagaki, M., 1999. Identification of a novel phosphorylation site on histone H3 coupled with mitotic chromosome condensation. J. Biol. Chem. 274, 25543–9.

Grandy, R.A., Whitfield, T.W., Wu, H., Fitzgerald, M.P., VanOudenhove, J.J., Zaidi, S.K., Montecino, M.A., Lian, J.B., van Wijnen, A.J., Stein, J.L., Stein, G.S., 2015. Genome-Wide Studies Reveal that H3K4me3 Modification in Bivalent Genes Is Dynamically Regulated during the Pluripotent Cell Cycle and Stabilized upon Differentiation. Mol. Cell. Biol. 36, 615–27. doi:10.1128/MCB.00877-15

Gray, A.M., Mason, A.J., 1990. Requirement for activin A and transforming growth factor--beta 1 pro-regions in homodimer assembly. Science 247, 1328–30.

Growney, J.D., Shigematsu, H., Li, Z., Lee, B.H., Adelsperger, J., Rowan, R., Curley, D.P., Kutok, J.L., Akashi, K., Williams, I.R., Speck, N.A., Gilliland, D.G., 2005. Loss of Runx1 perturbs adult hematopoiesis and is associated with a myeloproliferative phenotype. Blood 106, 494–504. doi:10.1182/blood-2004-08-3280

Guertin, A.D., Li, J., Liu, Y., Hurd, M.S., Schuller, A.G., Long, B., Hirsch, H.A., Feldman, I., Benita, Y., Toniatti, C., Zawel, L., Fawell, S.E., Gilliland, D.G., Shumway, S.D., 2013. Preclinical evaluation of the WEE1 inhibitor MK-1775 as single-agent anticancer therapy. Mol. Cancer Ther. 12, 1442–52. doi:10.1158/1535-7163.MCT-13-0025

Hagting, A., Jackman, M., Simpson, K., Pines, J., 1999. Translocation of cyclin B1 to the nucleus at prophase requires a phosphorylation-dependent nuclear import signal. Curr. Biol. 9, 680–689. doi:10.1016/S0960-9822(99)80308-X

Hagting, A., Karlsson, C., Clute, P., Jackman, M., Pines, J., 1998. MPF localization is controlled by nuclear export. EMBO J. 17, 4127–38. doi:10.1093/emboj/17.14.4127

Hajra, K.M., Chen, D.Y.-S., Fearon, E.R., 2002. The SLUG zinc-finger protein represses E-cadherin in breast cancer. Cancer Res. 62, 1613–8.

Hanai, J. -i., Chen, L.F., Kanno, T., Ohtani-Fujita, N., Kim, W.Y., Guo, W.-H., Imamura, T., Ishidou, Y., Fukuchi, M., Shi, M.-J., Stavnezer, J., Kawabata, M., Miyazono, K., Ito, Y., 1999. Interaction and Functional Cooperation of PEBP2/CBF with Smads: SYNERGISTIC INDUCTION OF THE IMMUNOGLOBULIN GERMLINE C PROMOTER. J. Biol. Chem. 274, 31577–31582. doi:10.1074/jbc.274.44.31577

Hata, A., Lagna, G., Massague, J., Hemmati-Brivanlou, A., 1998. Smad6 inhibits BMP/Smad1 signaling by specifically competing with the Smad4 tumor suppressor. Genes Dev. 12, 186–197. doi:10.1101/gad.12.2.186

Hay, E.D., 1968. Organization and fine structure of epithelium and mesenchyme in the developing chick embryo. Ep. Interact. 2, 31–35.

Heald, R., McKeon, F., 1990. Mutations of phosphorylation sites in lamin A that prevent nuclear lamina disassembly in mitosis. Cell 61, 579–89.

Hoffmann, I., Clarke, P.R., Marcote, M.J., Karsenti, E., Draetta, G., 1993. Phosphorylation and activation of human cdc25-C by cdc2--cyclin B and its involvement in the self-amplification of MPF at mitosis. EMBO J. 12, 53–63.

Hoi, C.S.L., Lee, S.E., Lu, S.-Y., McDermitt, D.J., Osorio, K.M., Piskun, C.M., Peters, R.M., Paus, R., Tumbar, T., 2010. Runx1 directly promotes proliferation of hair follicle stem cells and epithelial tumor formation in mouse skin. Mol. Cell. Biol. 30, 2518–36. doi:10.1128/MCB.01308-09

Hoogenkamp, M., Lichtinger, M., Krysinska, H., Lancrin, C., Clarke, D., Williamson, A., Mazzarella, L., Ingram, R., Jorgensen, H., Fisher, A., Tenen, D.G., Kouskoff, V., Lacaud, G., Bonifer, C., 2009. Early chromatin unfolding by RUNX1: a molecular explanation for differential requirements during specification versus maintenance of the hematopoietic gene expression program. Blood 114, 299–309. doi:10.1182/blood-2008-11-191890

Huang, D.W., Sherman, B.T., Lempicki, R.A., 2009a. Bioinformatics enrichment tools: paths toward the comprehensive functional analysis of large gene lists. Nucleic Acids Res. 37, 1–13. doi:10.1093/nar/gkn923

Huang, D.W., Sherman, B.T., Lempicki, R.A., 2009b. Systematic and integrative analysis of large gene lists using DAVID bioinformatics resources. Nat. Protoc. 4, 44–57. doi:10.1038/nprot.2008.211

Huang, G., Ye, S., Zhou, X., Liu, D., Ying, Q.-L., 2015. Molecular basis of embryonic stem cell self-renewal: from signaling pathways to pluripotency network. Cell. Mol. Life Sci. 72, 1741–57. doi:10.1007/s00018-015-1833-2

Ichikawa, M., Asai, T., Saito, T., Seo, S., Yamazaki, I., Yamagata, T., Mitani, K., Chiba, S., Ogawa, S., Kurokawa, M., Hirai, H., 2004. AML-1 is required for megakaryocytic maturation and lymphocytic differentiation, but not for maintenance of hematopoietic stem cells in adult hematopoiesis. Nat. Med. 10, 299–304. doi:10.1038/nm997

Ichikawa, M., Goyama, S., Asai, T., Kawazu, M., Nakagawa, M., Takeshita, M., Chiba, S., Ogawa, S., Kurokawa, M., 2008. AML1/Runx1 negatively regulates quiescent hematopoietic stem cells in adult hematopoiesis. J. Immunol. 180, 4402–8.

Ikenouchi, J., Matsuda, M., Furuse, M., Tsukita, S., 2003. Regulation of tight junctions during the epithelium-mesenchyme transition: direct repression of the gene expression of claudins/occludin by Snail. J. Cell Sci. 116, 1959–67. doi:10.1242/jcs.00389

Inoue, K., Ozaki, S., Shiga, T., Ito, K., Masuda, T., Okado, N., Iseda, T., Kawaguchi, S., Ogawa, M., Bae, S.-C., Yamashita, N., Itohara, S., Kudo, N., Ito, Y., 2002. Runx3 controls the axonal projection of proprioceptive dorsal root ganglion neurons. Nat. Neurosci. 5, 946–54. doi:10.1038/nn925

Ito, Y., 2004. Oncogenic potential of the RUNX gene family: “overview”. Oncogene 23, 4198–208. doi:10.1038/sj.onc.1207755

Itoh, F., Watabe, T., Miyazono, K., 2014. Roles of TGF-β family signals in the fate determination of pluripotent stem cells. Semin. Cell Dev. Biol. 32, 98–106. doi:10.1016/j.semcdb.2014.05.017

Itoh, S., Itoh, F., Goumans, M.-J., ten Dijke, P., 2000. Signaling of transforming growth factor-β family members through Smad proteins. Eur. J. Biochem. 267, 6954–6967. doi:10.1046/j.1432-1327.2000.01828.x

Itoh, S., ten Dijke, P., 2007. Negative regulation of TGF-beta receptor/Smad signal transduction. Curr. Opin. Cell Biol. 19, 176–84. doi:10.1016/j.ceb.2007.02.015

Itskovitz-Eldor, J., Schuldiner, M., Karsenti, D., Eden, A., Yanuka, O., Amit, M., Soreq, H., Benvenisty, N., 2000. Differentiation of human embryonic stem cells into embryoid bodies compromising the three embryonic germ layers. Mol. Med. 6, 88–95.

Jackson, R.J., Hellen, C.U.T., Pestova, T. V, 2010. The mechanism of eukaryotic translation initiation and principles of its regulation. Nat. Rev. Mol. Cell Biol. 11, 113–27. doi:10.1038/nrm2838

Jackson, S.A., Schiesser, J., Stanley, E.G., Elefanty, A.G., 2010. Differentiating Embryonic Stem Cells Pass through “Temporal Windows” That Mark Responsiveness to Exogenous and Paracrine Mesendoderm Inducing Signals. PLoS One 5, e10706. doi:10.1371/journal.pone.0010706

James, D., Levine, A.J., Besser, D., Hemmati-Brivanlou, A., 2005. TGFbeta/activin/nodal signaling is necessary for the maintenance of pluripotency in human embryonic stem cells. Development 132, 1273–82. doi:10.1242/dev.01706

Javed, A., Guo, B., Hiebert, S., Choi, J.Y., Green, J., Zhao, S.C., Osborne, M.A., Stifani, S., Stein, J.L., Lian, J.B., van Wijnen, A.J., Stein, G.S., 2000. Groucho/TLE/R-esp proteins associate with the nuclear matrix and repress RUNX (CBF(alpha)/AML/PEBP2(alpha)) dependent activation of tissue-specific gene transcription. J. Cell Sci. 113 (Pt 1, 2221–31.

Jin, Y.-H., Jeon, E.-J., Li, Q.-L., Lee, Y.H., Choi, J.-K., Kim, W.-J., Lee, K.-Y., Bae, S.-C., 2004. Transforming growth factor-beta stimulates p300-dependent RUNX3 acetylation, which inhibits ubiquitination-mediated degradation. J. Biol. Chem. 279, 29409–17. doi:10.1074/jbc.M313120200

Kagoshima, H., Shigesada, K., Satake, M., Ito, Y., Miyoshi, H., Ohki, M., Pepling, M., Gergen, P., 1993. The Runt domain identifies a new family of heteromeric transcriptional regulators. Trends Genet. 9, 338–41.

Kalluri, R., Neilson, E.G., 2003. Epithelial-mesenchymal transition and its implications for fibrosis. J. Clin. Invest. 112, 1776–1784. doi:10.1172/JCI20530

Kalluri, R., Weinberg, R.A., 2009. The basics of epithelial-mesenchymal transition. J. Clin. Invest. 119, 1420–8. doi:10.1172/JCI39104

Kanno, T., Kanno, Y., Chen, L.-F., Ogawa, E., Kim, W.-Y., Ito, Y., 1998. Intrinsic Transcriptional Activation-Inhibition Domains of the Polyomavirus Enhancer Binding Protein 2/Core Binding Factor α Subunit Revealed in the Presence of the β Subunit. Mol. Cell. Biol. 18, 2444–2454. doi:10.1128/MCB.18.5.2444

Kapinas, K., Grandy, R., Ghule, P., Medina, R., Becker, K., Pardee, A., Zaidi, S.K., Lian, J., Stein, J., van Wijnen, A., Stein, G., 2013. The abbreviated pluripotent cell cycle. J. Cell. Physiol. 228, 9–20. doi:10.1002/jcp.24104

Keita, M., Bachvarova, M., Morin, C., Plante, M., Gregoire, J., Renaud, M.-C., Sebastianelli, A., Trinh, X.B., Bachvarov, D., 2013. The RUNX1 transcription factor is expressed in serous epithelial ovarian carcinoma and contributes to

cell proliferation, migration and invasion. Cell Cycle 12, 972–86. doi:10.4161/cc.23963

Keller, G.M., 1995. In vitro differentiation of embryonic stem cells. Curr. Opin. Cell Biol. 7, 862–869. doi:10.1016/0955-0674(95)80071-9

Kim, W., Barron, D.A., San Martin, R., Chan, K.S., Tran, L.L., Yang, F., Ressler, S.J., Rowley, D.R., 2014. RUNX1 is essential for mesenchymal stem cell proliferation and myofibroblast differentiation. Proc. Natl. Acad. Sci. U. S. A. 111, 16389–94. doi:10.1073/pnas.1407097111

Kimura, K., Hirano, M., Kobayashi, R., Hirano, T., 1998. Phosphorylation and activation of 13S condensin by Cdc2 in vitro. Science 282, 487–90.

Kingsley, D.M., 1994. The TGF-beta superfamily: new members, new receptors, and new genetic tests of function in different organisms. Genes Dev. 8, 133–46.

Kitisin, K., Saha, T., Blake, T., Golestaneh, N., Deng, M., Kim, C., Tang, Y., Shetty, K., Mishra, B., Mishra, L., 2007. Tgf-Beta signaling in development. Sci. STKE 2007, cm1. doi:10.1126/stke.3992007cm1

Klunker, S., Chong, M.M.W., Mantel, P.-Y., Palomares, O., Bassin, C., Ziegler, M., Rückert, B., Meiler, F., Akdis, M., Littman, D.R., Akdis, C.A., 2009. Transcription factors RUNX1 and RUNX3 in the induction and suppressive function of Foxp3 + inducible regulatory T cells. J. Exp. Med. 206, 2701–2715. doi:10.1084/jem.20090596

Knezevic, K., Bee, T., Wilson, N.K., Janes, M.E., Kinston, S., Polderdijk, S., Kolb-Kokocinski, A., Ottersbach, K., Pencovich, N., Groner, Y., de Bruijn, M., Göttgens, B., Pimanda, J.E., 2011. A Runx1-Smad6 rheostat controls Runx1 activity during embryonic hematopoiesis. Mol. Cell. Biol. 31, 2817–26. doi:10.1128/MCB.01305-10

Komar, A.A., Hatzoglou, M., 2011. Cellular IRES-mediated translation: the war of ITAFs in pathophysiological states. Cell Cycle 10, 229–40.

Krajewska, M., Heijink, A.M., Bisselink, Y.J.W.M., Seinstra, R.I., Silljé, H.H.W., de Vries, E.G.E., van Vugt, M.A.T.M., 2013. Forced activation of Cdk1 via wee1 inhibition impairs homologous recombination. Oncogene 32, 3001–8. doi:10.1038/onc.2012.296

Kreahling, J.M., Gemmer, J.Y., Reed, D., Letson, D., Bui, M., Altiok, S., 2012. MK1775, a selective Wee1 inhibitor, shows single-agent antitumor activity against sarcoma cells. Mol. Cancer Ther. 11, 174–82. doi:10.1158/1535-7163.MCT-11-0529

Kubo, A., Shinozaki, K., Shannon, J.M., Kouskoff, V., Kennedy, M., Woo, S.,

Fehling, H.J., Keller, G., 2004. Development of definitive endoderm from embryonic stem cells in culture. Development 131, 1651–62. doi:10.1242/dev.01044

Kulkarni, A.B., Huh, C.G., Becker, D., Geiser, A., Lyght, M., Flanders, K.C., Roberts, A.B., Sporn, M.B., Ward, J.M., Karlsson, S., 1993. Transforming growth factor beta 1 null mutation in mice causes excessive inflammatory response and early death. Proc. Natl. Acad. Sci. U. S. A. 90, 770–4.

Kumagai, A., Dunphy, W.G., 1991. The cdc25 protein controls tyrosine dephosphorylation of the cdc2 protein in a cell-free system. Cell 64, 903–914. doi:10.1016/0092-8674(91)90315-P

Lacaud, G., Gore, L., Kennedy, M., Kouskoff, V., Kingsley, P., Hogan, C., Carlsson, L., Speck, N., Palis, J., Keller, G., 2002. Runx1 is essential for hematopoietic commitment at the hemangioblast stage of development in vitro. Blood 100, 458–66. doi:10.1182/blood-2001-12-0321

Lam, A.Q., Freedman, B.S., Morizane, R., Lerou, P.H., Valerius, M.T., Bonventre, J. V, 2014. Rapid and efficient differentiation of human pluripotent stem cells into intermediate mesoderm that forms tubules expressing kidney proximal tubular markers. J. Am. Soc. Nephrol. 25, 1211–25. doi:10.1681/ASN.2013080831

Lamouille, S., Xu, J., Derynck, R., 2014. Molecular mechanisms of epithelial-mesenchymal transition. Nat. Rev. Mol. Cell Biol. 15, 178–96. doi:10.1038/nrm3758

Lanoix, J., Belhumeur, P., Lussier, M., Royal, A., Bravo, R., Skup, D., 1991. Regulated expression of Krox-24 and other serum-responsive genes during differentiation of P19 embryonal carcinoma cells. Cell Growth Differ. 2, 391–9.

Laslett, A.L., Grimmond, S., Gardiner, B., Stamp, L., Lin, A., Hawes, S.M., Wormald, S., Nikolic-Paterson, D., Haylock, D., Pera, M.F., Pera, M., Reubinoff, B., Trounson, A., Pera, M., Trounson, A., Hoffman, L., Carpenter, M., Thomson, J., Itskovitz-Eldor, J., Shapiro, S., Waknitz, M., Swiergiel, J., Marshall, V., Jones, J., Reubinoff, B., Pera, M., Fong, C., Trounson, A., Bongso, A., Takagi, Y., Takahashi, J., Saiki, H., Morizane, A., Hayashi, T., Kishi, Y., Fukuda, H., Okamoto, Y., Koyanagi, M., Ideguchi, M., Ben-Hur, T., Idelson, M., Khaner, H., Pera, M., Reinhartz, E., Itzik, A., Reubinoff, B., Wei, C., Miura, T., Robson, P., Lim, S., Xu, X., Lee, M., Gupta, S., Stanton, L., Luo, Y., Schmitt, J., Xu, R., Chen, X., Li, D., Li, R., Addicks, G., Glennon, C., Zwaka, T., Thomson, J., Rosler, E., Fisk, G., Ares, X., Irving, J., Miura, T., Rao, M., Carpenter, M., Robson, P., Rao, R., Calhoun, J., Qin, X., Rekaya, R., Clark, J., Stice, S., Ginis, I., Luo, Y., Miura, T., Thies, S., Brandenberger, R., Gerecht-Nir, S., Amit, M., Hoke, A., Carpenter, M., Itskovitz-Eldor, J.,

Rao, M., Carpenter, M., Rosler, E., Fisk, G., Brandenberger, R., Ares, X., Miura, T., Lucero, M., Rao, M., Brandenberger, R., Khrebtukova, I., Thies, R., Miura, T., Jingli, C., Puri, R., Vasicek, T., Lebkowski, J., Rao, M., Bhattacharya, B., Cai, J., Luo, Y., Miura, T., Mejido, J., Brimble, S., Zeng, X., Schulz, T., Rao, M., Puri, R., Bhattacharya, B., Miura, T., Brandenberg, R., Mejido, J., Luo, Y., Yang, A., Joshi, B., Irene, G., Thies, R., Amit, M., Sperger, J., Chen, X., Draper, J., Antosiewicz, J., Chon, C., Jones, S., Brooks, J., Andrews, P., Brown, P., Thomson, J., Richards, M., Tan, S., Tan, J., Chan, W., Bongso, A., Rathjen, J., Lake, J., Bettess, M., Washington, J., Chapman, G., Rathjen, P., Rossant, J., Niwa, H., Toyooka, Y., Shimosato, D., Strumpf, D., Takahashi, K., Yagi, R., Rossant, J., Smith, A., Hu, M., Krause, D., Greaves, M., Sharkis, S., Dexter, M., Heyworth, C., Enver, T., Greaves, M., Chan, L., Furley, A., Watt, S., Molgaard, H., Orkin, S., Boyer, L., Lee, T., Cole, M., Johnstone, S., Levine, S., Zucker, J., Guenther, M., Kumar, R., Murray, H., Jenner, R., Cooper, S., Pera, M., Bennett, W., Finch, J., Schopperle, W., Kershaw, D., DeWolf, W., Cooper, S., Bennett, W., Andrade, J., Reubinoff, B., Thomson, J., Pera, M., Nichols, J., Zevnik, B., Anastassiadis, K., Niwa, H., Klewe-Nebenius, D., Chambers, I., Scholer, H., Smith, A., Zaehres, H., Lensch, M., Daheron, L., Stewart, S., Itskovitz-Eldor, J., Daley, G., Matin, M., Walsh, J., Gokhale, P., Draper, J., Bahrami, A., Morton, I., Moore, H., Andrews, P., Reubinoff, B., Itsykson, P., Turetsky, T., Pera, M., Reinhartz, E., Itzik, A., Ben-Hur, T., Loebel, D., Watson, C., Young, R. De, Tam, P., Enver, T., Soneji, S., Joshi, C., Brown, J., Iborra, F., Orntoft, T., Thykjaer, T., Maltby, E., Smith, K., Dawud, R., Sugahara, K., Mikami, T., Uyama, T., Mizuguchi, S., Nomura, K., Kitagawa, H., Oka, M., Tagoku, K., Russell, T., Nakano, Y., Hamazaki, T., Meyer, E., Yokota, T., Terada, N., Draper, J., Smith, K., Gokhale, P., Moore, H., Maltby, E., Johnson, J., Meisner, L., Zwaka, T., Thomson, J., Andrews, P., Pera, M., Herszfeld, D., Wolvetang, E., Langton-Bunker, E., Chung, T., Filipczyk, A., Houssami, S., Jamshidi, P., Koh, K., Laslett, A., Michalska, A., Guyomarc, S., Xi, R., Xie, T., Meshorer, E., Yellajoshula, D., George, E., Scambler, P., Brown, D., Misteli, T., Ye, M., Iwasaki, H., Laiosa, C., Stadtfeld, M., Xie, H., Heck, S., Clausen, B., Akashi, K., Graf, T., Hancock, W., Atkins, R., Larsson, S., Charlieu, J., Miyagawa, K., Engelkamp, D., Rassoulzadegan, M., Ross, A., Cuzin, F., Heyningen, V. van, Hastie, N., Challen, G., Martinez, G., Davis, M., Taylor, D., Crowe, M., Teasdale, R., Grimmond, S., Little, M., Smyth, G., Speed, T., 2007. Transcriptional analysis of early lineage commitment in human embryonic stem cells. BMC Dev. Biol. 7, 12. doi:10.1186/1471-213X-7-12

Lee, S.E., Sada, A., Zhang, M., McDermitt, D.J., Lu, S.Y., Kemphues, K.J., Tumbar, T., 2014. High Runx1 levels promote a reversible, more-differentiated cell state in hair-follicle stem cells during quiescence. Cell Rep. 6, 499–513. doi:10.1016/j.celrep.2013.12.039

Lee, S.L., Tourtellotte, L.C., Wesselschmidt, R.L., Milbrandt, J., 1995. Growth and differentiation proceeds normally in cells deficient in the immediate early gene NGFI-A. J. Biol. Chem. 270, 9971–7.

Levanon, D., Bettoun, D., Harris-Cerruti, C., Woolf, E., Negreanu, V., Eilam, R., Bernstein, Y., Goldenberg, D., Xiao, C., Fliegauf, M., Kremer, E., Otto, F., Brenner, O., Lev-Tov, A., Groner, Y., 2002. The Runx3 transcription factor regulates development and survival of TrkC dorsal root ganglia neurons. EMBO J. 21, 3454–63. doi:10.1093/emboj/cdf370

Li, H., Collado, M., Villasante, A., Matheu, A., Lynch, C.J., Cañamero, M., Rizzoti, K., Carneiro, C., Martínez, G., Vidal, A., Lovell-Badge, R., Serrano, M., 2012. p27(Kip1) directly represses Sox2 during embryonic stem cell differentiation. Cell Stem Cell 11, 845–52. doi:10.1016/j.stem.2012.09.014

Li, Q.L., Ito, K., Sakakura, C., Fukamachi, H., Inoue, K. ichi, Chi, X.Z., Lee, K.Y., Nomura, S., Lee, C.W., Han, S.B., Kim, H.M., Kim, W.J., Yamamoto, H., Yamashita, N., Yano, T., Ikeda, T., Itohara, S., Inazawa, J., Abe, T., Hagiwara, A., Yamagishi, H., Ooe, A., Kaneda, A., Sugimura, T., Ushijima, T., Bae, S.C., Ito, Y., 2002. Causal relationship between the loss of RUNX3 expression and gastric cancer. Cell 109, 113–24.

Lian, J.B., Balint, E., Javed, A., Drissi, H., Vitti, R., Quinlan, E.J., Zhang, L., Van Wijnen, A.J., Stein, J.L., Speck, N., Stein, G.S., 2003. Runx1/AML1 hematopoietic transcription factor contributes to skeletal development in vivo. J. Cell. Physiol. 196, 301–11. doi:10.1002/jcp.10316

Lian, X., Zhang, J., Azarin, S.M., Zhu, K., Hazeltine, L.B., Bao, X., Hsiao, C., Kamp, T.J., Palecek, S.P., 2013. Directed cardiomyocyte differentiation from human pluripotent stem cells by modulating Wnt/β-catenin signaling under fully defined conditions. Nat. Protoc. 8, 162–75. doi:10.1038/nprot.2012.150

Lichtinger, M., Ingram, R., Hannah, R., Müller, D., Clarke, D., Assi, S.A., Lie-A-Ling, M., Noailles, L., Vijayabaskar, M.S., Wu, M., Tenen, D.G., Westhead, D.R., Kouskoff, V., Lacaud, G., Göttgens, B., Bonifer, C., 2012. RUNX1 reshapes the epigenetic landscape at the onset of haematopoiesis. EMBO J. 31, 4318–33. doi:10.1038/emboj.2012.275

Lickert, H., Kutsch, S., Kanzler, B., Tamai, Y., Taketo, M.M., Kemler, R., 2002. Formation of Multiple Hearts in Mice following Deletion of β-catenin in the Embryonic Endoderm. Dev. Cell 3, 171–181. doi:10.1016/S1534-5807(02)00206-X

Lie-A-Ling, M., Marinopoulou, E., Li, Y., Patel, R., Stefanska, M., Bonifer, C., Miller, C., Kouskoff, V., Lacaud, G., 2014. RUNX1 positively regulates a cell adhesion and migration program in murine hemogenic endothelium prior to blood emergence. Blood 124, e11–20. doi:10.1182/blood-2014-04-572958

Liu, F., Stanton, J.J., Wu, Z., Piwnica-Worms, H., 1997. The human Myt1 kinase preferentially phosphorylates Cdc2 on threonine 14 and localizes to the endoplasmic reticulum and Golgi complex. Mol. Cell. Biol. 17, 571–583. doi:10.1128/MCB.17.2.571

Maduro, M.F., Meneghini, M.D., Bowerman, B., Broitman-Maduro, G., Rothman, J.H., 2001. Restriction of mesendoderm to a single blastomere by the combined action of SKN-1 and a GSK-3beta homolog is mediated by MED-1 and -2 in C. elegans. Mol. Cell 7, 475–85.

Maeda, M., Johnson, K.R., Wheelock, M.J., 2005. Cadherin switching: essential for behavioral but not morphological changes during an epithelium-to-mesenchyme transition. J. Cell Sci. 118, 873–87. doi:10.1242/jcs.01634

Mahmood, A., Aldahmash, A., 2015. Induction of primitive streak and mesendoderm formation in monolayer hESC culture by activation of TGF-β signaling pathway by Activin B. Saudi J. Biol. Sci. 22, 692–7. doi:10.1016/j.sjbs.2015.03.002

Mak, S.K., Kültz, D., 2004. Gadd45 proteins induce G2/M arrest and modulate apoptosis in kidney cells exposed to hyperosmotic stress. J. Biol. Chem. 279, 39075–84. doi:10.1074/jbc.M406643200

Massagué, J., 2000. How cells read TGF-beta signals. Nat. Rev. Mol. Cell Biol. 1, 169–78. doi:10.1038/35043051

Massagué, J., 1998. TGF-beta signal transduction. Annu. Rev. Biochem. 67, 753–91. doi:10.1146/annurev.biochem.67.1.753

Masui, Y., Markert, C.L., 1971. Cytoplasmic control of nuclear behavior during meiotic maturation of frog oocytes. J. Exp. Zool. 177, 129–45. doi:10.1002/jez.1401770202

McGowan, C.H., Russell, P., 1995. Cell cycle regulation of human WEE1. EMBO J. 14, 2166–75.

McGowan, C.H., Russell, P., 1993. Human Wee1 kinase inhibits cell division by phosphorylating p34cdc2 exclusively on Tyr15. EMBO J. 12, 75–85.

Meijer, L., Azzi, L., Wang, J.Y., 1991. Cyclin B targets p34cdc2 for tyrosine phosphorylation. EMBO J. 10, 1545–54.

Melnikova, I.N., Crute, B.E., Wang, S., Speck, N.A., 1993. Sequence specificity of the core-binding factor. J. Virol. 67, 2408–2411.

Menchón, C., Edel, M.J., Izpisua Belmonte, J.C., 2011. The cell cycle inhibitor p27Kip^{1} controls self-renewal and pluripotency of human embryonic stem cells by regulating the cell cycle, Brachyury and Twist. Cell Cycle 10, 1435–47.

Miake-Lye, R., Newport, J., Kirschner, M., 1983. Maturation-promoting factor induces nuclear envelope breakdown in cycloheximide-arrested embryos of Xenopus laevis. J. Cell Biol. 97, 81–91.

Micallef, L., Rodgers, P., 2014. eulerAPE: drawing area-proportional 3-Venn diagrams using ellipses. PLoS One 9, e101717. doi:10.1371/journal.pone.0101717

Mikkelsen, T.S., Ku, M., Jaffe, D.B., Issac, B., Lieberman, E., Giannoukos, G., Alvarez, P., Brockman, W., Kim, T.-K., Koche, R.P., Lee, W., Mendenhall, E., O'Donovan, A., Presser, A., Russ, C., Xie, X., Meissner, A., Wernig, M., Jaenisch, R., Nusbaum, C., Lander, E.S., Bernstein, B.E., 2007. Genome-wide maps of chromatin state in pluripotent and lineage-committed cells. Nature 448, 553–60. doi:10.1038/nature06008

Milacic, M., Haw, R., Rothfels, K., Wu, G., Croft, D., Hermjakob, H., D'Eustachio, P., Stein, L., 2012. Annotating cancer variants and anti-cancer therapeutics in reactome. Cancers (Basel). 4, 1180–211. doi:10.3390/cancers4041180

Miyazawa, K., Shinozaki, M., Hara, T., Furuya, T., Miyazono, K., 2002. Two major Smad pathways in TGF-beta superfamily signalling. Genes to Cells 7, 1191–1204. doi:10.1046/j.1365-2443.2002.00599.x

Miyazono, K., Maeda, S., Imamura, T., 2004. Coordinate regulation of cell growth and differentiation by TGF-beta superfamily and Runx proteins. Oncogene 23, 4232–7. doi:10.1038/sj.onc.1207131

Miyazono, K., Olofsson, A., Colosetti, P., Heldin, C.H., 1991. A role of the latent TGF-beta 1-binding protein in the assembly and secretion of TGF-beta 1. EMBO J. 10, 1091–101.

Moustakas, A., Heldin, C.-H., 2007. Signaling networks guiding epithelial-mesenchymal transitions during embryogenesis and cancer progression. Cancer Sci. 98, 1512–20. doi:10.1111/j.1349-7006.2007.00550.x

Mueller, P.R., Coleman, T.R., Dunphy, W.G., 1995. Cell cycle regulation of a Xenopus Wee1-like kinase. Mol. Biol. Cell 6, 119–34.

Mummery, C., Ward-van Oostwaard, D., Doevendans, P., Spijker, R., van den Brink, S., Hassink, R., van der Heyden, M., Opthof, T., Pera, M., de la Riviere, A.B., Passier, R., Tertoolen, L., 2003. Differentiation of human embryonic stem cells to cardiomyocytes: role of coculture with visceral endoderm-like cells. Circulation 107, 2733–40. doi:10.1161/01.CIR.0000068356.38592.68

Murphy, M., Stinnakre, M.G., Senamaud-Beaufort, C., Winston, N.J., Sweeney, C., Kubelka, M., Carrington, M., Bréchot, C., Sobczak-Thépot, J., 1997. Delayed early embryonic lethality following disruption of the murine cyclin A2

gene. Nat. Genet. 15, 83–6. doi:10.1038/ng0197-83

Murthy, M., Bocking, S., Verginelli, F., Stifani, S., 2014. Transcription factor Runx1 inhibits proliferation and promotes developmental maturation in a selected population of inner olfactory nerve layer olfactory ensheathing cells. Gene 540, 191–200. doi:10.1016/j.gene.2014.02.038

Nair, G., Abranches, E., Guedes, A.M. V., Henrique, D., Raj, A., Ying, Q.-L., Silva, J., Smith, A., Huang, S., Smith, A., Arias, A.M., Brickman, J.M., Hayashi, K., Lopes, S.M.C., de, S., Tang, F., Surani, M.A., Toyooka, Y., Shimosato, D., Murakami, K., Takahashi, K., Niwa, H., Marks, H., Chambers, I., Kalmar, T., Abranches, E., Abranches, E., Bekman, E., Henrique, D., Arias, A.M., Nichols, J., Schröter, C., Cross, M.A., Enver, T., Raj, A., Bogaard, P. van den, Rifkin, S.A., Oudenaarden, A. van, Tyagi, S., Singer, Z.S., MacArthur, B.D., Young, M.D., Wakefield, M.J., Smyth, G.K., Oshlack, A., Ying, Q.-L., Stavridis, M., Griffiths, D., Li, M., Smith, A., Kim, J., Chu, J., Shen, X., Wang, J., Orkin, S.H., Loh, K.M., Lim, B., Guttman, M., Maamar, H., Cabili, M.N., Rinn, J., Raj, A., Niwa, H., Miyazaki, J., Smith, A.G., Sharova, L. V., Faddah, D.A., Chapman, D.L., Agulnik, I., Hancock, S., Silver, L.M., Papaioannou, V.E., Zhang, X., Peterson, K.A., Liu, X.S., McMahon, A.P., Ohba, S., Trott, J., Arias, A.M., Turner, D.A., Trott, J., Hayward, P., Rué, P., Arias, A.M., Raj, A., Peskin, C.S., Tranchina, D., Vargas, D.Y., Tyagi, S., Suter, D.M., Grant, G.R., Anders, S., Huber, W., Pina, C., 2015. Heterogeneous lineage marker expression in naive embryonic stem cells is mostly due to spontaneous differentiation. Sci. Rep. 5, 13339. doi:10.1038/srep13339

Nieto, M.A., 2013. Epithelial plasticity: a common theme in embryonic and cancer cells. Science (80-.). 342, 1234850. doi:10.1126/science.1234850

Nigg, E.A., 1995. Cyclin-dependent protein kinases: key regulators of the eukaryotic cell cycle. Bioessays 17, 471–80. doi:10.1002/bies.950170603

Nishikawa, S., Nishikawa, S., Hirashima, M., Matsuyoshi, N., Kodama, H., 1998. Progressive lineage analysis by cell sorting and culture identifies FLK1+VE-cadherin+ cells at a diverging point of endothelial and hemopoietic lineages. Development 125, 1747–1757.

Niwa, H., Miyazaki, J., Smith, A.G., 2000. Quantitative expression of Oct-3/4 defines differentiation, dedifferentiation or self-renewal of ES cells. Nat. Genet. 24, 372–6. doi:10.1038/74199

Nomura, M., Li, E., 1998. Smad2 role in mesoderm formation, left-right patterning and craniofacial development. Nature 393, 786–90. doi:10.1038/31693

O'Connell, M.J., Cimprich, K.A., 2005. G2 damage checkpoints: what is the turn-on? J. Cell Sci. 118, 1–6. doi:10.1242/jcs.01626

Ogawa, E., Inuzuka, M., Maruyama, M., Satake, M., Naito-Fujimoto, M., Ito, Y., Shigesada, K., 1993a. Molecular cloning and characterization of PEBP2 beta, the heterodimeric partner of a novel Drosophila runt-related DNA binding protein PEBP2 alpha. Virology 194, 314–31. doi:10.1006/viro.1993.1262

Ogawa, E., Maruyama, M., Kagoshima, H., Inuzuka, M., Lu, J., Satake, M., Shigesada, K., Ito, Y., 1993b. PEBP2/PEA2 represents a family of transcription factors homologous to the products of the Drosophila runt gene and the human AML1 gene. Proc. Natl. Acad. Sci. U. S. A. 90, 6859–63.

Okuda, T., van Deursen, J., Hiebert, S.W., Grosveld, G., Downing, J.R., 1996. AML1, the target of multiple chromosomal translocations in human leukemia, is essential for normal fetal liver hematopoiesis. Cell 84, 321–30.

Osoegawa, K., Mammoser, A.G., Wu, C., Frengen, E., Zeng, C., Catanese, J.J., de Jong, P.J., 2001. A bacterial artificial chromosome library for sequencing the complete human genome. Genome Res. 11, 483–96. doi:10.1101/gr.169601

Osoegawa, K., Woon, P.Y., Zhao, B., Frengen, E., Tateno, M., Catanese, J.J., de Jong, P.J., 1998. An improved approach for construction of bacterial artificial chromosome libraries. Genomics 52, 1–8. doi:10.1006/geno.1998.5423

Osorio, K.M., Lee, S.E., McDermitt, D.J., Waghmare, S.K., Zhang, Y. V, Woo, H.N., Tumbar, T., 2008. Runx1 modulates developmental, but not injury-driven, hair follicle stem cell activation. Development 135, 1059–68. doi:10.1242/dev.012799

Osorio, K.M., Lilja, K.C., Tumbar, T., 2011. Runx1 modulates adult hair follicle stem cell emergence and maintenance from distinct embryonic skin compartments. J. Cell Biol. 193, 235–50. doi:10.1083/jcb.201006068

Otto, F., Thornell, A.P., Crompton, T., Denzel, A., Gilmour, K.C., Rosewell, I.R., Stamp, G.W., Beddington, R.S., Mundlos, S., Olsen, B.R., Selby, P.B., Owen, M.J., 1997. Cbfa1, a candidate gene for cleidocranial dysplasia syndrome, is essential for osteoblast differentiation and bone development. Cell 89, 765–71.

Palmer, B.D., Thompson, A.M., Booth, R.J., Dobrusin, E.M., Kraker, A.J., Lee, H.H., Lunney, E.A., Mitchell, L.H., Ortwine, D.F., Smaill, J.B., Swan, L.M., Denny, W.A., 2006. 4-Phenylpyrrolo[3,4-c]carbazole-1,3(2H,6H)-dione inhibitors of the checkpoint kinase Wee1. Structure-activity relationships for chromophore modification and phenyl ring substitution. J. Med. Chem. 49, 4896–911. doi:10.1021/jm0512591

Parker, L.L., Piwnica-Worms, H., 1992. Inactivation of the p34cdc2-cyclin B complex by the human WEE1 tyrosine kinase. Science 257, 1955–7.

Patel, N.M., Nozaki, S., Shortle, N.H., Bhat-Nakshatri, P., Newton, T.R., Rice, S., Gelfanov, V., Boswell, S.H., Goulet, R.J., Sledge, G.W., Nakshatri, H., 2000. Paclitaxel sensitivity of breast cancer cells with constitutively active NF-kappaB is enhanced by IkappaBalpha super-repressor and parthenolide. Oncogene 19, 4159–69. doi:10.1038/sj.onc.1203768

Pauklin, S., Vallier, L., 2013. The cell-cycle state of stem cells determines cell fate propensity. Cell 155, 135–47. doi:10.1016/j.cell.2013.08.031

Pazhanisamy, S., 2015. Adult Stem Cell and Embryonic Stem Cell Markers. Mater. Methods .

Pereira, L.A., Wong, M.S., Lim, S.M., Sides, A., Stanley, E.G., Elefanty, A.G., 2011. Brachyury and Related Tbx Proteins Interact with the Mixl1 Homeodomain Protein and Negatively Regulate Mixl1 Transcriptional Activity. PLoS One 6, e28394. doi:10.1371/journal.pone.0028394

Piaggio, G., Farina, A., Perrotti, D., Manni, I., Fuschi, P., Sacchi, A., Gaetano, C., 1995. Structure and growth-dependent regulation of the human cyclin B1 promoter. Exp. Cell Res. 216, 396–402. doi:10.1006/excr.1995.1050

Pines, J., 1995. Cyclins and cyclin-dependent kinases: a biochemical view. Biochem. J. 308, 697–711. doi:10.1042/bj3080697

Pines, J., Hunter, T., 1989. Isolation of a human cyclin cDNA: Evidence for cyclin mRNA and protein regulation in the cell cycle and for interaction with p34cdc2. Cell 58, 833–846. doi:10.1016/0092-8674(89)90936-7

Pozner, A., Goldenberg, D., Negreanu, V., Le, S.Y., Elroy-Stein, O., Levanon, D., Groner, Y., 2000. Transcription-coupled translation control of AML1/RUNX1 is mediated by cap- and internal ribosome entry site-dependent mechanisms. Mol. Cell. Biol. 20, 2297–307.

Ran, D., Shia, W.-J., Lo, M.-C., Fan, J.-B., Knorr, D.A., Ferrell, P.I., Ye, Z., Yan, M., Cheng, L., Kaufman, D.S., Zhang, D.-E., 2013. RUNX1a enhances hematopoietic lineage commitment from human embryonic stem cells and inducible pluripotent stem cells. Blood 121, 2882–90. doi:10.1182/blood-2012-08-451641

Reubinoff, B.E., Pera, M.F., Fong, C.Y., Trounson, A., Bongso, A., 2000. Embryonic stem cell lines from human blastocysts: somatic differentiation in vitro. Nat. Biotechnol. 18, 399–404. doi:10.1038/74447

Rodaway, A., Patient, R., 2001. Mesendoderm. Cell 105, 169–172. doi:10.1016/S0092-8674(01)00307-5

Sanford, L., Ormsby, I., Gittenberger-de Groot, A., Sariola, H., Friedman, R., Boivin, G., Cardell, E., Doetschman, T., 1997. TGFbeta2 knockout mice

have multiple developmental defects that are non-overlapping with other TGFbeta knockout phenotypes. Development 124, 2659–2670.

Santamaría, D., Barrière, C., Cerqueira, A., Hunt, S., Tardy, C., Newton, K., Cáceres, J.F., Dubus, P., Malumbres, M., Barbacid, M., 2007. Cdk1 is sufficient to drive the mammalian cell cycle. Nature 448, 811–5. doi:10.1038/nature06046

Scheitz, C.J.F., Tumbar, T., 2013. New insights into the role of Runx1 in epithelial stem cell biology and pathology. J. Cell. Biochem. 114, 985–993. doi:10.1002/jcb.24453

Schmierer, B., Hill, C.S., 2007. TGFbeta-SMAD signal transduction: molecular specificity and functional flexibility. Nat. Rev. Mol. Cell Biol. 8, 970–82. doi:10.1038/nrm2297

Segev, H., Fishman, B., Ziskind, A., Shulman, M., Itskovitz-Eldor, J., 2004. Differentiation of human embryonic stem cells into insulin-producing clusters. Stem Cells 22, 265–74. doi:10.1634/stemcells.22-3-265

Sela, Y., Molotski, N., Golan, S., Itskovitz-Eldor, J., Soen, Y., 2012. Human embryonic stem cells exhibit increased propensity to differentiate during the G1 phase prior to phosphorylation of retinoblastoma protein. Stem Cells 30, 1097–108. doi:10.1002/stem.1078

Shi, Y., Massagué, J., 2003. Mechanisms of TGF-β Signaling from Cell Membrane to the Nucleus. Cell 113, 685–700. doi:10.1016/S0092-8674(03)00432-X

Shull, M.M., Ormsby, I., Kier, A.B., Pawlowski, S., Diebold, R.J., Yin, M., Allen, R., Sidman, C., Proetzel, G., Calvin, D., 1992. Targeted disruption of the mouse transforming growth factor-beta 1 gene results in multifocal inflammatory disease. Nature 359, 693–9. doi:10.1038/359693a0

Smits, V.A.., Medema, R.H., 2001. Checking out the G2/M transition. Biochim. Biophys. Acta - Gene Struct. Expr. 1519, 1–12. doi:10.1016/S0167-4781(01)00204-4

Sokol, E.S., Sanduja, S., Jin, D.X., Miller, D.H., Mathis, R.A., Gupta, P.B., 2015. Perturbation-expression analysis identifies RUNX1 as a regulator of human mammary stem cell differentiation. PLoS Comput. Biol. 11, e1004161. doi:10.1371/journal.pcbi.1004161

Sroczynska, P., Lancrin, C., Kouskoff, V., Lacaud, G., 2009. The differential activities of Runx1 promoters define milestones during embryonic hematopoiesis. Blood 114, 5279–89. doi:10.1182/blood-2009-05-222307

Stark, G.R., Taylor, W.R., 2006. Control of the G2/M transition. Mol. Biotechnol.

32, 227–48. doi:10.1385/MB:32:3:227

Stein, G.S., Lian, J.B., Stein, J.L., van Wijnen, A.J., Choi, J.-Y., Pratap, J., Zaidi, S.K., 2009. Temporal and Spatial Parameters of Skeletal Gene Expression: Targeting RUNX Factors and their Coregulatory Proteins to Subnuclear Domains. Connect. Tissue Res. 44, 149–153. doi:10.1080/03008900390152241

Stifani, N., Freitas, A.R.O., Liakhovitskaia, A., Medvinsky, A., Kania, A., Stifani, S., 2008. Suppression of interneuron programs and maintenance of selected spinal motor neuron fates by the transcription factor AML1/Runx1. Proc. Natl. Acad. Sci. U. S. A. 105, 6451–6. doi:10.1073/pnas.0711299105

Strausfeld, U., Labbé, J.C., Fesquet, D., Cavadore, J.C., Picard, A., Sadhu, K., Russell, P., Dorée, M., 1991. Dephosphorylation and activation of a p34cdc2/cyclin B complex in vitro by human CDC25 protein. Nature 351, 242–5. doi:10.1038/351242a0

Sulzbacher, S., Schroeder, I.S., Truong, T.T., Wobus, A.M., 2009. Activin A-Induced Differentiation of Embryonic Stem Cells into Endoderm and Pancreatic Progenitors—The Influence of Differentiation Factors and Culture Conditions. Stem Cell Rev. Reports 5, 159–173. doi:10.1007/s12015-009-9061-5

Sun, P.D., Davies, D.R., 1995. The cystine-knot growth-factor superfamily. Annu. Rev. Biophys. Biomol. Struct. 24, 269–91. doi:10.1146/annurev.bb.24.060195.001413

Szutorisz, H., Dillon, N., 2005. The epigenetic basis for embryonic stem cell pluripotency. Bioessays 27, 1286–93. doi:10.1002/bies.20330

Tada, S., 2005. Characterization of mesendoderm: a diverging point of the definitive endoderm and mesoderm in embryonic stem cell differentiation culture. Development 132, 4363–4374. doi:10.1242/dev.02005

Taipale, J., Miyazono, K., Heldin, C.H., Keski-Oja, J., 1994. Latent transforming growth factor-beta 1 associates to fibroblast extracellular matrix via latent TGF-beta binding protein. J. Cell Biol. 124, 171–81.

Tajima, Y., Goto, K., Yoshida, M., Shinomiya, K., Sekimoto, T., Yoneda, Y., Miyazono, K., Imamura, T., 2003. Chromosomal region maintenance 1 (CRM1)-dependent nuclear export of Smad ubiquitin regulatory factor 1 (Smurf1) is essential for negative regulation of transforming growth factor-beta signaling by Smad7. J. Biol. Chem. 278, 10716–21. doi:10.1074/jbc.M212663200

Takasato, M., Er, P.X., Becroft, M., Vanslambrouck, J.M., Stanley, E.G., Elefanty, A.G., Little, M.H., 2014. Directing human embryonic stem cell differentiation

towards a renal lineage generates a self-organizing kidney. Nat. Cell Biol. 16, 118–26. doi:10.1038/ncb2894

Takizawa, C.G., Weis, K., Morgan, D.O., 1999. Ran-independent nuclear import of cyclin B1-Cdc2 by importin beta. Proc. Natl. Acad. Sci. U. S. A. 96, 7938–43.

Tassan, J.P., 1994. Cell cycle analysis of the activity, subcellular localization, and subunit composition of human CAK (CDK-activating kinase). J. Cell Biol. 127, 467–478. doi:10.1083/jcb.127.2.467

Thiery, J.P., Acloque, H., Huang, R.Y.J., Nieto, M.A., 2009. Epithelial-mesenchymal transitions in development and disease. Cell 139, 871–90. doi:10.1016/j.cell.2009.11.007

Thomson, J.A., Itskovitz-Eldor, J., Shapiro, S.S., Waknitz, M.A., Swiergiel, J.J., Marshall, V.S., Jones, J.M., 1998. Embryonic Stem Cell Lines Derived from Human Blastocysts. Sci. 282 , 1145–1147. doi:10.1126/science.282.5391.1145

Tombes, R.M., Peloquin, J.G., Borisy, G.G., 1991. Specific association of an M-phase kinase with isolated mitotic spindles and identification of two of its substrates as MAP4 and MAP1B. Cell Regul. 2, 861–74.

Tominaga, Y., Li, C., Wang, R.-H., Deng, C.-X., 2006. Murine Wee1 plays a critical role in cell cycle regulation and pre-implantation stages of embryonic development. Int. J. Biol. Sci. 2, 161–70.

Tonge, P.D., Andrews, P.W., 2010. Retinoic acid directs neuronal differentiation of human pluripotent stem cell lines in a non-cell-autonomous manner. Differentiation. 80, 20–30. doi:10.1016/j.diff.2010.04.001

Toyoshima, F., Moriguchi, T., Wada, A., Fukuda, M., Nishida, E., 1998. Nuclear export of cyclin B1 and its possible role in the DNA damage-induced G2 checkpoint. EMBO J. 17, 2728–35. doi:10.1093/emboj/17.10.2728

Toyoshima-Morimoto, F., Taniguchi, E., Shinya, N., Iwamatsu, A., Nishida, E., 2001. Polo-like kinase 1 phosphorylates cyclin B1 and targets it to the nucleus during prophase. Nature 410, 215–20. doi:10.1038/35065617

Vairapandi, M., Balliet, A.G., Hoffman, B., Liebermann, D.A., 2002. GADD45b and GADD45g are cdc2/cyclinB1 kinase inhibitors with a role in S and G2/M cell cycle checkpoints induced by genotoxic stress. J. Cell. Physiol. 192, 327–38. doi:10.1002/jcp.10140

Vallier, L., Touboul, T., Chng, Z., Brimpari, M., Hannan, N., Millan, E., Smithers, L.E., Trotter, M., Rugg-Gunn, P., Weber, A., Pedersen, R.A., 2009. Early Cell Fate Decisions of Human Embryonic Stem Cells and Mouse Epiblast

Stem Cells Are Controlled by the Same Signalling Pathways. PLoS One 4, e6082. doi:10.1371/journal.pone.0006082

Vandewalle, C., Comijn, J., De Craene, B., Vermassen, P., Bruyneel, E., Andersen, H., Tulchinsky, E., Van Roy, F., Berx, G., 2005. SIP1/ZEB2 induces EMT by repressing genes of different epithelial cell-cell junctions. Nucleic Acids Res. 33, 6566–78. doi:10.1093/nar/gki965

VanOudenhove, J.J., Grandy, R.A., Ghule, P.N., del Rio, R., Lian, J.B., Stein, J.L., Zaidi, S.K., Stein, G.S., 2016. Lineage-Specific Early Differentiation of Human Embryonic Stem Cells Requires a G2 Cell Cycle Pause. Stem Cells n/a–n/a. doi:10.1002/stem.2352

Vermeulen, K., Van Bockstaele, D.R., Berneman, Z.N., 2003. The cell cycle: a review of regulation, deregulation and therapeutic targets in cancer. Cell Prolif. 36, 131–149. doi:10.1046/j.1365-2184.2003.00266.x

Vesuna, F., van Diest, P., Chen, J.H., Raman, V., 2008. Twist is a transcriptional repressor of E-cadherin gene expression in breast cancer. Biochem. Biophys. Res. Commun. 367, 235–41. doi:10.1016/j.bbrc.2007.11.151

Viebahn, C., 1995. Epithelio-Mesenchymal Transformation during Formation of the Mesoderm in the Mammalian Embryo. Cells Tissues Organs 154, 79–97. doi:10.1159/000147753

Vodyanik, M.A., Bork, J.A., Thomson, J.A., Slukvin, I.I., 2005. Human embryonic stem cell-derived CD34+ cells: efficient production in the coculture with OP9 stromal cells and analysis of lymphohematopoietic potential. Blood 105, 617–26. doi:10.1182/blood-2004-04-1649

Wang, Q., Stacy, T., Binder, M., Marin-Padilla, M., Sharpe, A.H., Speck, N.A., 1996. Disruption of the Cbfa2 gene causes necrosis and hemorrhaging in the central nervous system and blocks definitive hematopoiesis. Proc. Natl. Acad. Sci. U. S. A. 93, 3444–9.

Watabe, T., Miyazono, K., 2009. Roles of TGF-beta family signaling in stem cell renewal and differentiation. Cell Res. 19, 103–15. doi:10.1038/cr.2008.323

Wei, C.L., Miura, T., Robson, P., Lim, S.-K., Xu, X.-Q., Lee, M.Y.-C., Gupta, S., Stanton, L., Luo, Y., Schmitt, J., Thies, S., Wang, W., Khrebtukova, I., Zhou, D., Liu, E.T., Ruan, Y.J., Rao, M., Lim, B., 2005. Transcriptome profiling of human and murine ESCs identifies divergent paths required to maintain the stem cell state. Stem Cells 23, 166–85. doi:10.1634/stemcells.2004-0162

Weinstein, M., Yang, X., Li, C., Xu, X., Gotay, J., Deng, C.-X., 1998. Failure of egg cylinder elongation and mesoderm induction in mouse embryos lacking the tumor suppressor smad2. Proc. Natl. Acad. Sci. 95, 9378–9383. doi:10.1073/pnas.95.16.9378

White, J., Dalton, S., 2005. Cell cycle control of embryonic stem cells. Stem Cell Rev. 1, 131–8. doi:10.1385/SCR:1:2:131

Wrana, J.L., Attisano, L., Cárcamo, J., Zentella, A., Doody, J., Laiho, M., Wang, X.-F., Massague, J., 1992. TGFβ signals through a heteromeric protein kinase receptor complex. Cell 71, 1003–1014. doi:10.1016/0092-8674(92)90395-S

Wu, M.Y., Hill, C.S., 2009. Tgf-beta superfamily signaling in embryonic development and homeostasis. Dev. Cell 16, 329–43. doi:10.1016/j.devcel.2009.02.012

Xu, C., 2002. Characterization and Enrichment of Cardiomyocytes Derived From Human Embryonic Stem Cells. Circ. Res. 91, 501–508. doi:10.1161/01.RES.0000035254.80718.91

Xu, C., Inokuma, M.S., Denham, J., Golds, K., Kundu, P., Gold, J.D., Carpenter, M.K., 2001. Feeder-free growth of undifferentiated human embryonic stem cells. Nat. Biotechnol. 19, 971–4. doi:10.1038/nbt1001-971

Xu, J., Lamouille, S., Derynck, R., 2009. TGF-beta-induced epithelial to mesenchymal transition. Cell Res. 19, 156–72. doi:10.1038/cr.2009.5

Xu, R.-H., Peck, R.M., Li, D.S., Feng, X., Ludwig, T., Thomson, J.A., 2005. Basic FGF and suppression of BMP signaling sustain undifferentiated proliferation of human ES cells. Nat. Methods 2, 185–90. doi:10.1038/nmeth744

Xu, R.-H., Sampsell-Barron, T.L., Gu, F., Root, S., Peck, R.M., Pan, G., Yu, J., Antosiewicz-Bourget, J., Tian, S., Stewart, R., Thomson, J.A., 2008. NANOG is a direct target of TGFbeta/activin-mediated SMAD signaling in human ESCs. Cell Stem Cell 3, 196–206. doi:10.1016/j.stem.2008.07.001

Yang, J., Mani, S.A., Donaher, J.L., Ramaswamy, S., Itzykson, R.A., Come, C., Savagner, P., Gitelman, I., Richardson, A., Weinberg, R.A., 2004. Twist, a master regulator of morphogenesis, plays an essential role in tumor metastasis. Cell 117, 927–39. doi:10.1016/j.cell.2004.06.006

Yang, J., Weinberg, R.A., 2008. Epithelial-mesenchymal transition: at the crossroads of development and tumor metastasis. Dev. Cell 14, 818–29. doi:10.1016/j.devcel.2008.05.009

Zambidis, E.T., Peault, B., Park, T.S., Bunz, F., Civin, C.I., 2005. Hematopoietic differentiation of human embryonic stem cells progresses through sequential hematoendothelial, primitive, and definitive stages resembling human yolk sac development. Blood 106, 860–70. doi:10.1182/blood-2004-11-4522

Zaret, K.S., Carroll, J.S., 2011. Pioneer transcription factors: Establishing competence for gene expression. Genes Dev. 25, 2227–2241.

doi:10.1101/gad.176826.111

Zeisberg, M., Neilson, E.G., 2009. Biomarkers for epithelial-mesenchymal transitions. J. Clin. Invest. 119, 1429–37. doi:10.1172/JCI36183

Zeng, C., McNeil, S., Pockwinse, S., Nickerson, J., Shopland, L., Lawrence, J.B., Penman, S., Hiebert, S., Lian, J.B., van Wijnen, A.J., Stein, J.L., Stein, G.S., 1998. Intranuclear targeting of AML/CBF regulatory factors to nuclear matrix-associated transcriptional domains. Proc. Natl. Acad. Sci. 95, 1585–1589. doi:10.1073/pnas.95.4.1585

Zeng, C., van Wijnen, A.J., Stein, J.L., Meyers, S., Sun, W., Shopland, L., Lawrence, J.B., Penman, S., Lian, J.B., Stein, G.S., Hiebert, S.W., 1997. Identification of a nuclear matrix targeting signal in the leukemia and bone-related AML/CBF- transcription factors. Proc. Natl. Acad. Sci. 94, 6746–6751. doi:10.1073/pnas.94.13.6746

Zhang, J., Tian, X.-J., Xing, J., 2016. Signal Transduction Pathways of EMT Induced by TGF-β, SHH, and WNT and Their Crosstalks. J. Clin. Med. 5. doi:10.3390/jcm5040041

Zhou, B.B., Elledge, S.J., 2000. The DNA damage response: putting checkpoints in perspective. Nature 408, 433–9. doi:10.1038/35044005

Zhu, H., Hu, S., Baker, J., 2014. JMJD5 regulates cell cycle and pluripotency in human embryonic stem cells. Stem Cells 32, 2098–110. doi:10.1002/stem.1724